NASA CR 62008

H
HONEYWELL

FINAL REPORT

AN ENGINEERING DESIGN STUDY
AND TEST PROGRAM FOR
THE PARAVULCOON RECOVERY SYSTEM

Prepared for
The National Aeronautics and Space Administration
Langley Research Center

Contract NAS 1-3169

26 February 1965

HONEYWELL | SYSTEMS AND RESEARCH DIVISION

26 February 1965

FINAL REPORT

AN ENGINEERING DESIGN STUDY
AND TEST PROGRAM FOR
THE PARAVULCOON RECOVERY SYSTEM

Prepared for
The National Aeronautics and Space Administration
Langley Research Center

Contract NAS 1-3169

Prepared by:

    A. J. Oberg
    Project Engineer

Reviewed by: *Kenneth J. Fraasch*

    K. J. Fraasch
    Project Supervisor

Approved by: *M. A. Sutton*

    M. A. Sutton
    Chief Engineer

Honeywell Inc.
Systems and Research Division
Minneapolis, Minnesota

FOREWORD

ABSTRACT

The Paravulcoon Recovery System is a concept for terminal recovery
which uses the buoyancy of an aerially deployed, ram air inflated,
and aerially heated balloon to hover the recovered body. In the pro-
gram reported here the feasibility of the aerial deployment, inflation,
and cold terminal descent phases of the system activation sequence
was investigated by means of a brief wind tunnel study and aerial drop
flight tests of a system with a 1000-pound payload. Although some
problems requiring further investigation and design were encountered,
the basic concept was found to be feasible.

CONTENTS

CONTENTS

ILLUSTRATIONS

CONTENTS

TABLES

SECTION I
SUMMARY

The Paravulcoon Recovery System is a concept for terminal recovery of space payloads and spent rocket boosters wherein the buoyancy of an aerially deployed, ram air inflated and heated balloon filled with hot air is used to accomplish the atmospheric flotation and controlled descent to touchdown of the recovered body. The aerial deployment and inflation phases of the system activation sequence have not been previously demonstrated with practical sized systems and are not amenable to analytical verification. Therefore, the purpose of the program reported here was to experimentally demonstrate the feasibility of these phases with a balloon suitable for the recovery of a 1000 pound object. In pursuing this objective, the program consisted of a brief wind tunnel study using 6-foot diameter balloon models, and four full-scale free flight tests using 54-foot diameter balloons.

The wind tunnel experimentation showed the planned mechanization of the concept to be sound, but also revealed a possible area of system instability. Further analysis and testing, however, showed this problem to be the result of the particular flow regime in which it was necessary to operate with the small model systems. Also, model instability was found to be readily tractable to "fixing" by mechanical design. In the full-scale free flight tests the feasibility of the deployment and inflation concept was completely demonstrated up to a deployment velocity of 204 fps and a dynamic pressure of 29 psf. While some problem areas requiring further study and development were revealed in these tests, nothing was encountered which would be expected to hinder the orderly development of a practical recovery system based on this concept.

SECTION II
INTRODUCTION AND PROGRAM DEFINITION

The Paravulcoon System is a terminal recovery scheme for space vehicles and boosters in which the buoyancy of hot air in an aerially deployed balloon is used to provide atmospheric flotation. This system concept has been previously established by means of analytical studies. However, the present study was devoted solely to experimentally demonstrating feasibility of just one portion of the over-all system sequence -- deployment and inflation of the balloon. Therefore, in order to define the purpose and nature of the program, the Paravulcoon System concept is briefly described, program objectives are outlined, and the plan to attain these objectives discussed. The experimental program is presented in terms of the model system design, test facilities and procedures used, test plans followed, and results of the several tests and studies. Finally, conclusions are drawn.

SYSTEM CONCEPT AND DESCRIPTION

The Paravulcoon Recovery System utilizes an open-throat, low permiability balloon filled with air as a drag and flotation device to accomplish terminal deceleration and controlled touch-down of a given payload. Following aerial deployment and ram air inflation of the balloon, buoyancy for flotation is provided by heating the air in the envelope. By controlling the air's temperature, ascent, hover, or descent can be accomplished as desired.

The basic operational concept of the system as studied in this program is sketched in Figure 1. Operation of the system begins with the payload stabilized by a primary decelerator system to descend at a subsonic velocity. At a predetermined altitude the Paravulcoon deployment event is initiated

DESCENT ON PRIMARY DECELERATOR

DEPLOYMENT

INFLATION

INITIAL HEAT

STATIC FLOTATION

CONTROLLED LANDING
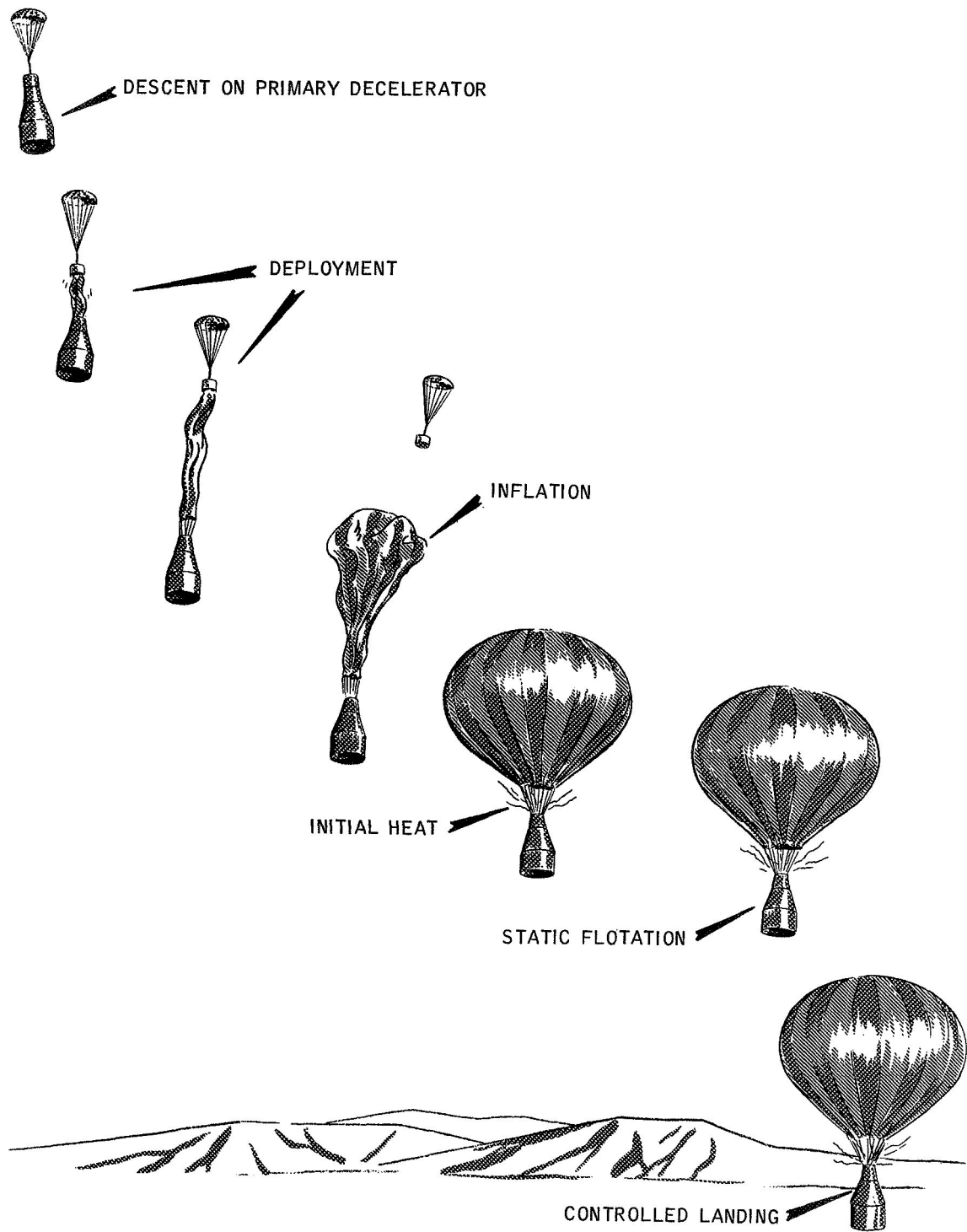
Figure 1. Over-All Paravulcoon System Sequence

as the balloon is extracted from its storage and streamed behind the payload body. As the system descends, the envelope is filled by ingesting air through its open throat. During this period, and when fully inflated by the ram air pressure, the balloon acts as a trailing aerodynamic drag body. Following inflation, the air in the envelope is heated through the open-throat by an initial heat generator. The resulting buoyancy of the hot air further decelerates the system until buoyant equilibrium is attained. By controlling the rate at which sustaining heat is added to replace steady-state heat losses, the payload may then be floated at a chosen altitude or lowered to the ground at a controlled rate. Float altitude is a function of balloon size and maximum air temperature, while float duration depends on the total fuel supply carried on board.

The total system to accomplish this sequence therefore consists of the balloon envelope, with its associated fittings and deployment mechanism, initial and sustaining heat generators with accompanying fuel tankage, and a control system which may include a radio link if needed.

PROGRAM OBJECTIVES

Consideration of the Paravulcoon System operational sequence suggests that the most critical phase with regard to concept feasibility is the aerial deployment and inflation of the balloon. To have a useful recovery system it must be practical to accomplish these events at reasonable velocities and dynamic pressures. Thus, it was felt by the National Aeronautics and Space Administration that the feasibility of the system concept should first be investigated before the other portions of the system are studied.

While it has been possible to analytically investigate the feasibility of some of the other sequence phases (Reference 1), deployment and inflation have been found to be the least amenable to such methods. Rather, these phases consist of a combination of aerodynamic, dynamic, and mechanical actions which are more readily analyzed by experimental observation. Furthermore, prior

practical experience with static hot gas balloons has provided some experimental information about envelope design for the buoyant condition, steady-state heat losses, and burner capabilities and design. However, the only experimental experience with aerial deployment and inflation prior to this program has been the two preliminary tests described in Reference 1 which used an 80-pound payload weight and a 25-foot diameter balloon.

Therefore, the primary objective of this program was to experimentally demonstrate the feasibility of aerially deploying and inflating a somewhat larger balloon with a more realistic payload at velocities up to 300 fps. Such tests, limited to deployment and inflation, could be accomplished using relatively simple drop vehicles. Alternatively, testing of the entire system sequence would require design, fabrication, and preliminary testing of heat generator and control systems for use in more complex and expensive test vehicles. Thus, this program's scope was strictly limited to demonstrating cold aerial deployment and inflation.

Since feasibility demonstration was the prime objective, it was not intended that optimized component or system designs would result from a program of this size and scope. However, it was anticipated that, in addition to feasibility and increased system understanding, there would be some fallout of performance characteristics and design data which might be applicable in designing larger systems.

PROGRAM PLAN

To meet the program objectives, the need for a primarily experimental investigation was indicated. Hence, a program plan was formulated which consisted of a relatively small number of cold drop flight tests preceded by a brief wind tunnel study.

Several attempts have been made to analytically describe the balloon inflation process. However, this process is a complex sequence of transient aero-mechanical motions, and thus does not lend itself to such an approach. Therefore, to better understand aerial deployment and inflation of larger Paravulcoon envelopes, and to provide a basis for design of the flight test equipment, a brief wind tunnel study program was conducted prior to start of the large scale flight tests. The Langley Spin Tunnel and the Langley Full-Scale Tunnel were made available for this investigation. Primary objective of the investigation was to study and observe deployment, inflation, and dynamic stability of the Paravulcoon envelope; the second objective was to measure the drag forces associated with the fully inflated balloon. A free flight drop test from a helicopter of one of the wind tunnel models was also included as part of this study.

As a result of phenomena observed in the basic wind tunnel study, a stability study consisting of an analytical investigation, a static drop of a large 40-foot diameter balloon, and a modification of a wind tunnel model, was undertaken before proceding on to the full-scale flight test program.

The large-scale cold drop flight tests were the principal means for attaining the program objectives. In order to observe some of the factors associated with increasing balloon size while avoiding handling of excessively heavy test equipment, a simulated payload weight of 1000 pounds was specified for these tests. This defined a test balloon envelope in the 50- to 60-foot diameter size range (actual flight test models were 54 feet in diameter). Since part of the study was aimed at proving deployment feasibility at increasing velocities, it was planned to conduct one drop test with a nominal deployment event velocity of 100 fps, two at 200 fps, and two at 300 fps. Total system studies suggest that Paravulcoon system activation at the latter value would be desirable from the standpoint of over-all system practicality. However, due to test results and damage to test equipment, the actual program was completed after two drops at an event velocity of 100 fps and two drops at 200 fps.

SECTION III
TEST MODELS AND SYSTEMS

For both the wind tunnel study and the full-scale free flight phases of this
program it was necessary to design and fabricate model Paravulcoon systems.
These models were intended to simulate a typical balloon-payload configuration
and so permit the study of the performance characteristics of a cold system.
The stability study required use of a special large balloon and a modification
of one of the wind tunnel models.

WIND TUNNEL MODEL

As indicated in Section II, the wind tunnel studies were intended to simulate
as realistically as possible the deployment, inflation, and terminal descent of
the larger full-scale systems which were test dropped later in the program.
Thus, considerations of similitude and scaling, as well as the requirements of
the Langley spin tunnel in which the major portion of the study was conducted,
governed design of the wind tunnel models. These models consisted of a
balloon envelope, a development bag and a forebody. When needed, drogue
parachutes were provided by the wind tunnel facility.

Since it was obviously not possible to dynamically scale the model balloons,
it was desirable to make them as large as possible. On the other hand, Langley
Research Center personnel estimated that need for freedom of movement, to-
gether with tunnel blockage limitations, would not permit use of larger than six-
foot diameter balloons in the spin tunnel. Although larger models could have
been accommodated in the full-scale tunnel, test convenience and economy pre-
cluded the use of larger models. Thus, it was decided to build only six-foot
diameter model envelopes for this study. This size gave a nominal geometric

scale factor of 1:10 with the full-scale envelopes for the 1000-pound flight tests (actual design resulted in a 54-foot diameter envelope and a scale of 1:9).

Examination of the system during the Paravulcoon activation sequence shows it consists of a rigid and relatively heavy body (the forebody) which separates from a flexible and relatively light body (the balloon) during deployment. Following streaming and during inflation, the flexible balloon material is subjected to transient dynamic and aerodynamic loads. Finally, the combined system descends terminally in a quasi-rigid configuration. Thus, several categories of scaling, not necessarily compatible, apply to the problem. These include geometric and weight scaling, aerodynamic flow scaling, aero-mechanical or aeroelastic scaling, inflation mass scaling, and the geometric and weight relationships between the system components.

It is apparent that geometric scaling could be readily accomplished with regard to the gross system and to the intercomponent geometry. One exception here was in the deployment mechanism indicated below.

Dynamic similitude relationships have been developed in Reference 2 for models of rigid, relatively homogeneous and dense bodies, such as aircraft. The following two apply to the present problem and have been proven by experience in the Langley Spin Tunnel:

$$\frac{W_m}{W_p} = \left(\frac{\ell_m}{\ell_p}\right)^3 \frac{\rho_m}{\rho_p} \tag{1}$$

$$\frac{V_m}{V_p} = \left(\frac{\ell_m}{\ell_p}\right)^{1/2} \left(\frac{\rho_m}{\rho_p}\right)^{1/2} \tag{2}$$

where

W = weight

V = descent velocity

ℓ = a linear dimension

ρ = air density

m = refers to wind tunnel model

p = refers to full-scale prototype

Although the derivation of these relationships is based on a rigid body, they have proven valid for relating the steady-state performance of parachutes. Thus, they also should be valid for use with the Paravulcoon models in their fully inflated terminal descent regime, provided they behave as a rigid, single-body system. Actually, if there are motions of the balloon relative to itself or to the payload, conclusions based on these relationships are subject to question.

The wind tunnel models were scaled for gross weight to simulate the terminal descent regime at various altitudes by varying the total weight of the model systems. For example, if they were assumed to be 1:10 scale models of a 1000-pound system, 1 1/2-pound and 6-pound models would represent the performance of the full-scale system at altitudes of approximately 15,000 feet and 50,000 feet, respectively. This was pure altitude-weight similitude with no allowance for the dissimilarity in flow regimes discussed in the following paragraph.

Since the same aerodynamic fluid was used in both the wind tunnel and full-scale tests, it was not possible to provide aerodynamic flow similarity by having equal Reynolds numbers in both cases. In fact, the six-foot diameter envelopes and the low terminal descent velocities encountered resulted in fully inflated operation in the spin tunnel in the transition regime of laminar to turbulent flow-for-flow about spherical objects (the larger balloons operate in fully turbulent flow). This caused considerable trouble and will be discussed in detail under "Results". As the drag coefficient varies strongly with Reynolds number in the transition regime, using drag data obtained from the wind tunnel models to predict larger system performances is of dubious validity.

Consideration of the other scaling factors indicated that the balloon envelope should be extremely light, thin and flexible compared to the full-scale envelope, or conversely, that the tunnel fluid should be denser than air. Unfortunately, such a material was not available and the model envelope could not be properly scaled in relation to the transient aerodynamic forces or to its own mechanical and dynamic motions during deployment and inflation. Also, proper weight distribution between the envelope and the forebody could not be achieved. Thus, while the terminal descent phase could be quantitatively simulated for various altitudes, the wind tunnel models could only quantitatively define the deployment and inflation performance of a six-foot diameter system. Any extrapolation of these latter results to larger systems must be of a strictly qualitiative nature.

A total of four envelopes were fabricated to the basic design shown in Figure 2 in the variations listed in Table 1.

Table 1. Wind Tunnel Model Envelope Configurations

Model Number	Material Type	Throat Diameter / Envelope Max Diameter
125	1.1 oz/yd^2 nylon	0.25
820	0.8 oz/yd^2 nylon	0.20
825	0.8 oz/yd^2 nylon	0.25
830	0.8 oz/yd^2 nylon	0.30
840*	0.8 oz/yd^2 nylon	0.40

*840 was recut from 820 during the test program.

10 IN. DIAMETER
END CAP

72.00 IN.

ENVELOPE
MATERIAL: ACRYLIC
COATED NYLON
NUMBER OF GORES: 12

TYPICAL LOAD CATENARY

LOAD LINES

18.00 IN. NOM.
THROAT DIAMETER
(25% THROAT)

ENVELOPE DIMENSIONS
DIAMETER = 6 FEET
CONE ANGLE = 96°
INFLATED VOLUME = 105.3 FEET^3
SURFACE AREA = 108.1 FEET^2
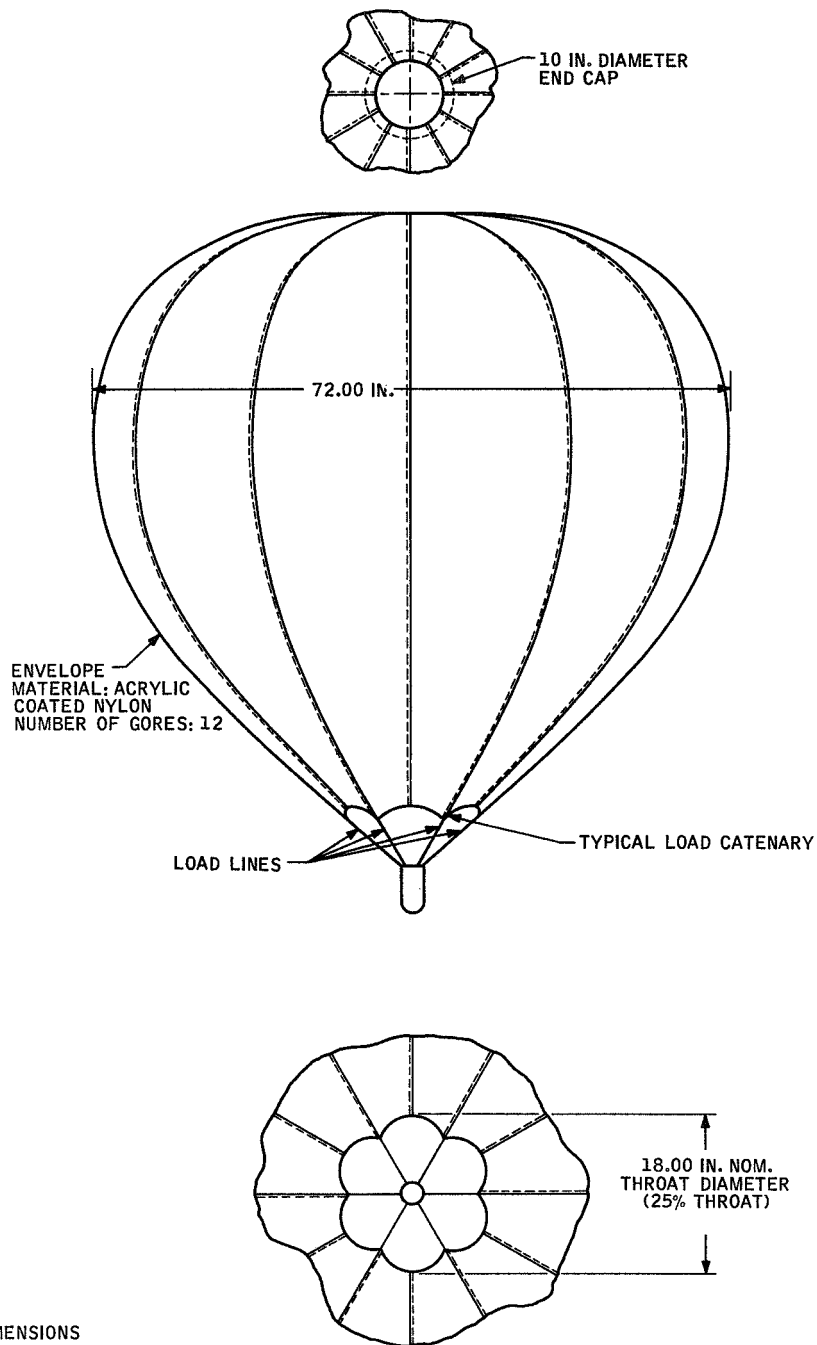
Figure 2.   Wind Tunnel Model Balloon Envelope

The shape shown is a theoretical "natural shape" for buoyancy, and except for the number of gores and load lines (12 versus 20), is the same shape as the envelopes used in the full-scale flight tests. All models were fabricated from nylon cloth coated with acrylic to reduce the envelope's permiability. Since these model envelopes had a relatively small number of gores, particular care was taken in their assembly to ensure that a circular and symmetrical shape was obtained. The 1.1 oz/yd^2 nylon is the same material used for the flight test envelopes; thus scalewise is too heavy and too rigid. As the 0.8 oz/yd^2 nylon was the lightest suitable material which could be obtained in time for these tests, it was used for the geometric variations. Unfortunately, it was also too heavy and stiff. These envelopes were used in conjunction with the two forebodies described below and with several load line configurations to allow the parametric variation of the throat-load line-forebody geometry. Appendix A details these variations. To observe the effect of a positively-opened throat, a rigid wire ring was inserted in the envelope throat for a few tests.

The model forebodies were made in the same configuration as the test vehicle used in the flight tests. However, since the flight test vehicle was only 30 inches in diameter, the geometrically-scaled 1:10 size forebody was only three inches in diameter. Due to the model envelope fabric's bulk, this was too small a body to contain and from which to deploy a model envelope. Therefore, two forebody models were made; a six-inch diameter forebody (the deployment forebody) for observation of envelope deployment; and a three-inch diameter forebody (the inflation forebody) for study of balloon inflation behind a geometrically-scaled forebody.

The deployment forebody along with an envelope packed in a nylon lined deployment bag, is sketched in Figure 3. This sketch also shows the deployment release mechanism consisting of three spring-tensioned retaining clips restrained by a rubber band. When the model system was in unrestrained "flight" suspended from a parachute in the wind tunnel, this band was severed by a smoldering time fuse element to initiate the deployment event.
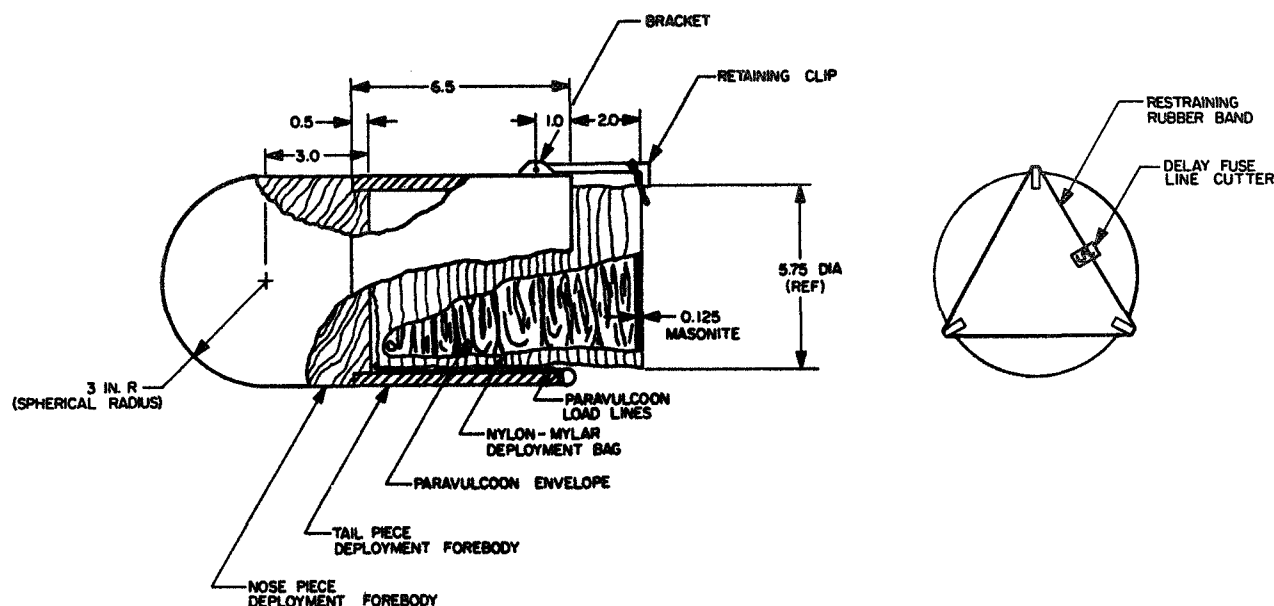
Figure 3. Model Deployment Forebody

Figure 4 shows the inflation forebody with an envelope packed in an externally-attached deployment bag. Using this arrangement a psuedo-deployment event could be obtained by securing the trailing deployment bag to the forebody by four restraining lines. At event, these lines were released by means of spring loaded clips held in place by a nylon cord. To initiate release with the model system on the wind tunnel mounting fixture and lifted by a parachute, the nylon cord was severed by an electric line cutter. The wooden nose of this forebody was drilled so that it could be mounted on the wind tunnel restraining fixture. Lead weights and shot were used in both forebodies to vary their weight for altitude simulation and the parametric study of inflation characteristics.

As shown in Figures 3 and 4, the deployment bag was a simple open-ended nylon tube with a nylon liner and a hardboard base. The crown of the envelope was slipped under a rubber band to secure it to this base during deployment until the envelope was streamed to its full length.
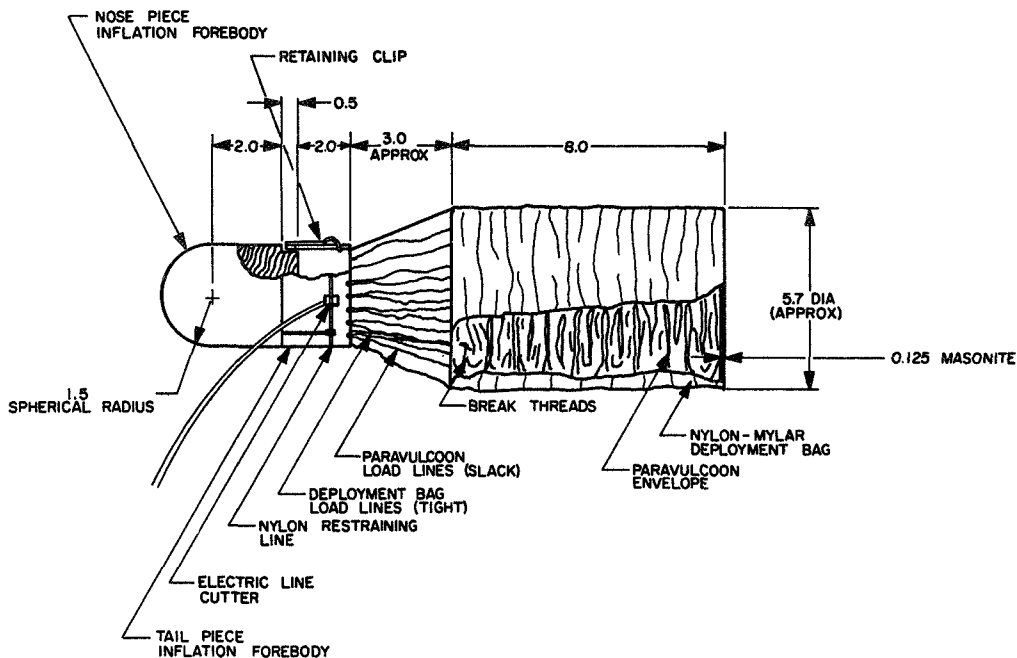
Figure 4. Model Inflation Forebody

Figure 5 shows the number 125 envelope fully inflated in the Vertical Wind Tunnel. The three-inch inflation forebody is attached.

BALLOON TERMINAL STABILITY STUDY

Following the basic wind tunnel tests, the number 125 model envelope was modified for use in the stability study by Langley Research Center personnel, as shown in Figure 6. This modification consisted of adding a three-inch wide fabric skirt or fence around the envelope, near its equator. The fence was supported by uniformly spaced fabric gusset pieces.

As part of the stability study, a 40-foot diameter hot gas balloon envelope from the stock of the contractor was used for a special free drop test. This was a
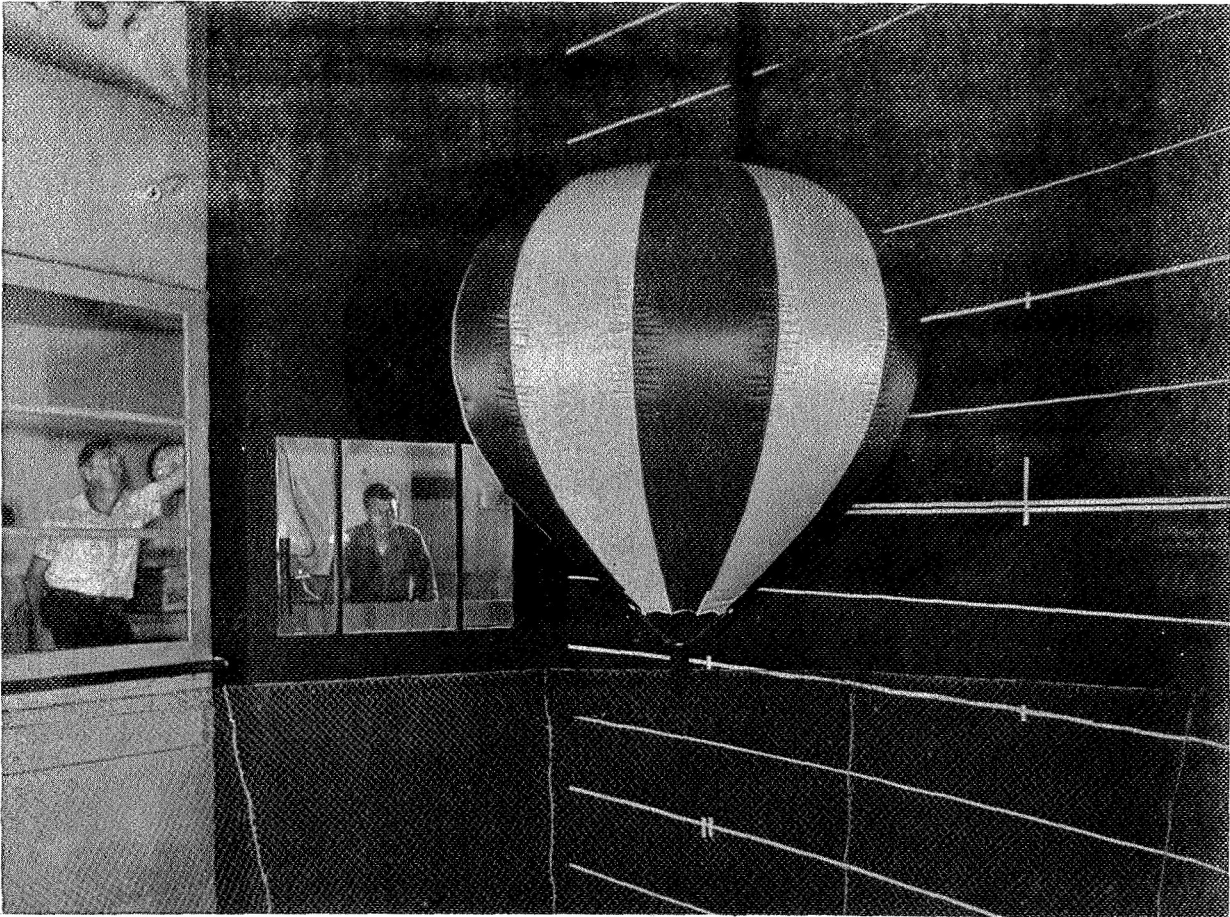
Figure 5. Inflated Model Paravulcoon in the 20-Foot Vertical
Free Spinning Wind Tunnel

natural shape envelope with 16 gores and a 30 percent throat opening made of
0.8 oz/yd^2 nylon laminated to 0.5 mil nylon (unit weight about 0.01 lb/ft^2).
Total balloon weight was 72 pounds. The payload used with this test was a
bag of 300 pounds of jettisonable steel shot. This ballast could be released
by the action of a pressure switch, battery, and line cutter.
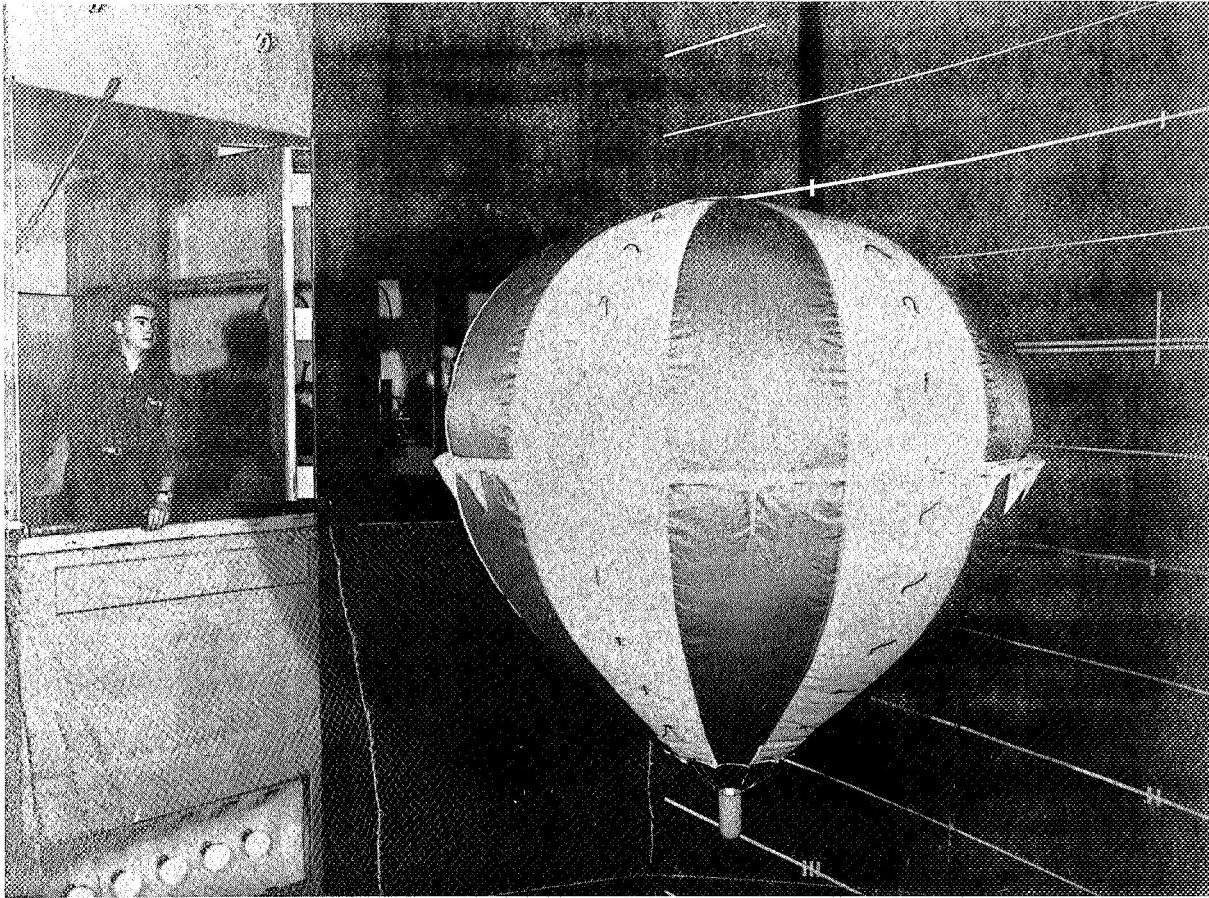
Figure 6. Model Balloon Modified with Fence

FULL SCALE SYSTEM

Since the full scale free flight tests were the principal means of accomplishing
the program objectives, design of the necessary test systems received con-
siderable attention. These systems consisted of the following: the actual balloon
envelope under test; a flight test vehicle to allow the system to be air dropped
and to simulate a payload; a deployment system to release, extract, and deploy
the balloon from the forebody; and the associated on-board instrumentation.

Balloon

System studies indicated that a Paravulcoon envelope capable of simulating the recovery of a 1,000-pound payload should be 54 feet in diameter. All envelopes used in this program were designed and fabricated in this size in the "natural" shape. This is an analytically determined shape in which, theoretically, the envelope material is not subjected to any circumferential stresses when the balloon is floating in the static buoyant mode. All stresses and loads are carried over meridional load paths only. Although this is the optimum shape for the buoyant flight mode, it may not necessarily be the optimum shape for the inflation or cold descent modes or for nonequilibrium modes.

The basic test balloon configuration designated X-54 is shown in Figure 7. This design resulted from stress considerations based on the estimated deployment and inflation environment, and static and dynamic tests of several of the design features. These tests included testing webbing-to-envelope attachment methods and configurations for the throat region, plus gore seam evaluation tests. As a result, the load line attachment straps of one-inch nylon webbing were used and were terminated in the multifingered "crow's foot" arrangement shown in Figure 7. The tests also provided a rational basis for seam construction specifications.

This design consisted of 20 gores of acrylic coated 1.1 oz/yd^2 rip stop nylon with 20 load lines of nylon-covered 1/8-inch steel aircraft cable. Due to the width of the available material, the gores were formed of 40 half gores and assembled with 20 straight seams and 20 curved seams with the load lines connected to 20 load catenaries. The 16.2-foot diameter, 30 percent throat opening was selected as a result of experience in the wind tunnel model study. Since it was originally expected that deployment would impose somewhat severe loads on the crown of the balloon, this region was reinforced with an 8-foot, 7 1/2-inch diameter end cap.

The basic X-54 balloon characteristics are listed in Table 2.
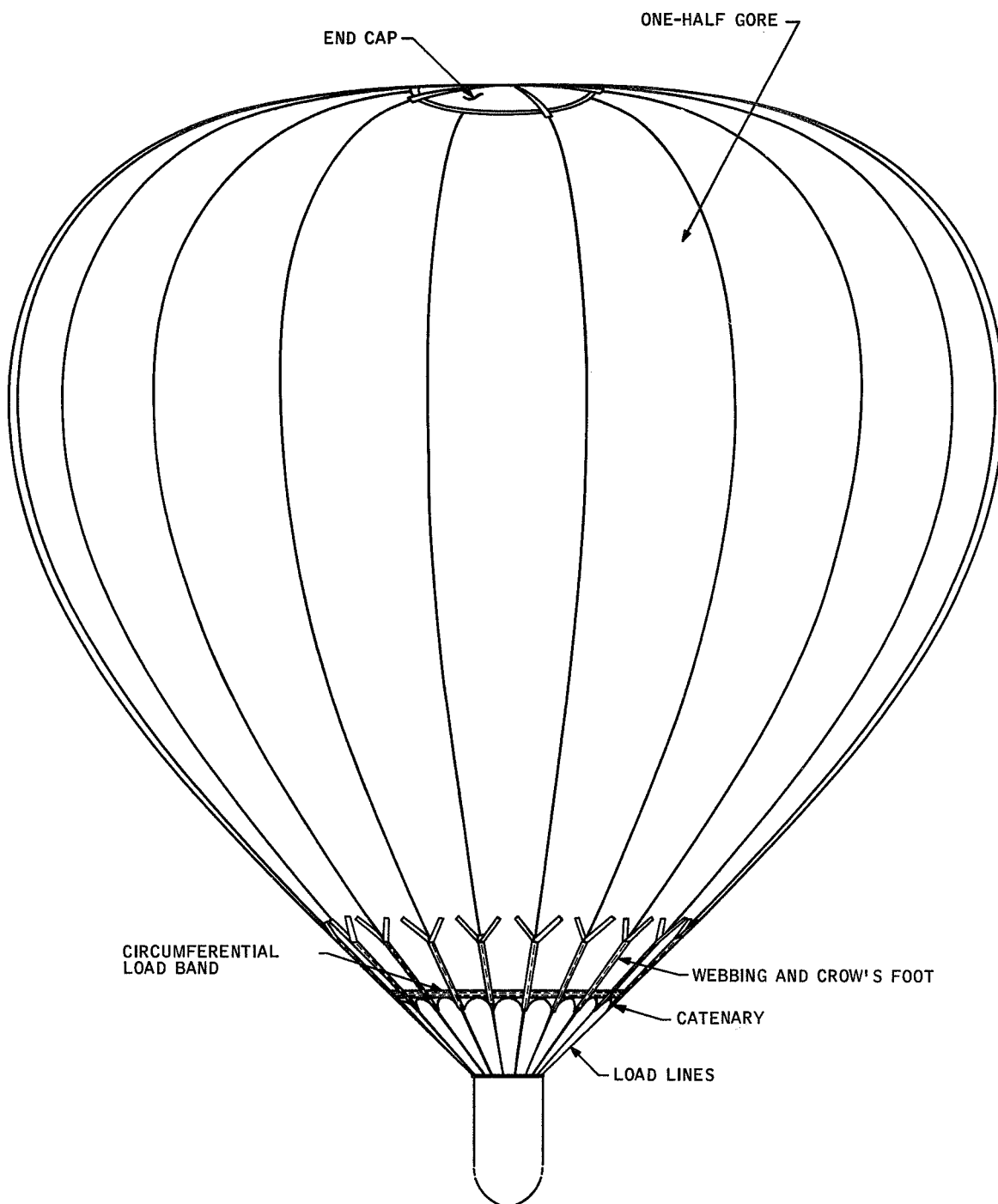
Figure 7. X-54 Balloon Configuration

Table 2. X-54 Paravulcoon Characteristics

Diameter	54 feet
Volume	76,842 feet^3
Surface Area	8,754 feet^2
Inflated Height	56.1 feet
Gore Length	85.1 feet
Number of Gores	20
Weight (approximate)	110 pounds
Packed Volume (approximate)	6.0 feet^2

After one flight test it was found that stress concentrations in the crown area made redesign of this portion of the envelope necessary. Since all of the envelope loads are brought to a theoretical confluence at the envelope apex, the structure must be reinforced in this area without creating load path discontinuities. In this vein, the redesigned envelope, X-54-1, incorporated a method of construction designated as Simulated Variable Thickness (SVT). This arrangement made it possible to better carry the meridional load on each gore across the envelope top to its diametrically opposite gore without abrupt changes in fabric thickness. This is achieved as sketched in Figure 8 by shaping each gore with a minimum constant width at its upper end, overlapping the excess material progressively, thus creating the equivalent of a gradual buildup of fabric thickness toward the apex of the envelope. Simple static tests of this configuration were performed in support of the envelope design revision.

The several envelope configurations fabricated for the program are listed in Table 3.
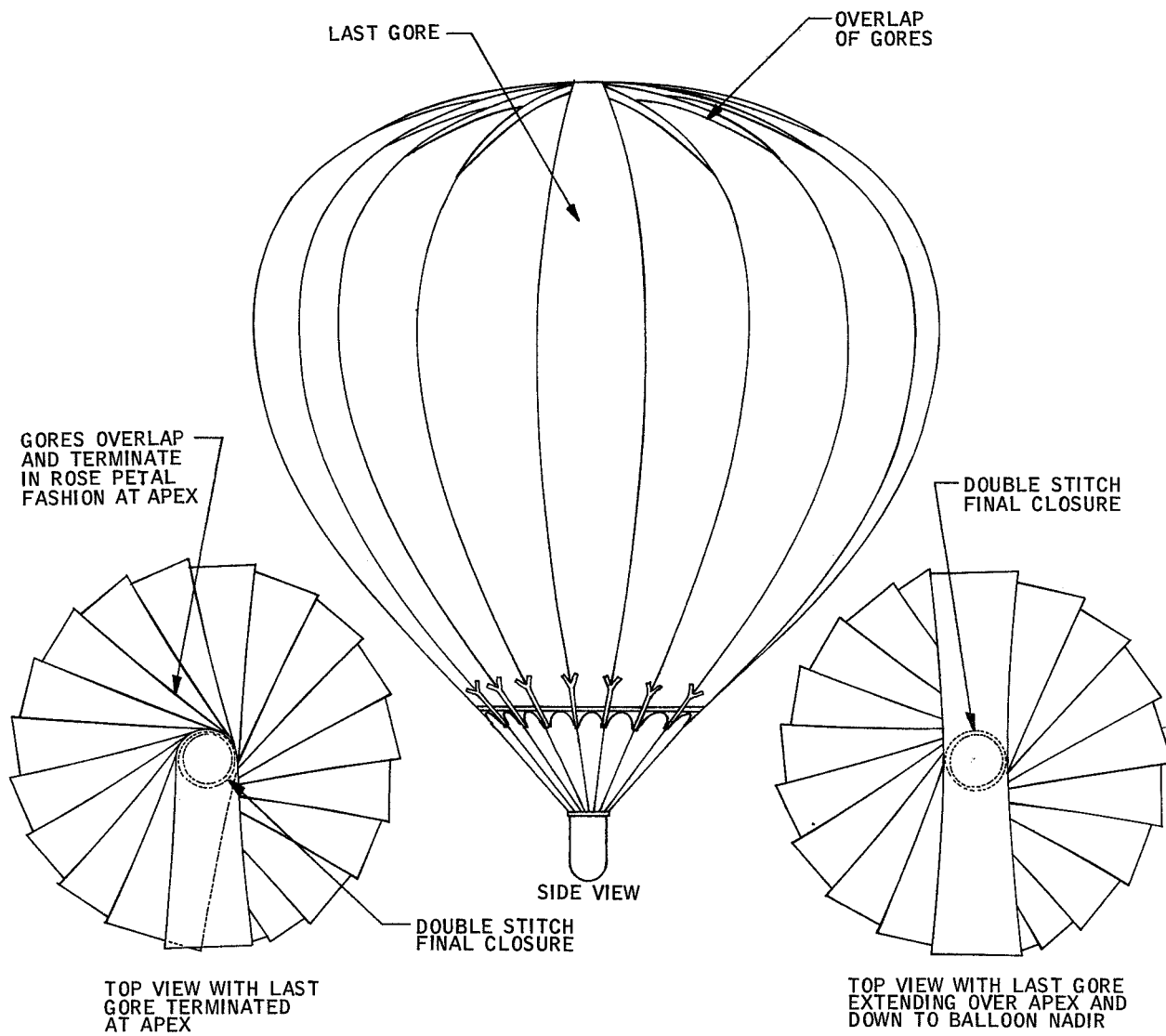
Figure 8. Simulated Variable Thickness Balloon Configuration

Table 3. Envelope Configurations

Envelope Number	Envelope Design Designation	Remarks
101	X-54	Original Design
102	X-54	Original Design
103	X-54-1	SVT Top
101	X-54 (modified)	SVT Top Spliced onto Original Design
103	X-54-1(modified)	Damage to Envelope Repaired

The modified designs were obtained by splicing the gores in a seven-foot long zig-zag pattern around the balloon circumference. This was done on envelope number 101 to change the original X-54 design to an SVT top. In this case, continuous gores were carried over the apex from the splice line just above the balloon equator. This was also done on the modified number 103 envelope. A similar splice was used in the lower part of eight half-gores of this envelope to repair test-incurred damage.

Test Vehicle

The flight vehicle for these tests filled a dual purpose: 1) it simulated a descending 1000-pound space payload for recovery and 2) it made possible the necessary test mechanics to accomplish the basic program objectives. Since no particular payload geometry was specified, the vehicle design was governed solely by the latter requirements. The mechanics of the test sequence will be described in the following section. However, in this role, the vehicle accomplished these things:

- Allowed the system to be dropped from the test aircraft

- Permitted a stable descent of the drogue parachute

- Provided a container for the packed balloon in the deployment bag prior to the deployment event

- Allowed simulation of the deployment event

- Allowed the attachment of the balloon load lines to the simulated payload in a realistic geometry

- Carried the necessary test controls and on-board instrumentation.

Furthermore, since the cold Paravulcoon could only decelerate rather than hover the payload, it was necessary for the vehicle to survive the predicted ground impact so that the equipment could be used for subsequent tests.

The requirements of system stability and nonrotation during the drogue-stabilized drop prior to the deployment event dictated an aerodynamically clean and, if possible, statically stable body. The need to absorb both the parachute and Paravulcoon opening and suspension loads around the aft end of the balloon compartment dictated a structurally rigid body, rather than a heavy nose attached to a lightweight balloon storage container. The planned deployment mechanism dictated a smooth and unobstructed balloon compartment and rear opening. Also, for these initial tests, it was felt it would be undesirable to try to extract and deploy an envelope of this size from an opening smaller than 28 to 30 inches in diameter until more experience had been gained with the deployment mechanics. (It should be noted here that on the basis of subsequent test experience, such a large opening probably is not necessary.)

Since hemispherical steel tank heads are readily available from commercial sources, the vehicles were designed in the hemisphere-cylinder shape shown in Figure 9. A steel hemisphere, approximately 30 inches in diameter, was welded to a 45-inch long, 1/4-inch thick steel cylinder, to form a 60- by
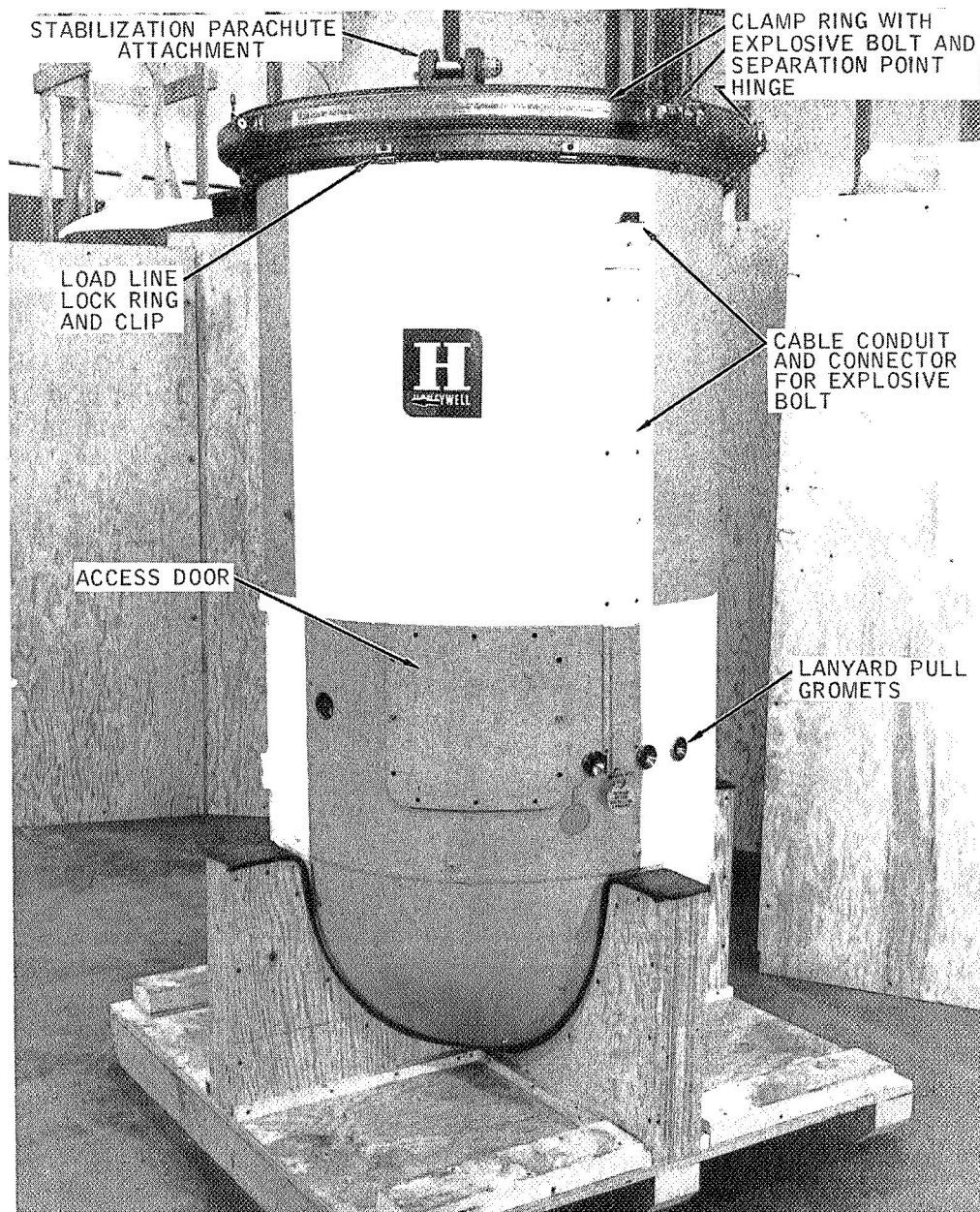
Figure 9. Flight Test Vehicle

30-inch vehicle. The steel cylinder, together with an aft load ring, provided both the necessary structure and balloon stowage compartment without need for additional structural members. Lead ballast in the nose was used to attain the desired vehicle weight, and a removable deck, cushioned by plastic foam against ground impact, was provided to mount the controls and instrumentation. These could be reached through an access door. An aluminum bulkhead was provided to support the balloon in the deployment bag during the parachute opening period.

Since this vehicle was marginally stable, the use of stabilizing fins was investigated. However, it was decided that if these fins should become slightly misaligned during handling or launch, the resultant vehicle rotation would be more detrimental to a successful balloon deployment than would the questionable vehicle stability. Also, simple spin tunnel tests indicated that the total system would be stable with the drogue parachute sizes planned for the tests.

Analysis and previous experience indicated that the test envelope would rupture at the ground impact velocities predicted for the system. When the vehicle reaches the ground, the envelope settles down over the throat of the envelope, thus blocking it off and preventing further exhausting of air. The inertia of the moving mass of air in the balloon then overpressures the envelope and ruptures it. To prevent this, several designs for jettisoning the vehicle ballast prior to impact were investigated. Due to the weight of the various other components, it was not possible to attain impact slow enough to ensure that the envelope would not rupture. Therefore, the jettisoning of weight was discarded as an unjustified system complication and expense.

Deployment System

Prior to deployment, the test envelope was stowed in its deployment bag in the after section of the flight test vehicle. The deployment sequence was as is sketched in Figure 10. At the deployment event the deployment bag with the

APEX BREAK LINE

ENVELOPE REEFING LINE

VEHICLE LID

DEPLOYMENT BAG (ATTACHED TO LID)

PARAVULCOON LOAD LINES

REEFED & STREAMERED ENVELOPE FULLY DEPLOYED

DEPLOYMENT BAG OPENED & REEFED ENVELOPE PARTIALLY DEPLOYED

DEPLOYMENT BAG CONTAINING PACKED ENVELOPE IS EXTRACTED FROM TEST VEHICLE AS LID AND VEHICLE SEPARATE

LID RESTRAINING CLAMP RELEASED

TEST EVENT BEGINS WHEN VEHICLE LID IS RELEASED

DROGUE PARACHUTE (SELECTED TO YIELD THE DESIRED TEST VELOCITY)

TEST VEHICLE

TEST VEHICLE & DROGUE CHUTE DESCENDING AT A STABLE VELOCITY.

Figure 10.   Envelope Deployment Sequence

envelope was released from its stowage and extracted from the vehicle. The envelope was then streamed from the bag to its full length behind the vehicle, ready to begin inflation. Thus, the principal components of the deployment system are the release mechanism, the deployment bag, and the associated controls.

Release Mechanism -- As indicated in Figure 10, the test deployment event occurred with the test vehicle descending vertically on the drogue parachute at the desired event velocity. At event, it was necessary to transfer the parachute suspension load from the test vehicle to the deployment bag in order to extract the deployment bag. Ideally, this release must be reliable and not impart jerks to the suspension lines or tumbling moments to the test vehicle.

Use of standard parachute load line release devices was first considered. However this was discarded as the multipoint parachute bridle attachment required for stability necessitated a multipoint release system. This would have created problems with reliability, simultaneous load release, and smooth transference of the parachute load from the vehicle structure to the deployment bag.

Instead, the solid rear-closure plate and clamp band arrangement shown in Figures 9 and 11 were selected. In this scheme, the deployment bag was bolted to the closure plate, and three brackets were provided on the closure plate to attach the drogue parachute bridle. The plate was clamped to the vehicle with a pair of semicircular clamp bands. These bands fitted over the beveled edge of the closure plate and the corresponding edge of the aft structural ring of the vehicle, as shown in Figure 12. The bands were held in the clamped position by two explosive bolts. In this design, the radial and side loads caused by parachute opening shock were carried by the closure plate through the clamp bands and mating surfaces to the vehicle structure. In turn, when the clamp bands were released by firing the explosive bolts, the parachute bridle directly attached to the deployment bag made it possible for the vehicle to drop away and thus extract the deployment bag and deploy the balloon.
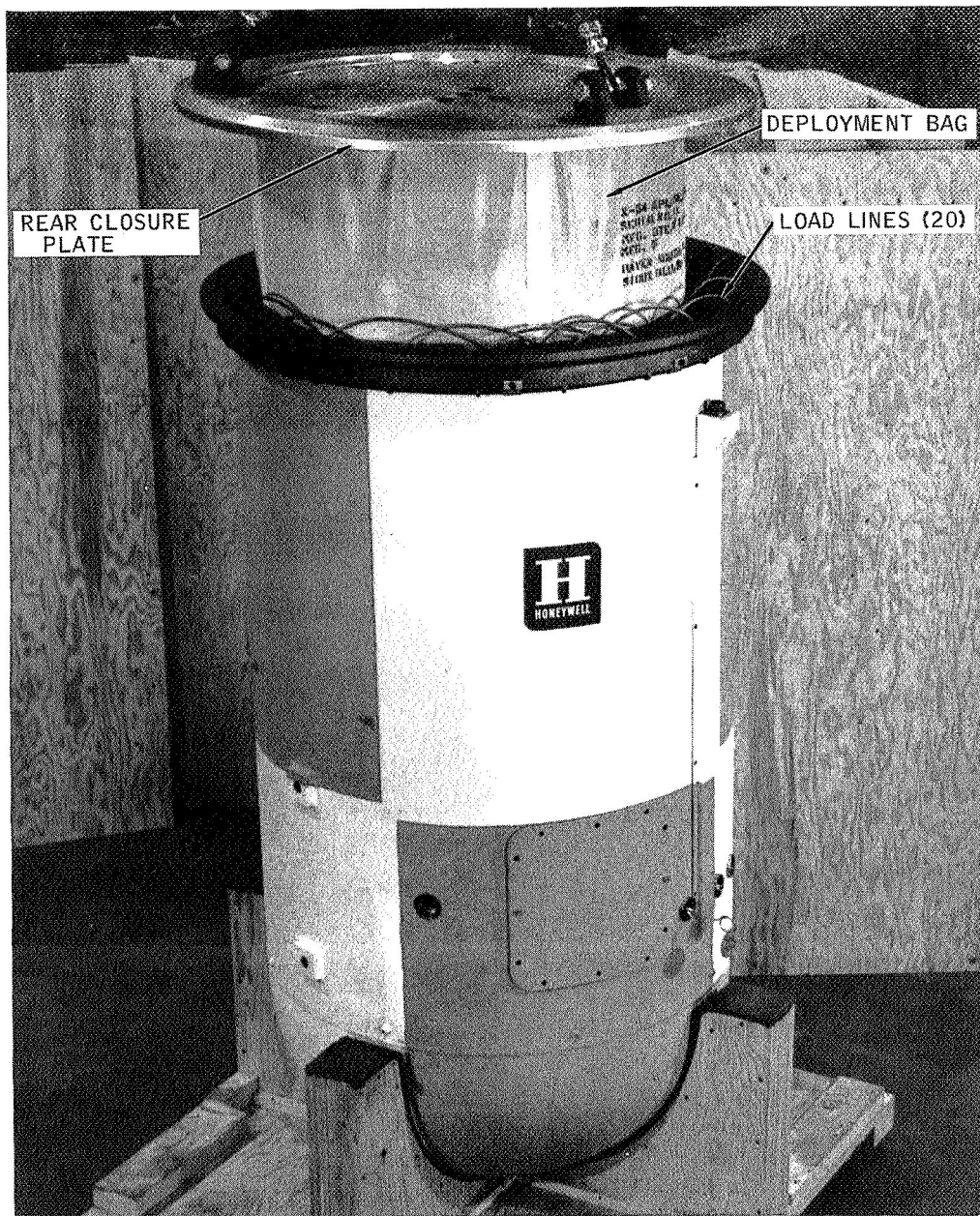
Figure 11. Paravulcoon Extraction Sequence (deployment bag partially extracted)
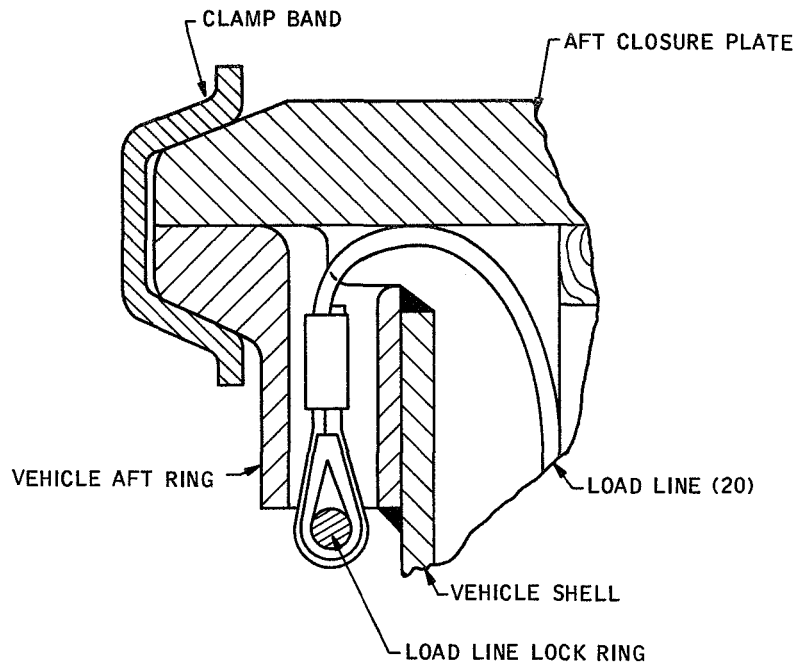
Figure 12. Flight Test Vehicle - Aft Closure Detail

The vehicle ends of the balloon load lines were secured to the aft ring as illustrated in Figure 12. The thimble of each line was passed through an individual hole in the aft ring and held in place by a semicircular lock ring clamped to the underside of the aft ring. This lock ring can also be seen in Figure 9. In the stowed position each load line was passed over the end of the vehicle shell under the rear closure plate and thence down between the shell and the deployment bag as shown in Figure 11. This design provided a simple disconnect between the vehicle and the load lines while at the same time it allowed the load lines to deploy with the deployment bag without fouling the bag. Smoothed edges on the holes permitted the load lines to swing out to the 42-degree angle necessary when the balloon was fully inflated.

The structural design of all aft closure and release components was based on the maximum predicted opening loads of the largest parachute to be used, plus a substantial load factor. Balloon attachment points were based on the maximum planned deployment event velocity. However, these parts were also made as

light as possible to keep the vehicle center of gravity near the nose. Static tests of the rear closure release showed that with either one or both of the explosive bolts firing, it did not appear possible for the rear closure to fail to separate. Fastex motion pictures indicated that the separation was clean, positive, and uniform. With only one bolt firing the closure plate appeared to tilt slightly on separation.

Deployment Bag -- In the planned deployment sequence the deployment bag contained the folded envelope and load lines during the pre-event stowage and during extraction from the vehicle. Following extraction the bottom of the deployment bag opened and permitted the envelope to smoothly stream out to its full length as the vehicle and deployment bag separated. Analysis of the mechanics of this sequence indicated that the bag closure must sustain a momentary load of eight g's as the bag is extracted from its stowage in the vehicle. Then, a brief time later, when the bag and the vehicle have separated about six feet, the bag closure must open so that the envelope can stream out without hindrance.

Since this sequence is so crucial to deployment success, considerable attention was given to the deployment bag design. The final design was the result of a number of static and dynamic tests on several possible schemes. This design consisted of an aluminum plate and clamp ring arrangement for attaching a 2. 2-oz/yd^2 nylon fabric bag reinforced by 1 1/2-inch nylon webbing, to the under side of the vehicle rear closure plate. The bag was actually an overlength tapered cylinder whose excess length formed the bottom of the bag when it was closed. A Teflon-coated glass fabric liner was also included in the bag to minimize friction during deployment. As shown in Figure 13, the bag was closed at the bottom by a four-piece aluminum break-away spool which was secured by a nylon closure strap. The strap was fastened by a cone and grommet arrangement locked by a pull pin of aircraft cable. As illustrated in Figure 13, the pull pin cable was swaged to one of the load lines so that as the load lines straightened out, the pin was pulled and the envelope released after the vehicle and its rear closure plate had separated about six feet. Since the bag was
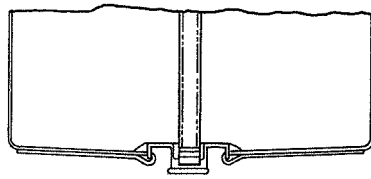
SIDE VIEW

BOTTOM VIEW

CLOSED

BREAK AWAY
SPOOL

CONE

GROMMET

NYLON CLOSURE
STRAP

PULL PIN

SWAGING

LOAD LINE

RELEASE DETAIL

1 1/2 IN. WEBBING
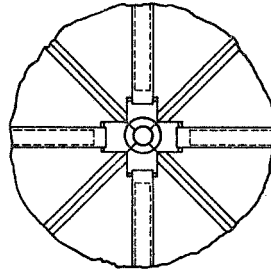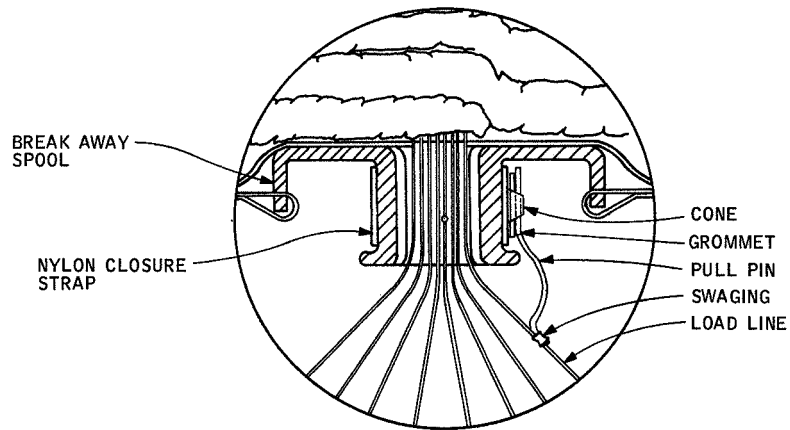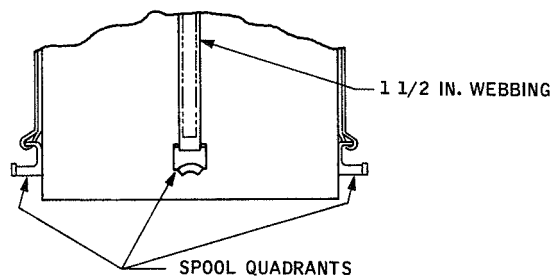
SPOOL QUADRANTS

OPEN

Figure 13. Deployment Bag Closure Design

designed overlong, the break-away spool quandrants ended up on the outside
of the bag after opening as detailed in Figure 13. This provided a completely
smooth passage for the streaming envelope.

To prevent premature release of the envelope crown from the bag before the
envelope was fully streamed, a 100-pound test break cord was attached
between the balloon crown and a fitting at the top of the deployment bag. A
backup scheme incorporating a 10-second delay, pyrotechnic reefing line
cutter (Figure 14) was also provided to ensure that the break cord was positively
severed. For one test, the throat of the envelope was temporarily reefed to
prevent ingestion of air until the balloon was fully streamed. This was jury
rigged as shown in Figure 15. A single 500-test nylon line was tied around the
base of the envelope just above the load catenary.. Two, 2-second delay,
pyrotechnic reefing line cutters initiated by the straightening of the load lines
were attached to sever this line. The action of either cutter was sufficient to
dis-reef the envelope.

Figure 16 shows the rear closure plate with the loaded deployment bag attached,
suspended above the vehicle in the position just prior to the release of the break-
away spool.

Controls -- The deployment event was initiated by the firing of the explosive
bolts by a present timer signal. The firing circuit consisted of safing switches;
manually set mechanical timers; batteries; a junction box; and the actual
explosive bolts. All components were redundantly wired in accepted explosive
practice to provide the maximum reliability of initiating the event while main-
taining system safety. Aircraft-type connectors were provided at all points
requiring field disconnects, including the connections to the explosive bolts,
as shown in Figures 9 and 11.

The spring-driven timers were started by the pulling of wire lanyards attached
to the vehicle launching skid. Stainless steel gromets were located in the
vehicle's outer shell to guarantee the pulling of these wires at all angles

ENVELOPE CROWN STRAP

100 POUND TEST
NYLON BREAK CORD

CUTTER
TRIP CORD

10 SEC DELAY
PYROTECHNIC
REEFING LINE
CUTTER
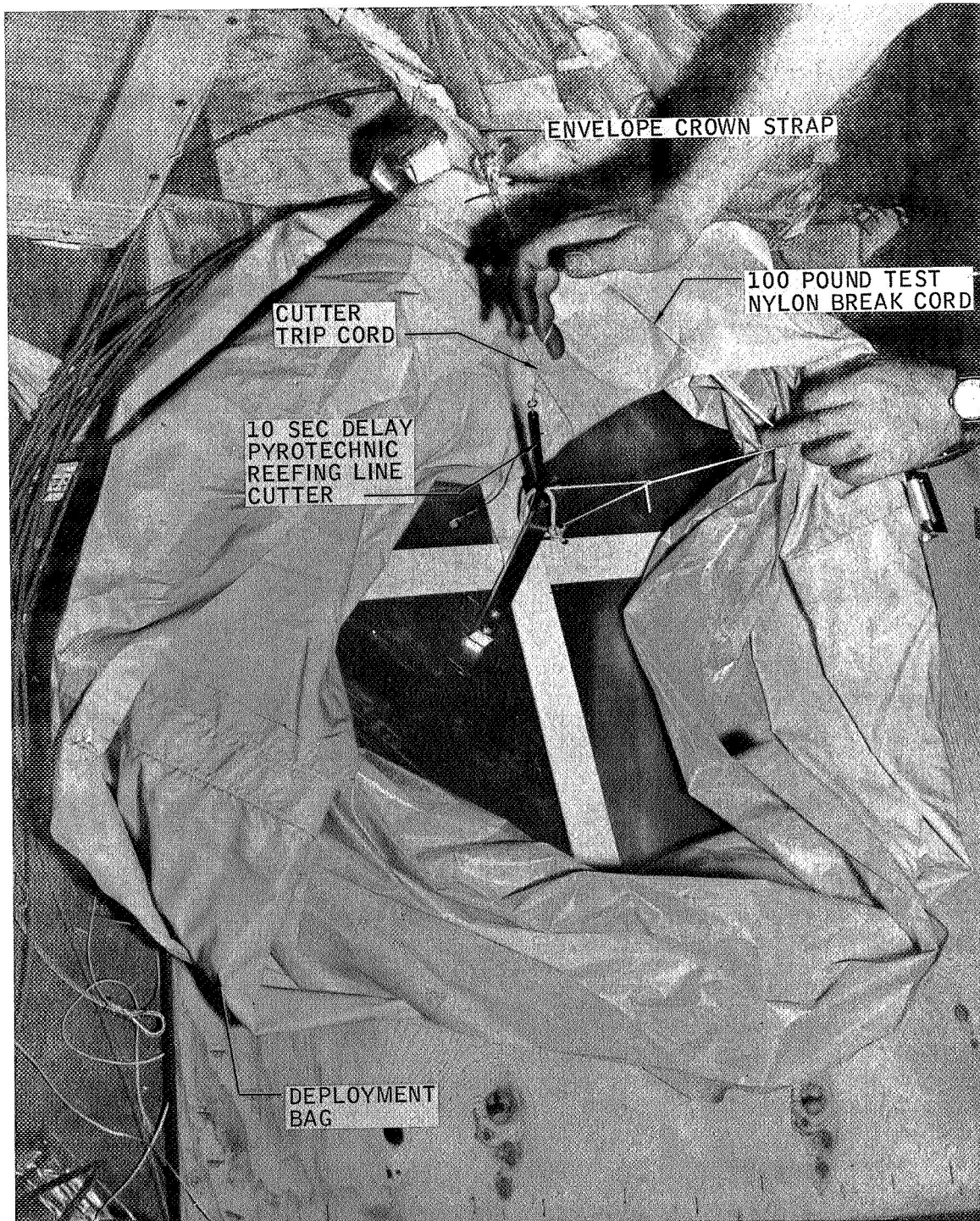
DEPLOYMENT
BAG

Official U.S. Navy Photograph

Figure 14. Deployment Bag Break Cord and Backup
Cutter Arrangement
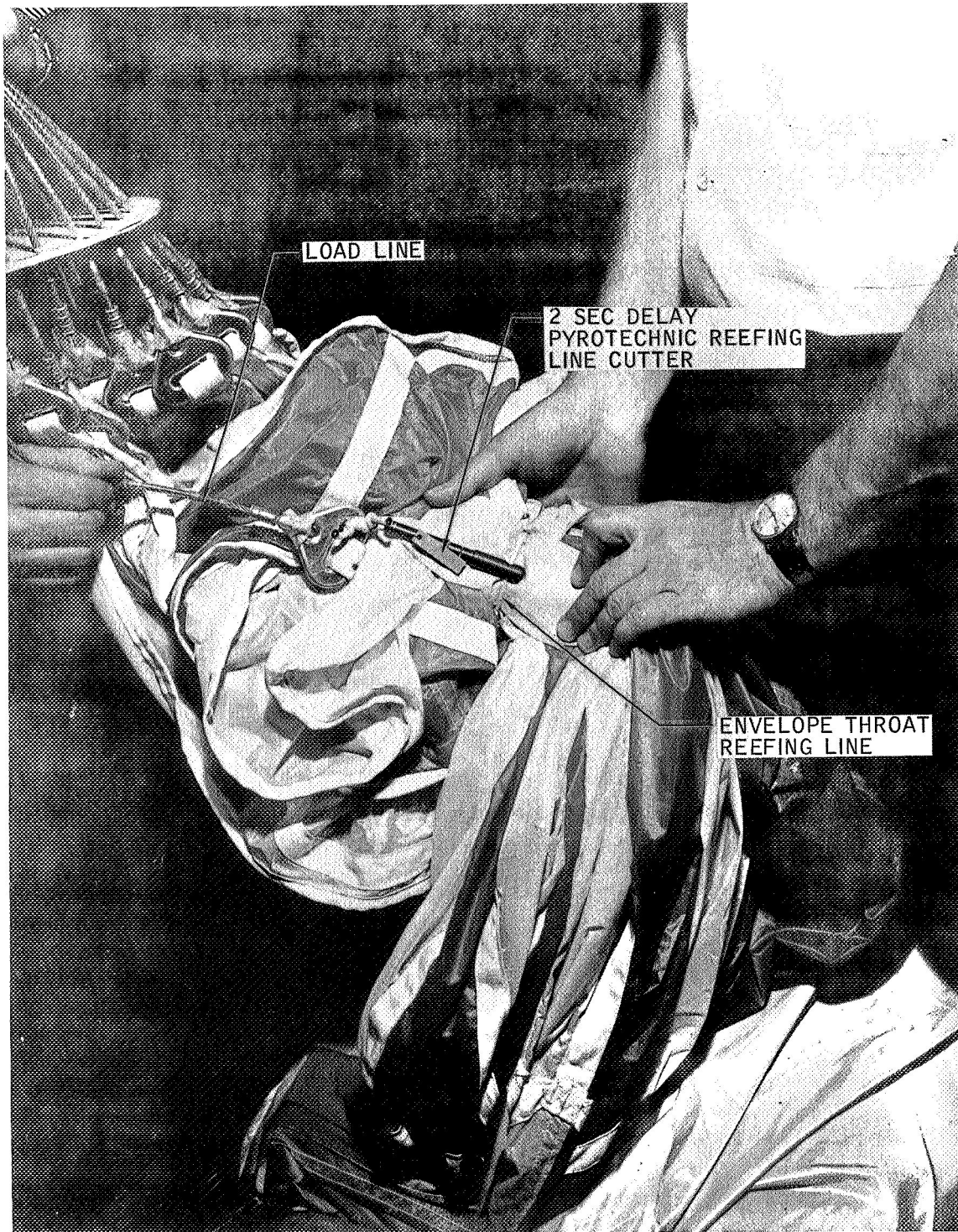
Official U.S. Navy Photograph

Figure 15. Manner of Temporarily Reefing Envelope Throat
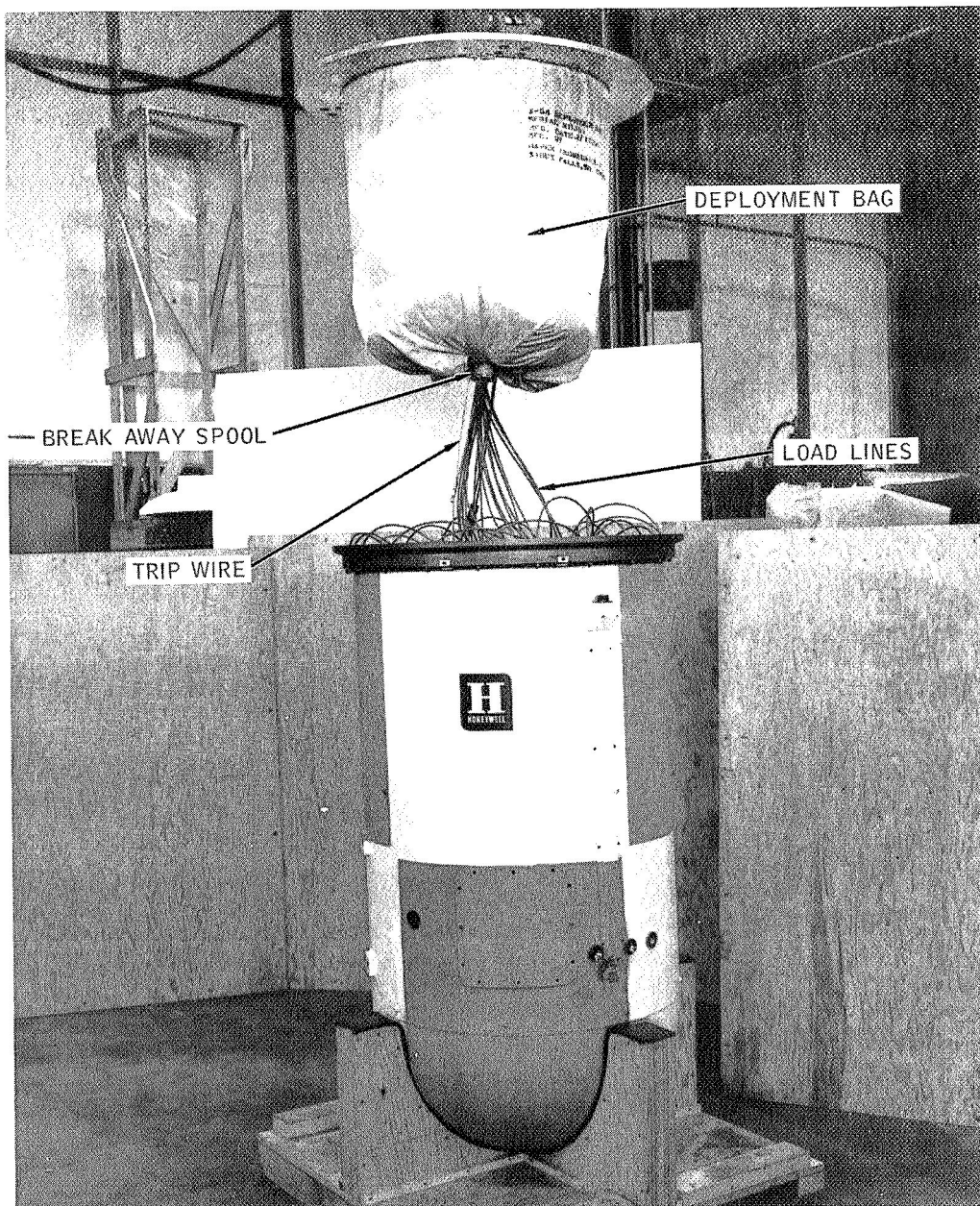
Figure 16. Paravulcoon Extraction Sequence (deployment bag just prior to release of breakaway spool)

between the vehicle and the skid. The functional reliability of the complete control system was bench and static tested prior to final vehicle assembly.

The various control system components are shown assembled on the vehicle instrument deck in Figure 17.

Instrumentation

Instrumentation carried on board the flight test vehicle was limited to telemetry and an "up camera".

All telemetry systems used for these tests were furnished, installed, and operated by the U. S. Air Force, 6511th Test Group (Parachute). Their purpose was to measure forces imparted to the test vehicle during deployment and inflation of the Paravulcoon. To accomplish this with minimum equipment, a 10-g Statham unbounded strain gage accelerometer was mounted on the vehicle after bulkhead to sense vehicle axial accelerations. After the first test the accelerometer was changed to a 25-g size, the mechanical mass of the mounting was increased, and a resiliant damper was added to the mount to reduce "ringing" of the accelerometer by extraneous cross-axis vibrations. A second channel was used to transmit an "event" signal. The time of event was sensed by a switch connected to the vehicle rear closure plate by a lanyard. All telemetry electronics were mounted on the vehicle instrument deck.

A gun sight aiming point (GSAP) camera used as an "up camera" on some of the flights was mounted on the vehicle aft bulkhead and aimed out the rear opening to photograph the actions of the balloon throat. It was started when the rear closure plate was separated by the switch that actuated the telemetry event signal. Camera lens settings were based on pretest ground experimentation.
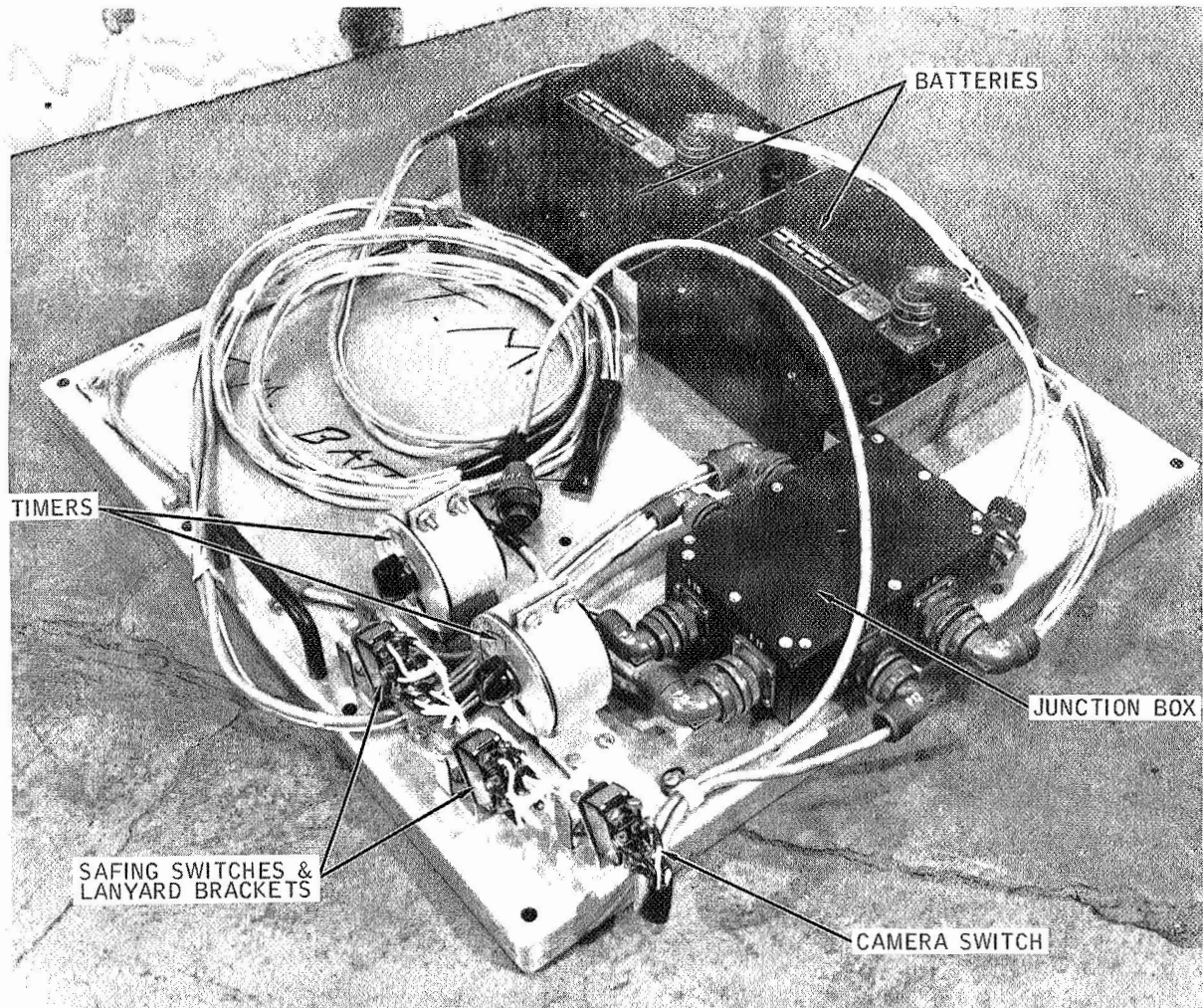
Figure 17. Flight Test Vehicle Instrument Deck

SECTION IV
TEST FACILITIES, EQUIPMENT, AND PROCEDURES

While some specialized static tests were conducted as part of the design of the
flight test equipment, all of the basic tests used to attain the program objectives
were made either under controlled wind tunnel conditions or as free drop
flight tests. In this section the test facilities and equipment are described and
the procedures and test modes utilized in accomplishing the tests outlined.
With exception of the 40-foot balloon drop conducted by the contractor, all tests
were conducted in government facilities by government personnel with con-
tractor personnel present.

WIND TUNNEL STUDY

Wind tunnel and free flight facilities and procedures were utilized for the wind
tunnel study program.

Wind Tunnels

The Langley Spin Tunnel and the Langley Full Scale Tunnel located at the
Langley Research Center were made available for this study. The spin tunnel
provides upward directed velocities from 10 to 90 fps. With this arrangement,
an unrestrained model of suitable weight and drag can be "floated" on the
upward airstream to simulate vertical free descent. The model is thus free
to accelerate and decelerate without restriction, thereby permitting observa-
tion of its dynamic characteristics. A mounting fixture was also available
for use in this tunnel which permitted vertical restraint of the model through
a strain gage link in its nose in more typical wind tunnel fashion. In this
infinite mass mode the model is not free to decelerate with respect to the

airstream as its drag increases. The full scale tunnel provides higher
velocities (up to 150 fps) and permits use of larger models, but with the
model restrained in the more conventional horizontal mode. Each of these
tunnels operates at sea level density at approximately atmospheric pressure.

Due to its greater convenience and readier availability, it was decided to
begin the study in the vertical tunnel. The full scale tunnel was to be used
only if its greater velocity or greater test section size should be found
necessary.

Tests in the spin tunnel were made in either the restrained or the dynamic mode
with the former used primarily to observe envelope deployment. In these
tests the model forebody was flexibly attached to a fixed support in the tunnel
by means of a rod and a swivel. The model envelope was accordion folded into
the deployment bag, which was inserted in the forebody or restrained behind
it, depending on which forebody model was used. Then the entire system was
streamed above the support by a drogue parachute attached to the deployment
bag. The deployment event was initiated by the release of the deployment bag
with the electric cutter.

Dynamic tests were used to study envelope deployment, inflation, stability,
and drag. The dynamic deployment tests were the same as the restrained
variety, except that the system was "floated" in the airstream on the drogue
parachute with the deployment velocity governed by the parachute size.
Inflation, stability, and drag were studied by hand launching the system into
the tunnel in a manner similar to that shown in Figure 18. After the excess
air had been rolled from the envelope, the balloon was held by the throat to
prevent premature ingestion of air, and allowed to stream in the tunnel air-
stream. The system was then released and the tunnel velocity was continuously
adjusted to keep the system supported in the airstream as the envelope
inflated. With this arrangement, tunnel velocity is a direct indication of system
drag, provided the model is not moving up or down in the tunnel.
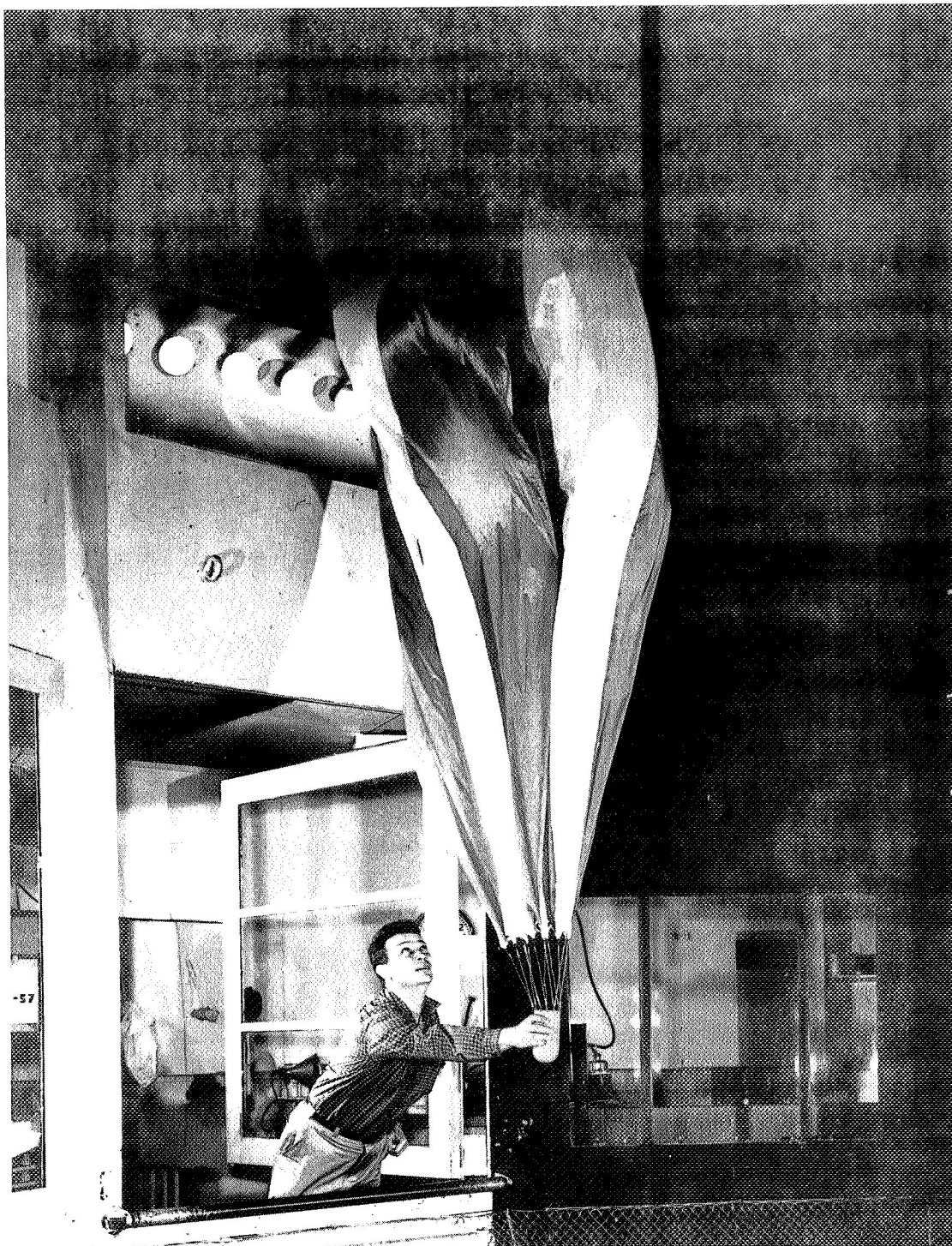
Figure 18. Hand Launch of Model Paravulcoon in 20-Foot Vertical
Free Spinning Wind Tunnel

Basic instrumentation for these tests was motion pictures, which included a tunnel velocity indicator and a timer superimposed on the photographs. Inflation was timed by stopwatch, and steady state tunnel velocity was obtained using tachometer readings and the tunnel calibration table. Force measurements by means of a strain gage mounted between the forebody and the fixed support as originally planned did not prove practical, due to excessive model system buffeting and oscillation.

In the full scale wind tunnel, the number 125 model envelope with the inflation forebody was restrained by a swivel connection in a horizontal position to a vertical halyard installed in the tunnel throat. To ensure that there were no wall effects, the model was positioned well away from the tunnel ground plane. The tunnel was started and envelope inflation and stability was observed.

Helicopter Drop Flight Test

The Langley Research Center Drop Range was used for a free flight drop test of one of the wind tunnel models. The model was dropped from a helicopter in the deployment configuration with a 9-inch Fist Ribbon parachute for a drogue. Earlier tests in the vertical wind tunnel had established that a parachute of this size would provide a 90 to 100 fps stabilized descent of the model system. It suspended the forebody with the envelope packed in a deployment bag by a 55 1/2-inch towline and a bridle of three 11 1/4-inch legs. A four-second delay pyrotechnic reefing line cutter was used to release the deployment bag, initiating the deployment event. Test instrumentation consisted of motion pictures taken from the ground using cameras with 12- and 24-inch telescopic lenses mounted on power driven tracking mounts. Pictures were also taken from the drop helicopter.

BALLOON TERMINAL STABILITY STUDY

Special tests made in connection with the stability study included streamer launched tests of the modified envelope in the vertical wind tunnel, and the large envelope free drop.

The latter test was conducted near Sioux Falls, South Dakota. For this test, the 40-foot envelope, complete with ballast and unarmed jettisoning device, was lifted by its crown in a streamed configuration under a manned hot gas balloon. In this position it was released and simply allowed to descend and inflate. Before impact the ballast was jettisoned to prevent balloon rupture at impact. Motion pictures were made from the ground, using a 300 mm telephoto lens.

FULL SCALE FREE FLIGHT PROGRAM

The full scale, free flight tests consisted essentially of dropping a test system from an aircraft, with photographic coverage of the test sequence from the air and ground as the principal instrumentation. Since this is very similar to the free drop testing of parachutes, it was found that the U. S. Department of Defense, Joint Parachute Test Facility, El Centro, California, is best suited for this type of operation. As this facility is also experienced in engineering, rigging, and performance of aerial cargo drops as a routine operation, all of these tests were conducted there with the technical support of the U. S. Air Force, 6511th Test Group (Parachute).

The following details are discussed in this section:

- Overall flight test sequence
- Rigging design for extracting the system from the drop aircraft and deployment of the parachutes

- Range instrumentation used

- Basic test procedures

Additional details are included in Appendix B.

Flight Test Sequence

Sole purpose of the flight test sequence was to accomplish a deployment event and subsequent balloon inflation with the system in vertical descent at pre-chosen altitudes and velocities. It was decided that this could be most easily accomplished by suspending the simulated payload from a drogue parachute. The parachute size was chosen to give the system the desired velocity at the selected event altitude. Since the object of the program was to demonstrate Paravulcoon feasibility, rather than develop aerial drop techniques, the flight test sequence was based upon recommendations and designs of 6511th Test Group (Parachute) personnel, along with the requirements of the tests.

It was recommended that the simplest way to aerially deploy the test system was to drop the test vehicle mounted on a wooden skid from the rear door of a C-130 transport aircraft. Although dropping from below a hovering helicopter would have eliminated the skid and directly established a vertical descent, range personnel considered this to be less satisfactory and more inconvenient for a test system of this weight.

The overall test sequence used as sketched in Figure 19 proceeded as follows:

- C-130 in level flight at specified altitude and speed vectored to drop point by range ground control.

- At drop command from range ground control, test vehicle on skid extracted from aircraft rear door by parachute.
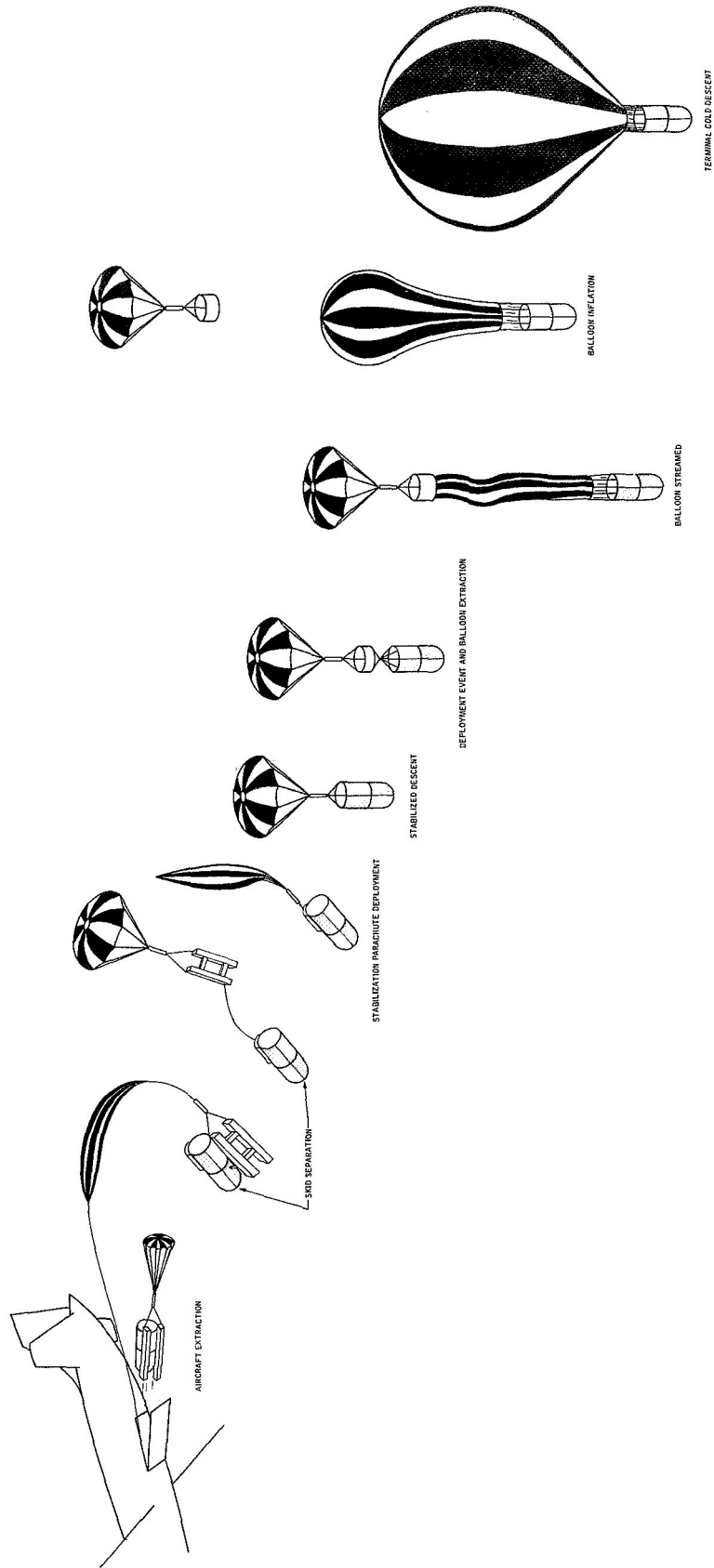
Figure 19. Paravulcoon Flight Test Sequence

- Skid recovery parachute streamed and vehicle released from skid.

- As vehicle separates from skid --

  Stabilization parachute streamed by static line to skid.
  Vehicle safing switches released and control timers
    started by pulling of lanyards attached to skid.

- Stabilization parachute opens and test system steadies out to terminal equilibrium descent.

- Deployment event initiated by control timers.

  Explosive bolts fire.
  Vehicle rear closure plate released by opening of clamp
    bands.
  Deployment bag extracted from vehicle as parachute and
    vehicles separate.
  Balloon envelope streamed from bottom of deployment bag.

- Balloon inflation begins (when throat reefing is used, inflation begins when throat is disreefed by cutters).

- Following deployment, the deployment bag and vehicle rear closure plate descend to ground impact supported on the stabilization parachute.

- After envelope is fully inflated, system descends to ground impact at equilibrium velocity.

It was predicted that the test envelope would rupture at ground impact. This is a cold system test problem only and does not occur with the controlled touchdown of a complete system using heat.

Extraction and Parachute Deployment Rig Design

The aircraft extraction and parachute deployment rigging used to accomplish
the pre-event test sequence was designed, fabricated, and rigged by 6511th
Test Group (Parachute) personnel. The actual design is included in
Appendix B.

In Figure 20 the test vehicle is shown on the extraction skid with all rigging
ready for loading on the drop aircraft. A rear view of the same assembly just
prior to aircraft takeoff is shown in Figure 21. In this design, a small para-
chute was catapulted out into the airstream behind the aircraft at the drop
command to pull the skid assembly out of the aircraft. As the skid left the
aircraft, a static line streamed out the skid recovery parachute. At the same
time, a second static line from the aircraft pulled the mechanical cutters
severing the nylon straps securing the vehicle to the skid. The skid recovery
parachute pulled the skid away from the vehicle. As they separated, the
stabilization parachute was streamed behind the vehicle by a static line to the
skid. This system performed satisfactorily and without incident in each of the
flight tests. Approximately 1.5 to 3 seconds elapsed from the skid extraction
to drogue parachute inflation. Photographs of actual pre-event drop sequences
are shown in Figures 22 and 23.

Range Instrumentation

With only a minimum of on-board instrumentation carried on the flight test
vehicle, the principal means of data acquisition in these tests was photo-
graphic.

Test system space-time histories, system oscillation characteristics, and
test sequence times were computed by the test facility from photographic
data produced by the range cinetheodolite tracking system. Meterological
data was based on weather balloon flights made within one hour of the particular
drop test.
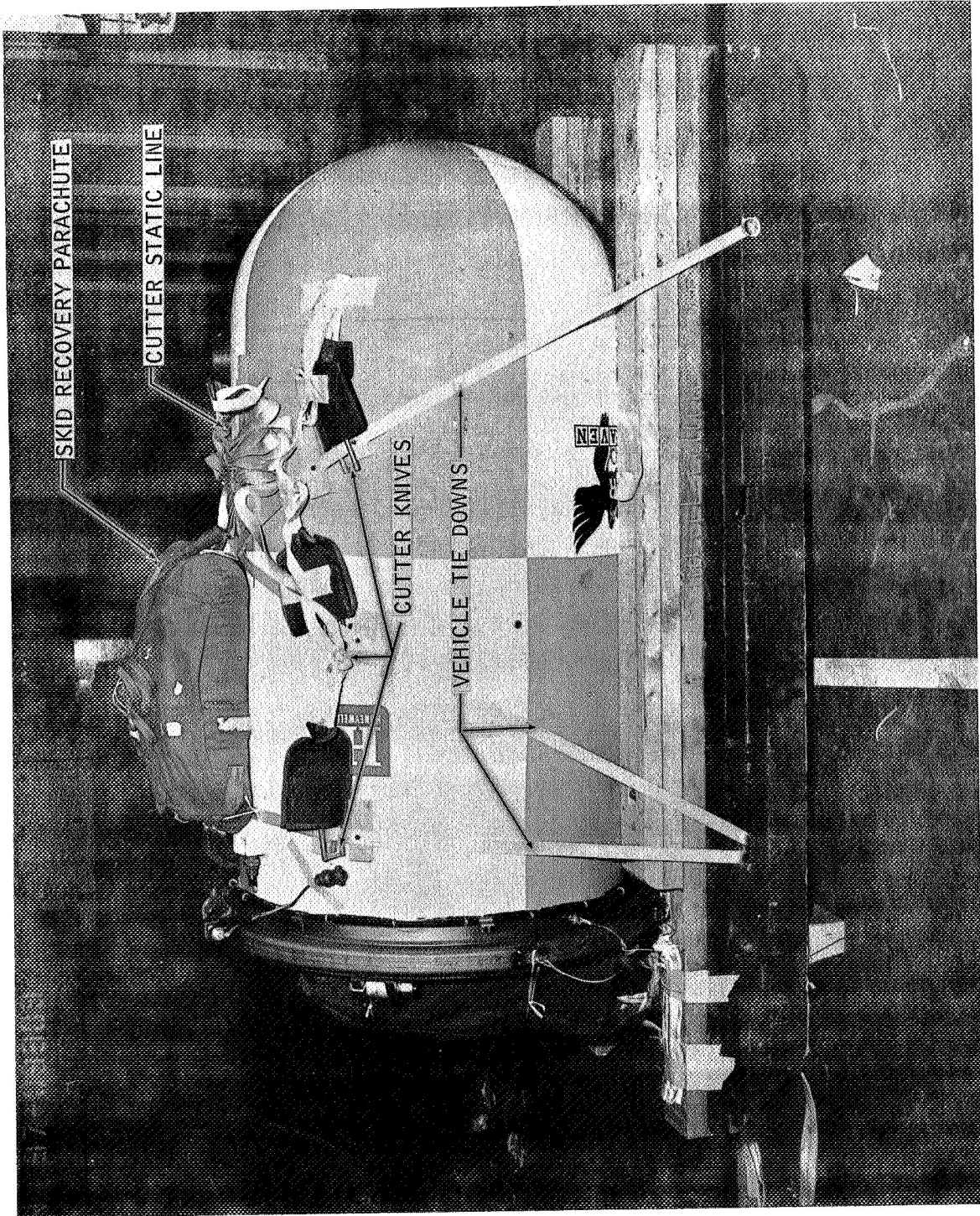
Official U. S. Navy Photograph

Figure 20. Flight Test Vehicle Rigged on Skid with Parachutes
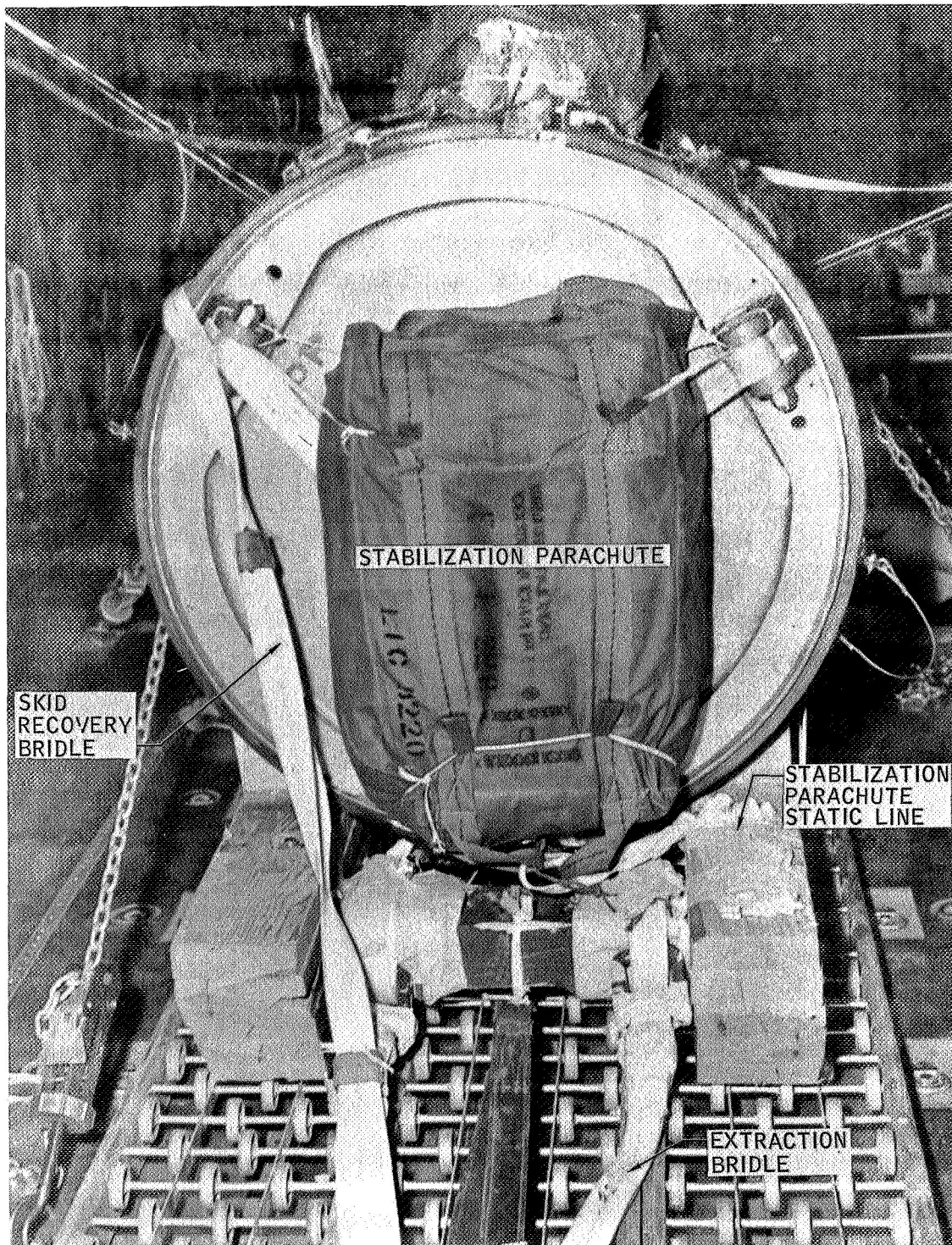
Official U.S. Navy Photograph

Figure 21. Flight Test Vehicle on Drop Aircraft (rear view)
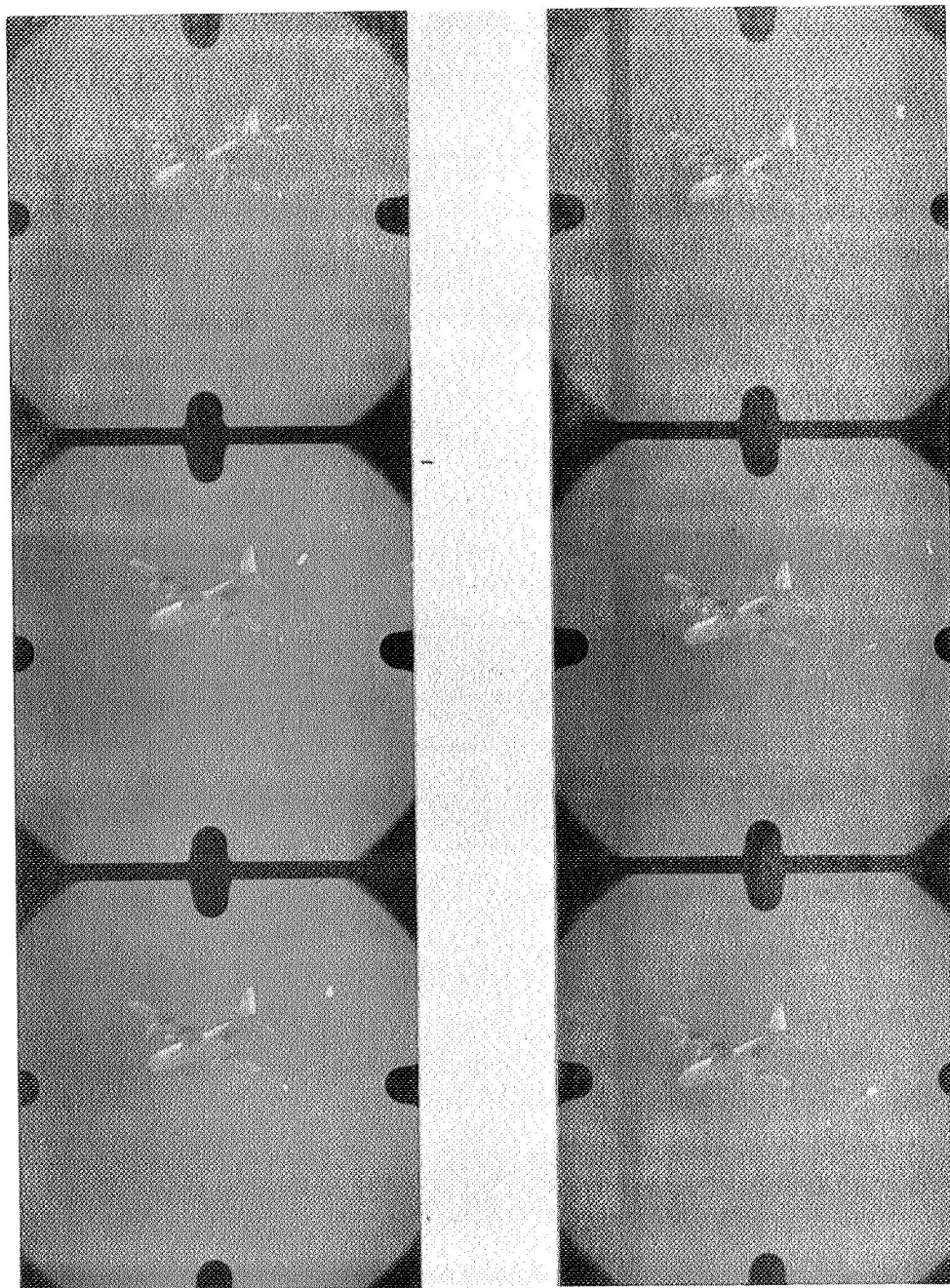
Official U.S. Navy Photograph

Figure 22. Pre-event Flight Test Sequence Showing Extraction
Parachute and Deployment of the Skid Recovery and
Stabilization Parachute
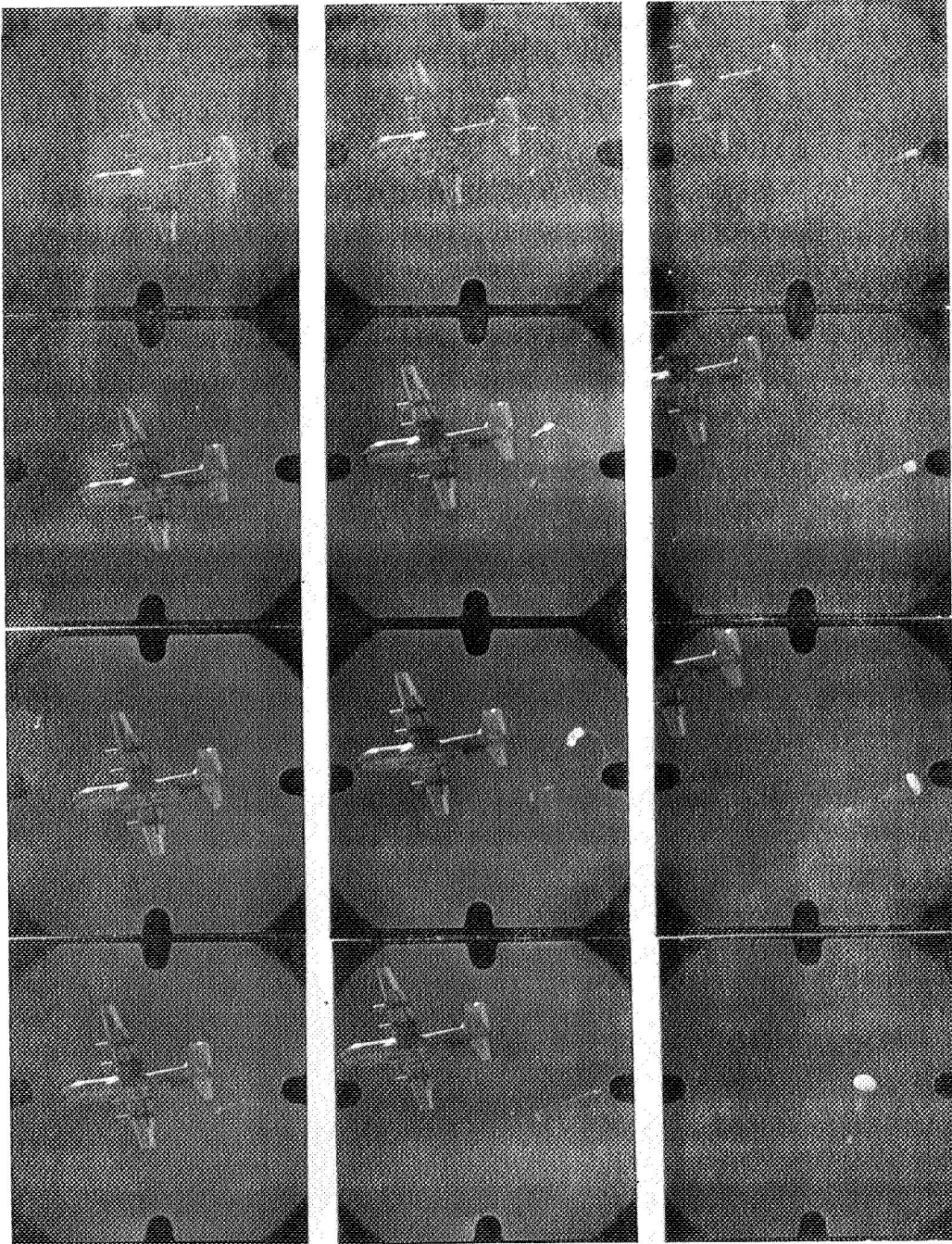
Official U. S. Navy Photograph

Figure 23. Typical Pre-event Flight Test Sequence

System performance details were obtained from direct observation, together with study of 16 mm color motion pictures taken at 50 and 100 frames per second. Ground-to-air photographs were made using 12-, 24-, 60-, and 100-inch telescopic lenses. Air-to-air motion pictures were taken from the drop aircraft and two chase aircraft.

Test Procedures

The actual range drop procedures have been described above; however, prior to each test it was necessary to assemble and check out the test system. To maximize test system reliability and minimize safety hazards to personnel, procedures and check off lists were prepared covering test system assembly and use.

Barring a test system failure, the only procedure whose design might have directly affected program conclusions was the packing of the envelope in the deployment bag. Therefore, this process was carefully designed and checked out. It is illustrated in Appendix B.

SECTION V
TEST PLAN

Both the wind tunnel model study and the full scale free flight test program
were begun on the basis of formal test plans. As testing progressed, various
phenomena and factors encountered necessitated changes and deviations from
the original plans. The stability study tests were added to the program because
of instability problems revealed by the wind tunnel study. In this section, the
specific test parameters chosen to accomplish the three portions of the program
are defined.

WIND TUNNEL STUDY

The wind tunnel study was mainly conducted in the Langley Spin Tunnel with a
brief test in the Langley Full Scale Tunnel. A single helicopter drop flight test
was used to corroborate the spin tunnel findings.

Langley Spin Tunnel

Prior to the wind tunnel tests, a test plan was prepared in which deployment,
inflation, stability, and steady state drag were to be investigated step-by-step
at various velocities, using the several parametric variations possible with the
models. It was expected that deployment and inflation could be most easily
observed under best control by first using the fixed mount in the Langley Spin
Tunnel. Then, having this experience, unrestrained tests were to be conducted
in the spin tunnel to observe system dynamic characteristics.

However, when the actual tests were begun it was quickly discovered that restrained tests were very difficult to perform. The rapid increase in model system drag, which occurred after a small amount of envelope inflation, increased the loading on the balloon more rapidly than the tunnel could be slowed down to simulate the resultant deceleration of a free system. Also, the tunnel mounting fixture was not sufficiently rigid to sustain the balloon buffeting and oscillation which occurred at these velocities. On the other hand, it was discovered that unrestrained dynamic tests were relatively easy to accomplish in the spin tunnel. Therefore, the initial test plan was abandoned. Most of the study was then devoted to unrestrained tests of various parametric model configurations to observe inflation and stability characteristics, with only a few restrained and unrestrained tests to observe balloon deployment.

While data was obtained in more than one category in many of the test runs, the revised tests were directed toward obtaining understanding in these four areas:

- Envelope deployment
- Envelope inflation
- System stability
- Drag measurements

A complete summary of all the test runs is included in Appendix A.

Most of the deployment runs were made using drogue parachutes sized to give event velocities from 30 to 35 fps. Also, a static test was run at 83 fps, and a dynamic test was made at 62 fps. However, in the dynamic deployment runs the partially inflated balloon rapidly rose to the top of the tunnel and was flattened against the top screen by the airstream. Since wind tunnel personnel were concerned that this would seriously damage the wind tunnel, deployment runs were limited to the minimum number necessary.

To investigate both inflation and stability, the whole range of parametric possibilities of envelope material, envelope throat size, forebody size, and load line geometry previously described were tested with various weights in the forebody (see Appendix A). Terminal descent was simulated at altitudes from 15,000 feet to over 50,000 feet. Naturally, not all of the possible combinations were investigated as test experience soon indicated those areas of greatest interest. Since in all these runs the systems were hand launched, the tunnel velocity for each run was regulated to match the particular system drag and weight.

The only test runs made solely for drag measurements were made with the envelope throat tied shut to prevent ingestion of air to obtain the drag of the envelope in the streamed configuration.

Langley Full Scale Tunnel

Two inflation and stability tests were made using the number 125 envelope in the Langley Full Scale Tunnel at velocities of 10 and 15 fps, respectively.

Helicopter Drop Flight Test

The number 125 envelope and the six-inch deployment forebody were used for the helicopter free drop test. The package was vertically dropped at 2000 feet altitude, and the estimated event velocity was 100 fps. The payload and balloon weighed 3098 grams, which simulated terminal descent at approximately 50,000 feet (500 square feet), while the complete package dropped from the helicopter weighed 3130 grams.

BALLOON TERMINAL STABILITY STUDY

The spin tunnel tests of the modified model envelope were made with the forebody weighted to give total system weights from 875 grams to 3500 grams, with corresponding terminal descent altitudes of approximately 21,000 feet and 53,000 feet.

The 40-foot diameter envelope with the 300-pound load was released in the streamed configuration at approximately 7200 feet MSL altitude (5800 feet above ground level). The ballast was jettisoned at about 1500 feet above ground level.

FULL SCALE FREE FLIGHT PROGRAM

Since the Paravulcoon system had not been previously flight tested in this size range, it was planned to first become familiar with the system charac- teristics and check out test equipment and procedures with a single flight at an event velocity of 100 fps. Following this it was intended to devote the remainder of the tests to the 200-and 300-fps cases which system studies have indicated would have a more practical application.

On the basis of the wind tunnel experience and the program objectives, it was decided to conduct all the flight tests at an event altitude of 15,000 feet. This provided a sufficient fall distance in case the inflation should require an unexpectedly long time. Also it was a convenient altitude for both the drop and chase aircraft and a good altitude for ground-to-air photography. The planned nominal test event conditions are listed in Table 4.

Table 4. Nominal Deployment Event Conditions

Drop Test No.	Altitude (Feet)	Velocity (fps)	Dynamic Pressure (psf)
1	15,000	100	7.48
2	15,000	200	29.9
3	15,000	200	29.9
4	15,000	300	67.3
5	15,000	300	67.3

A parametric trajectory study was made to determine the drop altitudes, stabilization parachute sizes, and timer settings necessary to achieve the desired event conditions. The resultant values are given in Table 5.

Table 5. System Drop Condition Specifications

Test Number	Drop Conditions				
	Stabilization Parachute			Drop Altitude (feet)	Timer Setting (seconds)
	Estimated $C_D S$ Required (feet^2)	Type	Diameter (feet)		
1	172.5	Ring Slot	20.0	16,145	15.0
2 and 3	39.0	Reefed 15 feet Ring Slot	Reefed Diameter 6.0	17,700	20.0
4 and 5	15.7	Ribless Guide Surface	5.0	18,620	22.0

All parachutes were furnished by the 6511th Test Group (Parachute). Thus, the sizes specified depended on the particular equipment in stock. Since no parachutes with a $C_D S$ value in the vicinity of 39. 0 ft.^{2} were available, a permanently-reefed, 15-foot ring slot parachute was used for the 200-fps tests. Timer settings and drop distances on the stabilization parachute were made somewhat longer than was necessary to reach a vertical trajectory so that any possible system oscillations could be stabilized out.

As the design of the vehicle was completed and the parachute sizes were specified, it became apparent that the steel rear closure plate's weight might cause problems when used with the smaller parachutes. There was concern that when suspended from these parachutes the steel plate might not have a sufficient separation velocity from the vehicle and deploying envelope to guarantee the severing of the break cord. Furthermore, the plate's descent velocity might be fast enough to produce a collision with the Paravulcoon after inflation. Use of an aluminum plate was investigated, but the aluminum design was found to have inadequate stiffness to handle the opening shock loads predicted for the 20-foot parachute. However, in this case, the parachute is large enough so that the separation rate problem does not occur with the steel plate. Because the opening shocks estimated for the smaller parachutes were so much less, an aluminum rear closure plate was designed for use with them. This plate was about 100 pounds lighter than the steel one and thus alleviated the problem. Therefore, a steel rear closure plate was provided for the 100-fps test and aluminum plates were fabricated for the higher speed tests.

As will be discussed in the following section, actual test occurrences resulted in a four-drop test program consisting of two drops at 100 fps nominal event velocity and two at 200 fps. Also, since it is difficult to obtain accurate drag predictions for reefed parachutes, it was necessary to change the reefing specifications for the second 200-fps test. Actual test conditions for the four tests are summarized in Table 6.

Table 6. Actual Flight Test Conditions and Equipment

Drop Test Number	1	2	3	4
Date	4-17-64	4-28-64	5-8-64	5-15-64
Stabilization Parachute	20' Ring Slot	20' Ring Slot	15' Ring Slot Reefed to 6'	15' Ring Slot Reefed to 5'
Reported Drop Conditions:				
Altitude (ft)	16,145	16,145	17,855	18,760
Speed (KIAS)	131	130	131	131
Timer Setting (seconds)	15	15	20	20
Event Conditions				
Altitude (feet)	15,300	15,107	15,494	16,690
Velocity (fps)	111	105	176	204
Dynamic Pressure (psf) (actual from flight data)	10.0	8.1	22.8	29.3
Envelope Used				
Number	102	103	101	103
Type	X-54	X-54-1	X-54 (Modified)	X-54-1 (Repaired)
Remarks	No "up" camera	---	---	Envelope throat temporarily reefed with two-second delay cutters

Table 7 itemizes the weights of the test systems dropped in the four full scale free flight tests.

Table 7. Flight Test System Weights*

Drop Test Number	1	2	3	4
Total weight suspended on stabilization parachute	1302	1293	1214	1209
Total weight descending after event	1214	1115	1215	1127
Total weight suspended from Paravulcoon	1005	1015	1015	1020

* All weights in pounds.

SECTION VI
RESULTS AND DISCUSSION

Program results are presented and discussed here in terms of the three
major program phases: wind tunnel study, stability study, and full scale
free flight program. The results of the first two studies are also summarized
before moving on to the full scale study.

WIND TUNNEL STUDY

As previously noted, the wind tunnel study consisted primarily of the spin
tunnel studies, plus a brief test in the full scale and a helicopter drop flight
test.

Spin Tunnel Studies

The basic spin tunnel studies can best be considered in terms of the envelope
deployment, the envelope inflation characteristics, system stability, and
system drag.

Deployment -- Prior to the wind tunnel investigation, it was anticipated that
envelope deployment would be a significant problem area and that a major portion
of the wind tunnel effort would be devoted to its study. However, after the
first tests at the relatively low velocities which had to be used for the deploy-
ment tests, it was concluded that deployment presented no problems.

In every test, the envelope streamed smoothly from the deployment bag and
immediately began to inflate by ingesting air through the throat. Actual time
from release until the deployment bag cleared the streamed envelope was
less than one second, and there did not appear to be any significant opening

shock transmitted to the forebody. Examination of the test films revealed that an ingested air bubble moved up the streaming balloon directly behind the deployment bag. Due to the stiffness of the model envelope fabric, this effect was not obvious during the wind tunnel tests. However, a similar bubble which occurred later in a full scale test was judged to be the cause of a balloon deployment failure.

Actually, all the problems encountered were involved in the test technique, rather than in envelope deployment, since drag on the envelope built up rapidly enough to simulate the Paravulcoon system deceleration   In the static runs, this resulted in severe buffeting and oscillation of the balloon, with resultant local overloading and failure of the load lines. In the dynamic runs, the partially inflated balloon rapidly rose to the top of the tunnel and was flattened against the top screen by the airstream.

Most of these runs were made at event velocities from 30 to 35 fps (dynamic pressure about 1.0 psi). Using the approximate rate of descent scaling relationship with the 1/10 scale model (Equation 2), this corresponds to about 90 to 100 fps for the prototype at 15,000 to 20,000 feet in altitude (dynamic pressure about 7.0 psi). However, since it was impossible to scale the mechanical and dynamic features of the model envelope, such a quantitative extrapolation is at best approximate. The static test at 83 fps and the dynamic test at 62 fps corresponded to flight test rates of descent of 260 fps and 200 fps, respectively. No deployment problems were observed at these velocities.

It should be noted that while the model deployment was smooth and trouble free, the model envelope was much stiffer and also heavier per unit area than the full scale test balloon. Therefore, the wind tunnel deployment tests were primarily an indication of over-all deployment mechanism feasibility and did not necessarily simulate model envelope transient aerodynamics, dynamics, or loading.

Inflation -- Although the inflation mode was also observed during the deployment tests, most of the inflation data was obtained from the hand-launched dynamic tests. As in the deployment studies, the model envelopes were too stiff and the scaling factors insufficiently understood for direct quantitative extrapolation of inflation data to larger systems. However, four characteristics were observed in these studies which appear to be qualitatively applicable to Paravulcoon systems of any size: :

- All model configurations had a positive tendency to inflate

- System drag increased rapidly to almost the fully inflated value after only a small percentage of the inflation was completed

- The system was completely stable during the inflation period

- For a given configuration, inflation times were quite reproducible.

In every case tested, the envelope began to ingest air as soon as its throat was released. The drag immediately increased and quickly reached a value near that of the fully inflated balloon. During the remainder of the inflation period, the drag gradually increased to the steady state value. Thus, inflation took place at a nearly constant velocity which, with the light models used in these tests, ranged from 8 to 18 fps with one heavy case at 27 fps. This rapid deceleration suggests that the problems of deployment and inflation can be studied separately, and that inflation is relatively independent of the deployment event velocity.

During this period, the motions of the envelope fabric appeared quite random, with a continuous movement of the folds of material and some opening and closing of the throat area. While several attempts have been made, a satisfactory analytical description of this phase has not yet been obtained.

There was no sign during this period of the system instability which was encountered after the envelope was fully inflated (to be discussed in the following section).

In spite of the random appearance of the inflation period, inflation time for a given configuration was surprisingly reproducible. Values ranged from four seconds with a rigid ring in the throat to over 40 seconds for the lightest configurations. Since tunnel velocity during inflation was nearly constant, the equivalent inflation distance (which is really the significant parameter systems-wise) is essentially proportional to inflation time. Typical values ranged from 200 feet or less, to over 300 feet. The effect of parametric variations of the models on inflation time is discussed in Appendix A.

In general, inflation was found to be somewhat slow. However, when the rigid throat ring was used, the rapid inflation was so violent that it could not possibly be sustained in a large system. So, while desirability of a positive inflation aid was reversed, need for a controlled gradual inflation was also indicated. Since the model envelope fabric was relatively stiff, the many and sometimes severe fabric and envelope motions associated with the long inflation period encountered in the full scale flight tests were not observed in these model studies.

Stability -- The major problem encountered in the wind tunnel study was an instability exhibited by the system during the cold descent period after the balloon was fully inflated. This occurred in the form of an indentation on the windward side of the balloon which came to be referred to as the "dimple". A typical indented configuration is sketched in cross-section in Figure 24. The indentation resulted in a quasi-steady rotation of the system, usually referred to as coning, or oscillations of varying degrees of intensity.

During the wind tunnel study proper, the effect of model variations on this dimple and instability was observed. This was done as part of the tests described in the discussion of inflation, where the model was hand launched in the streamed configuration. Based on notes from the direct test observations and subsequent analysis of the test films, the efforts of these configurations on the dimple and resultant system motion are summarized in Table 8. In this table the size of the indentation is placed in three categories, its tendency to remain formed is noted, and the nature of the system motion is described.
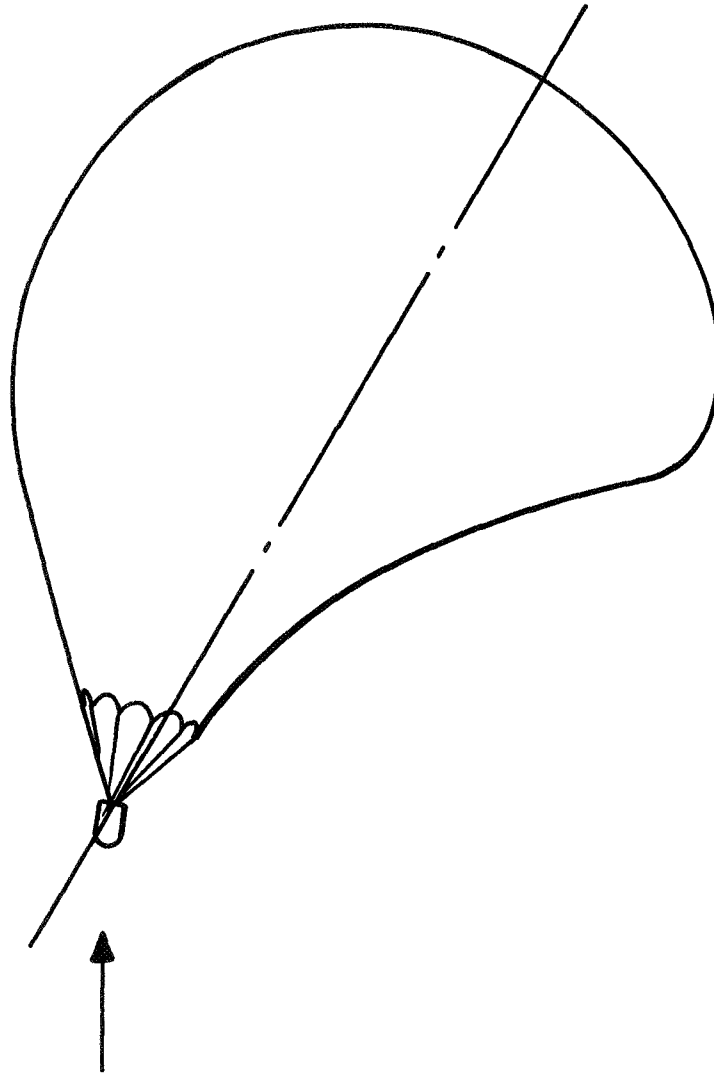
Figure 24. Typical Cross-Section of Indented Model Balloon

Table 8. Summary of Terminal Descent Characteristics (Wind Tunnel Model)

Envelope	Configuration (Inflation from Streamer)	Total Weight (lbs)	Dimple Size			Dimple Persistance		Nature of Motion	C_D
			Small	Average	Large	Unstable	Stable		
125	Normal - 3-Inch Forebody	2.82	X			X		Slow oscillatory rotation	0.837
125	Normal - 3-Inch Forebody	3.74		X		X		Slow oscillatory rotation	0.575
125	Normal - 3-Inch Forebody	8.26			X		X	Rapid coning rotation	1.035
125	Normal - 6-Inch Forebody	4.16		X			X	Moderate coning rotation	0.790
125	Normal - 6-Inch Forebody	6.66		X			X	Rapid coning rotation	0.926
125	3-Inch Extension - 3-Inch Forebody	3.74		X			X	Slow coning rotation	0.575
125	6-Inch Extension - 3-Inch Forebody	3.74		X			X	Slow coning rotation	0.812
125	12-Inch Extension - 3-Inch Forebody	3.78	X				X	Slow coning rotation	0.821
125	17-Inch Throat Ring - 3-Inch Forebody	2.91	X			X		Slow oscillatory rotation	0.865
125	17-Inch Throat Ring - 3-Inch Forebody	8.38	X				X	Rapid coning rotation	0.767
125	12-Inch Load Lines - 3-Inch Forebody	1.79		X			X	Slight oscillatory rotation	0.687
125	12-Inch Load Lines - 3-Inch Forebody	2.81	X			X		Oscillatory (no rotation)	0.652
125	12-Inch Load Lines - 3-Inch Forebody	3.76	X			X		Oscillatory (no rotation)	0.524
820	Normal - 3-Inch Forebody	3.50		X			X	Moderate coning rotation	0.665
820	Normal - 3-Inch Forebody	6.35			X		X	Rapid coning rotation	1.067
825	Normal - 3-Inch Forebody	1.53	X			X		Slow oscillatory rotation	0.708
825	Normal - 3-Inch Forebody	3.48			X		X	Slow oscillatory rotation	0.753
825	Normal - 3-Inch Forebody	6.34			X		X	Rapid coning rotation	0.959
830	Normal - 3-Inch Forebody	1.52	X			X		Slight oscillatory rotation	0.704
830	Normal - 3-Inch Forebody	1.52	X			X		Oscillatory (no rotation)	0.704
830	Normal - 3-Inch Forebody	2.53	X			X		Translation (no rotation)	0.752
830	Normal - 3-Inch Forebody	3.47	X			X		Translation (no rotation)	0.752
830	Normal - 3-Inch Forebody	6.34			X		X	Moderate coning rotation	0.733
830	12-Inch Load Lines - 3-Inch Forebody	3.48	X			X		Translation (no rotation)	-
840	Normal - 3-Inch Forebody	1.53	X			X		Translation (no rotation)	0.710
840	Normal - 3-Inch Forebody	2.55	X			X		Translation (no rotation)	0.755
840	Normal - 3-Inch Forebody	3.50	X			X		Oscillatory (no rotation)	0.813

Of necessity, these lumpings are somewhat arbitrary as they represent an attempt to categorize a rather subjective phenomena. The dimple was considered unstable if it tended to form, disappear, and reform in a flip-flop manner. This was usually accompanied by a corresponding translation, oscillation, or oscillatory rotation of the system. The dimple was considered stable if it persisted once it was formed. In these latter cases, the dimple remained in a single position relative to the airstream as shown in Figure 24 and the entire system rotated or coned about this position in a quasi-stable mode. Although the dimple remained in a fixed position, the envelope fabric moved continuously through the dimple as the system rotated.

It is seen that the geometric variations only moderately influenced the terminal stability of the model systems. An increase in throat size had some tendency to reduce the dimple size, as did the use of over length load lines, which tended to hold the throat open. On the other hand, the extension lines and the rigid ring had a negligible effect on the dimple phenomena.

However, increasing the model system weight markedly increased instability, ranging up to the severe buffeting observed in the static mount tests, which are equivalent to an infinite weight. If the weight-altitude scaling relationship of Equation 1 is valid for these cases, where the balloon is being distorted and the system is no longer acting as a single rigid body, this model performance can be related to the performance of the 1000-pound systems at higher altitudes. Thus, for the lighter models, which would correspond to altitudes from 15,000 to 25,000 or 30,000 feet, the motions were flip-flop oscillations, translations, or oscillatory rotations, while with the heavier models, which would correspond to 50,000 feet and higher, a strong and quasi-stable coning rotation was observed.

The problem posed by this instability was considered sufficiently serious to warrant additional analytical and experimental investigation, since a practical recovery system must be stable in all phases of its activation sequence. These studies showed the instability to be primarily the result of the particular flow regime in which the model balloons were operating, and will be discussed in the following section.

Drag -- In the spin tunnel, drag measurements are readily obtained by "floating" the model on the airstream and computing the drag coefficient from the following expression:

$$C_D = \frac{2W}{\rho SV^2} \tag{3}$$

where:

C_D = aerodynamic drag coefficient

ρ = air density, (slugs/ft^3)

W = system weight, (pounds)

S = reference area (ft^2), (for the model systems, the maximum cross-sectional area of the undistorted balloon)

V = airstream velocity, (ft/sec)

Drag measurements were attempted for all the various model configurations and the drag coefficients computed by Equation 3 are listed in Table 8. However, it was not possible to obtain a fully inflated condition without some dimple. Thus, the drag coefficients tabulated represent the net drag of the dimpled configurations. Also as previously noted, these tests were all conducted in the critical Reynolds number regime which limits the validity of the application of this data to other flow conditions.

Net drag coefficient values of 0.524 to 1.067 were observed while Hoerner[3] gives values of 0.47 for a sphere and 1.17 for a hollow hemisphere in the same Reynolds number range. Since the dimpled configuration tends to give a shape approaching a hollow hemisphere, an increase in dimple size would be expected to cause the net drag coefficient to approach that of the hemisphere. Indeed, this seems to be essentially the case. Also, while an increase in the relative throat opening had some tendency to reduce the dimple size, it also caused a more severe deviation from a spherical shape and thus was also accompanied by an increase in the observed drag coefficients.

Drag coefficients of 0.018 to 0.027, based on the fully-inflated balloon area, were recorded for the envelope in a streamed configuration. Based on the banner area of the streamer (streamer width × streamer length) in the manner used in Reference 3, these coefficients become 0.162 to 0.206. These values were found to straddle a curve extrapolated in terms of the length-to-breadth parameter from the data reported in Reference 3 for a banner.

Other Wind Tunnel Model Tests

When initially considering the instability found with the wind tunnel models, it was suggested that there was an outside chance that this phenomena was due to tunnel blockage or wall interference effects resulting from using such large models in the 20-foot spin tunnel. The model tests in the full scale tunnel and the helicopter drop flight test were conducted to check out this factor.

Full Scale Tunnel -- Essentially the same dimpling and coning rotation was observed in the full scale tunnel as had been experienced in the spin tunnel.

Helicopter Drop Flight Test -- This test was successful as planned with the time to event 6.4 seconds and the total time to ground impact one minute, 45.5 seconds. Deployment at an estimated event velocity of 100 fps appeared to be exactly the same as in the spin tunnel, with no problems. Envelope inflation was also the same as in the wind tunnel with the system stable during this period. Unfortunately, the terminal descent of the inflated balloon was also the same as for the corresponding wind tunnel case which simulated the terminal descent of a 1000-pound system at about 50,000 feet altitude. A large dimple formed and a stable coning rotation continued until ground impact.

Therefore, this free drop test tended to corroborate the observations of the deployment, inflation, and terminal descent characteristics of six-foot diameter model Paravulcoons made in the spin tunnel.

BALLOON TERMINAL STABILITY STUDY

Having uncovered a possible system stability problem in the small model tests, it was necessary to further investigate this problem before moving on to the full-scale cold drop flight tests. Three problems were pursued in this investigation: Determination of the cause and explanation of the instability; probability of encountering the same instability during flight tests of larger balloons; and a possible mechanical "fix" which can be applied to larger balloons if found necessary.

Analysis

A theoretical study was made to establish an explanation for the unstable behavior exhibited by the model balloon. Based on a consideration of flow around a sphere, theories of the dimple formation and the instability were formulated.

Sphere Flow -- Since the natural shape balloon is essentially a 96-degree cone-sphere configuration with the aft side somewhat flattened, a review of the characteristics of flow about a sphere gives some suggestions for the explanation of the model instability.

The most striking feature of flow around a sphere is the sudden large change in flow distribution and drag coefficient in the Reynolds number range of 1×10^5 to 4×10^5. This is the critical range between laminar or subcritical flow and turbulent or supercritical flow. As illustrated in Figure 25, these two flow regimes have quite different flow patterns. For the laminar case, the flow separates from the sphere surface at a position angle of 80 to 90 degrees from the stagnation point, while in the turbulent case the separation occurs at 105 to 120 degrees. These patterns are accompanied by markedly different pressure distributions, as shown in Figure 26. In both cases, the pressure drops off rapidly as the flow moves away from the stagnation point. However, the big

SEPARATED
WAKE

LAMINAR
(SUBCRITICAL)

TURBULENT
(SUPER CRITICAL)

Figure 25. Flow Around a Sphere

$R_{supercr.} = 4.35 \times 10^5$

$R_{subcr.} = 1.63 \times 10^5$

$\dfrac{p - p_\infty}{q}$

-1.0

0

30   60   90   120   180   270   360

SUBCRITICAL

SUPERCRITICAL

-1.0

θ - DEGREES
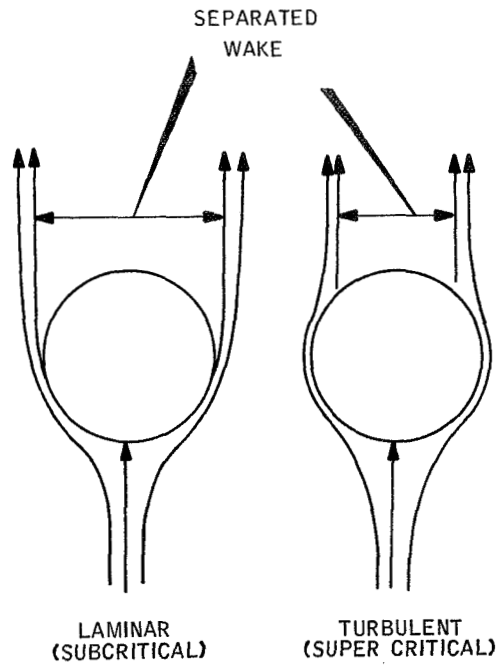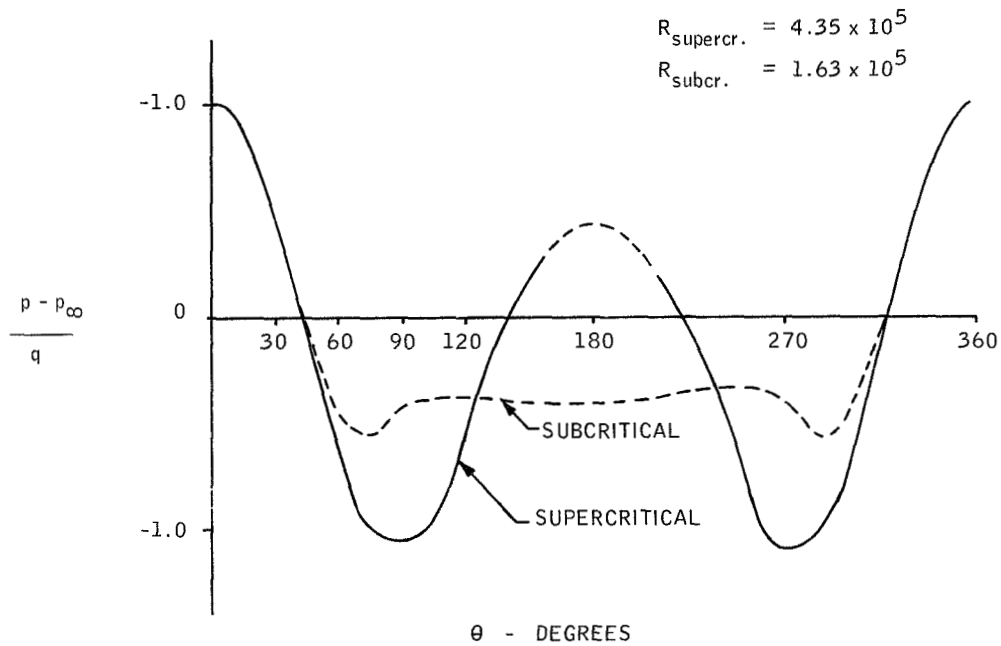
Figure 26. Pressure Distribution Around Spheres

difference in the present pattern occurs in the equatorial region of a sphere. This implies that when operating in the critical Reynolds number range small geometrical or flow variations can result in large pressure distribution variations along the sides of a sphere.

Unfortunately, as indicated in the plot of Figure 27, all the model balloon tests had to be conducted in or just above the critical range. Since the full-scale flight test envelopes which are 10 times larger operate at a Reynolds number an order of magnitude greater, flow about them will be well into the super-critical regime. Thus, it appears that geometrical or flow variations about them should not result in such radical pressure variations in their equatorial region.

Dimple -- A typical dimpled model balloon in rotation to the air stream is sketched in Figure 28. It can be seen that at an angle of attack on one surface of the balloon, the "windward" side, assumes an orientation which is more normal to the oncoming stream than it is at zero angle of attack. This results in a sizable increase of pressure over this surface. At the same time, the "lee" side of the balloon will be oriented less normal to the stream and consequently the pressures over this surface will be somewhat reduced. Similarly, the throat of the balloon is oriented less normal to the stream, and hence this portion of the flow is also at a reduced pressure. Thus, the pressures over the throat will be lower on the average than for the zero angle-of-attack orientation. Since presumably for an envelope of low permiability any flow inside the envelope will be confined primarily to the inlet region, internal flow velocities relative to the envelope will be at least an order of magnitude less than the external relative velocities. As a result, any pressure variations over the inside envelope surface will be small compared to the external pressure variation, and the mean internal pressure will be approximately equal to the mean throat pressure.
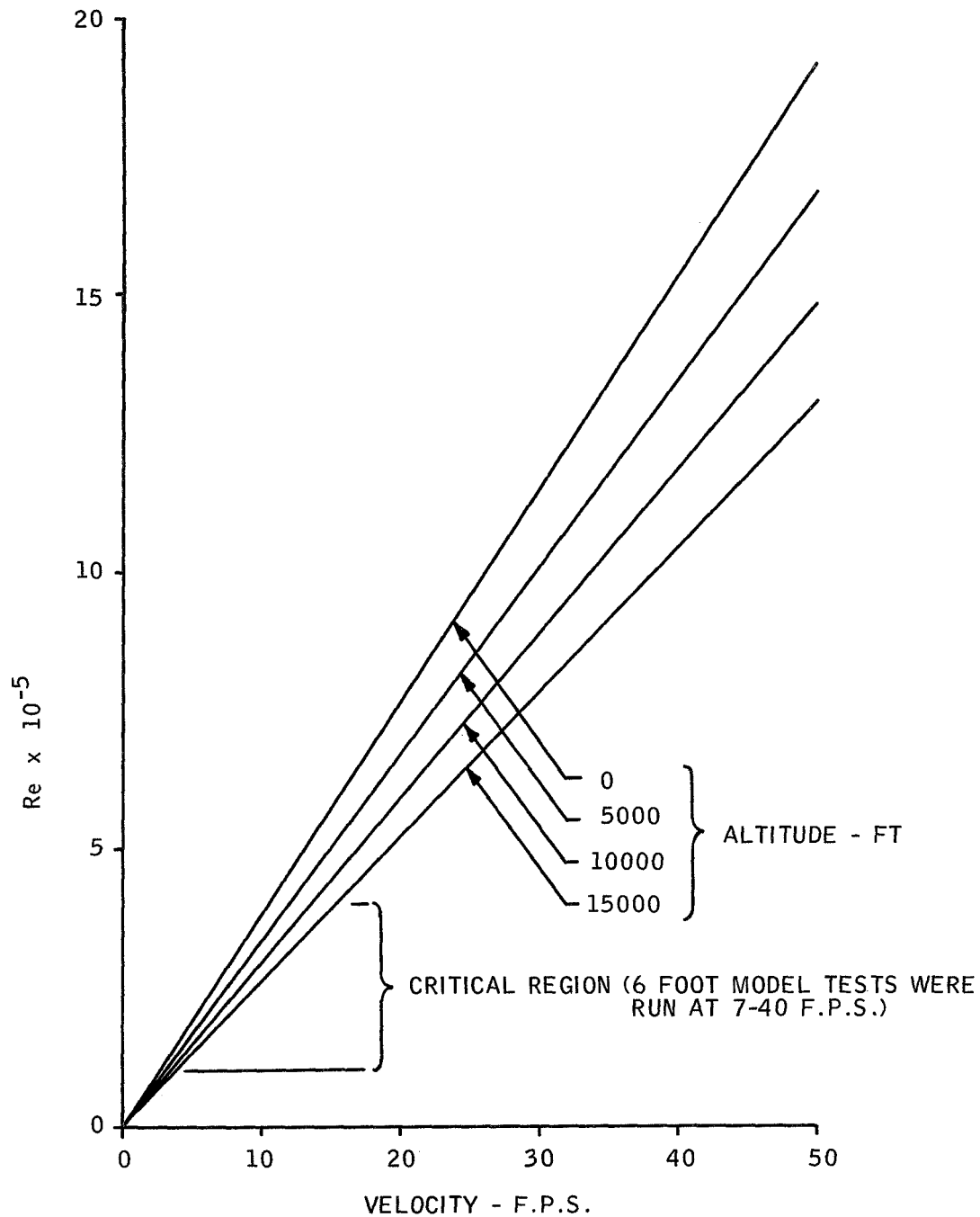
Figure 27. Reynolds Number versus Velocity and Altitude
for a Six-Foot Diameter Sphere
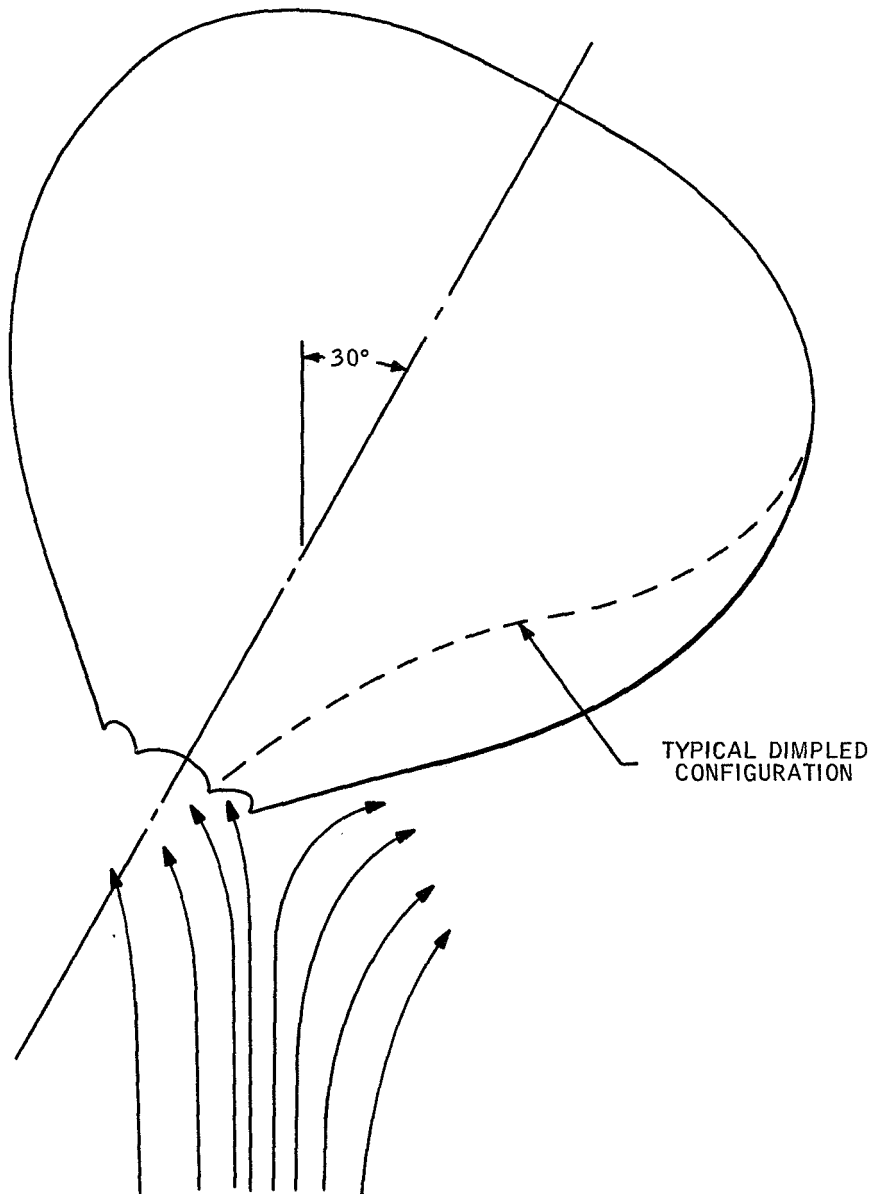
30°

TYPICAL DIMPLED
CONFIGURATION

Figure 28. Typical Dimpled Balloon Orientation

Therefore, the dimple phenomena is explained by this existence of a lower
pressure in the region of the flow over the throat than is present over the
concave portion of the dimple. Similarly, at locations on the surface where
the envelope shape is convex (fully inflated), the throat pressure must exceed
the external pressure as there is no other internal pressure source to main-
tain the inflated shape.

Stability -- Assuming that the dimple is caused by the reduced pressure which
occurs at the throat during an oscillation, two questions remain unanswered:
What causes the lateral instability, and what are the restoring forces which
result in a quasi-equilibrium state at some angle of attack? The answer to
these questions appears to lie with the sensitive variation of the pressure
distribution with respect to the location of the separation point around the
balloon. If for some reason the separation point should shift slightly forward
on one side, this side of the balloon will experience higher pressures in the
region from 45 to 135 degrees from the stagnation point and an upsetting
moment is produced. At least three causes of the shift in separation point
can be postulated.

First, the aerodynamics of the actual system differ from those of the sphere
not only due to shape, but also due to the presence of the forward payload.
Disturbances produced by the payload will be carried in the flow stream around
the balloon and may significantly affect the location of the separation point.
Studies of the drag of a sphere in the wake of a forebody[3], indicate that a
normally supercritical flow may become subcritical due to local reduction
of the Reynolds number. Second, the wake formation process may induce
perturbing forces causing fluctuations in the location of the separation point.
This is particularly true at low Reynolds numbers below the range of interest
here. However, definite periodicity in wakes has been observed well into the
supercritical regime at Reynolds numbers as high as 7×10^6. Third, the sys-
tem will always be subjected to some amount of random turbulence when
operating in the atmosphere and to a lesser extent in the wind tunnel. Therefore,

it is to be expected that the balloon and payload system will be subjected to transient moments and the motion of the system will depend on the variation of the upsetting and restoring forces as functions of angle of attack.

It is of interest to consider the origin of the forces and moments which tend to maintain the balloon at an angle of attack. In the quasi-stable "tilted" orientation with a dimple formed, the summation of the moments about the center of gravity must be zero. Location of the center of gravity in the dimpled condition is not precisely known and depends in addition on the relative magnitudes of payload and balloon. However, in most cases the center of gravity of a Paravulcoon system may be expected to be near the payload, so it is easily seen that the payload contributes a restoring moment. The moment of the pressure distribution over the dimple is also restoring, and since these pressures are higher than those over the corresponding loca- tions on the lee side, one must look for somewhat higher pressures over the upper half of the balloon on the lee side to account for the angle of attack. The tunnel test films reveal that the lee side of the balloon has a nearly vertical profile. This implies that pressures over the lower (upstream) surfaces are less than for the zero angle-of-attack position, while over the mid-latitudes and upper surfaces the pressures will be higher. By constrast, the windward side of the balloon will be subject to a flow separation at the short radius bend along the upper edge of the dimple, and pressures over surfaces above this point will be sharply reduced. The balloon thus assumes a resultant altitude in which these upsetting and restoring moments are in balance.

Studies of the aerodynamic characteristics of inflatable deceleration systems[4] having geometries very similar to the Paravulcoon, have revealed the same coning and oscillating motion. Spheres and cone-spheres were tested in sub- critical and supercritical flow. The subcritical tests showed that a cone- sphere configuration with a laminar to turbulent trip fence in the shape of a torus around the body at a position angle of 75 degrees was the most promising system. The fence effectively stabilized the system, eliminated the coning, and reduced the oscillations to ±5 degrees.

In the supercritical region, all configurations tested without a fence proved unstable. The addition of a three-percent flow separation fence at a position angle of 105 degrees eliminated coning and oscillation. The use of the fence resulted in excellent pitch and roll stability characteristics and increased the drag. Since the purpose of the fence was to control the point of separation, it was undoubtedly placed ahead of the normal separation point for the particular Reynolds number. This would account for the increased drag.

Thus, the use of a circumferential fence near the balloon equator may be an effective means to ensure balloon stability in some coning situations. Depending on the flow conditions involved, such a fence may act as either a boundary layer trip or an initiator for boundary layer separation.

Conclusions -- The observed coning and oscillating motion of the six-foot model appears to be due to unsteady, asymmetric separation of the boundary layer from the balloon. It has been shown from existing data that large pitching moments occur from the resulting asymmetric flow patterns. The cause of the asymmetric separation may be attributed to: (1) The effects of the forebody on the flow field, (2) unsteady wake formation, and (3) tunnel and atmospheric turbulence. All of these causes will exert a greater effect on tests run in the critical region, 3 to 10 feet per second for the 6-foot model, than on larger models with the resultant higher Reynolds number.

Presence of the dimple when the system is at an angle of attack is plausibly explained in terms of increased pressures over the windward side of the balloon and reduced pressure over the throat region due to the angle of attack.

Finally, a trip or separation fence may provide an effective mechanical means of balloon stabilization if needed, particularly at the lower flight altitudes.

Large Balloon Drop

The large balloon free drop was made to obtain a preliminary look at the over-all stability of larger sized balloons. In this drop the system descended approximately 1500 feet while inflating. During this period the envelope appearance and inflation characteristics were very similar to those previously observed with the six-foot models. At the completion of inflation, the envelope rotated approximately two revolutions in one direction and then slowly rotated one revolution in the reverse direction. Further rotation was random, slow, and self-damping. Descent was estimated to be at 15 to 20 fps. Since the drop occurred some distance from the camera, the image in the film was too small to justify any firm conclusions on the behavior of the fully-inflated balloon. However, there did not appear to be any observable tendency toward persistent indentation or instability.

Modified Model Envelope

The modification of the model envelope with the fence was the first try toward a mechanical fix of the instability problem. Such a fence should provide a well-defined flow separation line, as previously discussed. As seen in Figure 6, the tufts attached to the envelope surface indicate that the entire balloon surface behind the fence was in a region of separated flow when operating fully inflated in the spin tunnel.

With a total weight of 875 grams simulating the terminal descent of the 1000-pound system at about 15,000 feet altitude, the inflated modified balloon showed slight oscillation, no indentations, and some tendency to translate or wander in the tunnel. For the higher weight simulating the larger system at altitudes above 50,000 feet, the modified system translated about two balloon diameters and then stopped abruptly and reversed direction. This resulted in indentations in the fabric. In both cases the system would not rotate, even when a rotation was intentionally started.

Rates of descent from 8 to 14 fps were observed. These correspond to approximately the same drag coefficients as were reported for the basic wind tunnel model systems.

SUMMARY OF MODEL STUDIES

During the wind tunnel and associated studies, no phenomena or problems were encountered which would be expected to disprove the feasibility of the system concept or interfere with the orderly accomplishment of the full-scale flight tests. Envelope deployment was smooth and uneventful. The inflation of the envelope was positive, and while perhaps a little lengthy in duration, could be accomplished in a repeatable time. Also, the system was stable during the inflation period and exhibited a nearly constant drag of approximately the same magnitude as that of the fully inflated balloon. An instability problem was encountered when testing the fully inflated six-foot diameter model balloons. However, analysis indicated that this problem was caused by the critical Reynolds number range in which the models operated and probably should not be a problem with larger systems. Also, should the cold inflated instability problem occur again, wind tunnel tests of a modified six-foot model balloon indicate that a relatively simple fix is available, at least for the 1000-pound systems at altitudes up to 15,000 or 20,000 feet.

In general, the test observations suggest that from the inflation and stability standpoint the envelope throat opening should be as large as system heat loss considerations will allow. Furthermore, should the envelope configuration be redesigned to other than the natural shape, the lower section should probably be made more conical to eliminate the slack fabric observed in some of the tests and expedite inflation.

FULL-SCALE FREE FLIGHT PROGRAM

In all four full-scale flight tests, the basic flight test sequence, procedures, and equipment accomplished the tests as intended. Only the usual minor modifications and repairs were required during the course of the test program. Of particular importance to the over-all program results is the observation that in each test the system descending on the stabilization parachute was in stable, nearly vertical flight without rotations or oscillations during the period prior to the event. Also, in every flight the release of the vehicle rear closure clamp bands at event appeared to be clean, as did the start of the separation of the rear closure plate and the vehicle. Therefore, only the results dealing with the Paravulcoon system characteristics will be discussed in detail in this section. First, the specific results and observations of each of the four tests will be presented. These results will then be discussed in terms of the over-all flight test program.

Drop Test No. 1

The first drop test was essentially successful and the program objectives were 80 to 90 percent accomplished. As noted above, the test sequence was proven completely satisfactory; envelope deployment at this velocity was demonstrated; ram inflation of the envelope, albeit somewhat slow, was demonstrated; and the terminal cold-inflated stability of a system of this size and weight was demonstrated for altitudes below 11,000 feet. A system rate of descent in the latter mode considerably below the predicted value was also revealed. However, at about 1610 feet the top of the envelope failed and the system plummeted to a 160 to 170 fps ground impact with the balloon streamed. The envelope was damaged beyond repair. A smoothed trajectory plot of this test beginning just before the event is shown in Figure 29.
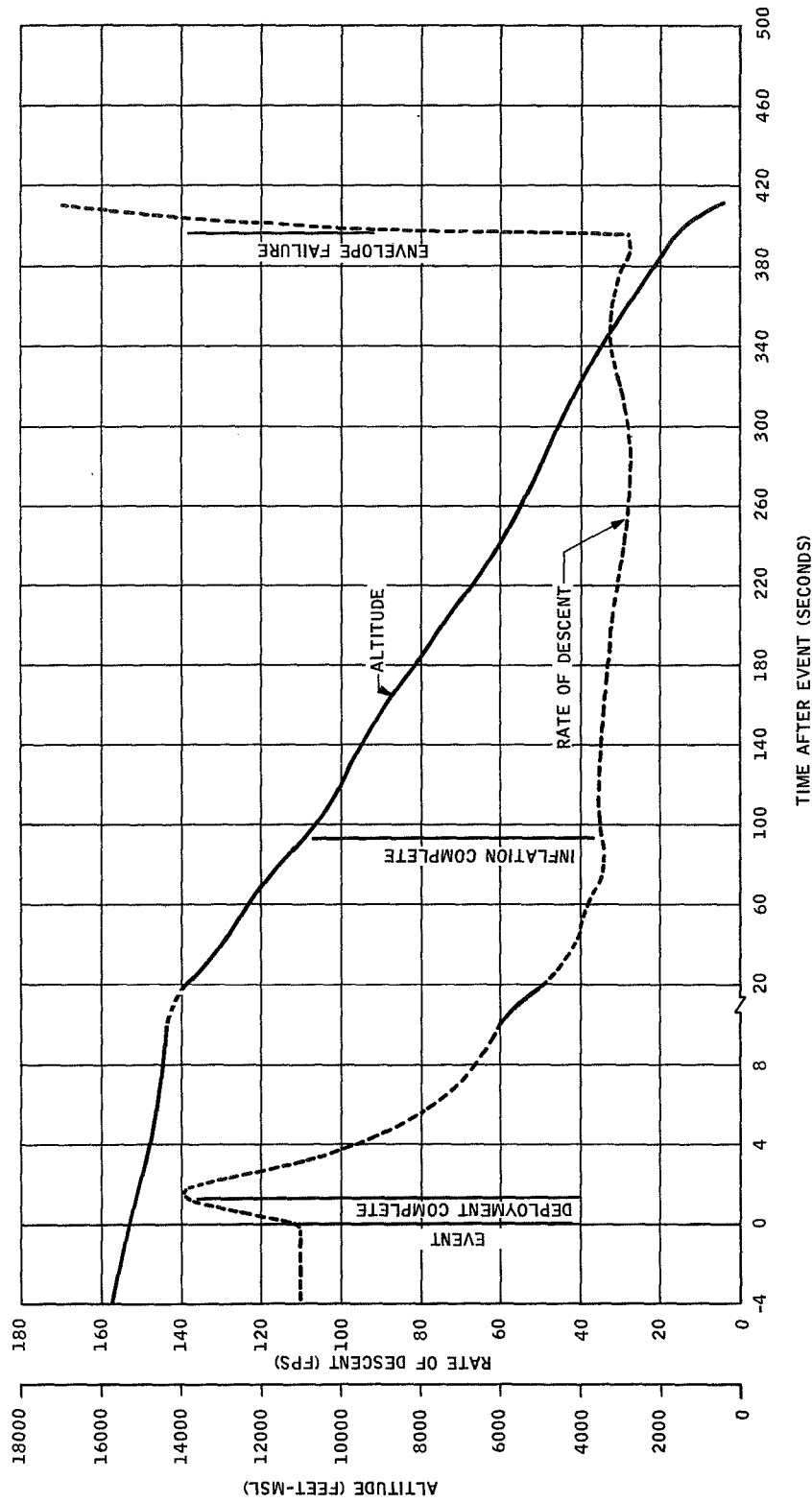
Figure 29. Smoothed Flight Test Trajectory – Drop Test No. 1

The deployment proceeded as had been planned and was very similar to the earlier model results. As the vehicle and the rear closure plate separated, the envelope streamed cleanly and rapidly from the deployment bag. Separation of the envelope crown from the break cord securing it to the deployment bag lid was clean and did not appear to cause any undue load on the envelope. It was agreed that use of the backup reefing line cutter on this cord was superfluous and unnecessary. This sequence required only about 1.3 seconds for completion. As shown in Figure 29, the system accelerated to a velocity of about 140 fps as it fell away from the parachute before the envelope began to inflate. The on-board accelerometer indicated peak axial loads on the vehicle of only 1 to 1.5 g's during this period.

Two phenomena were revealed during this deployment which had not been obvious with the model envelopes. When the envelope mouth cleared the deployment bag opening, it immediately ingested ram air which resulted in a flared out bubble of balloon which followed the deployment bag the full length of the envelope. Ground photographs of this phenomena are shown in Figure 30. Also, when streaming out, the envelope was pushed to one side by the strong crosswind (about 70 fps at event altitude). Thus, the envelope appeared to be coming out of one side of the deployment bag opening. This is not obvious in Figure 30, due to camera angle.

Envelope inflation began immediately after deployment, and, as indicated in Figure 29, the rapid buildup of system drag caused the descent velocity to drop from 140 fps to 60 fps within 10 seconds after event. In the initial phases, this sequence appeared quite similar to the inflation of the wind tunnel model envelopes. However, due to the much lighter relative weight of the fabric there was much more small scale motion in the 54-foot envelope. Descent during this period was stable at velocities ranging from 70 fps down to 50 fps. Peak axial loads on the vehicle of 2 to 3.5 g's were measured during this period. However, the steady load during this time was 1 to 1.5 g's.
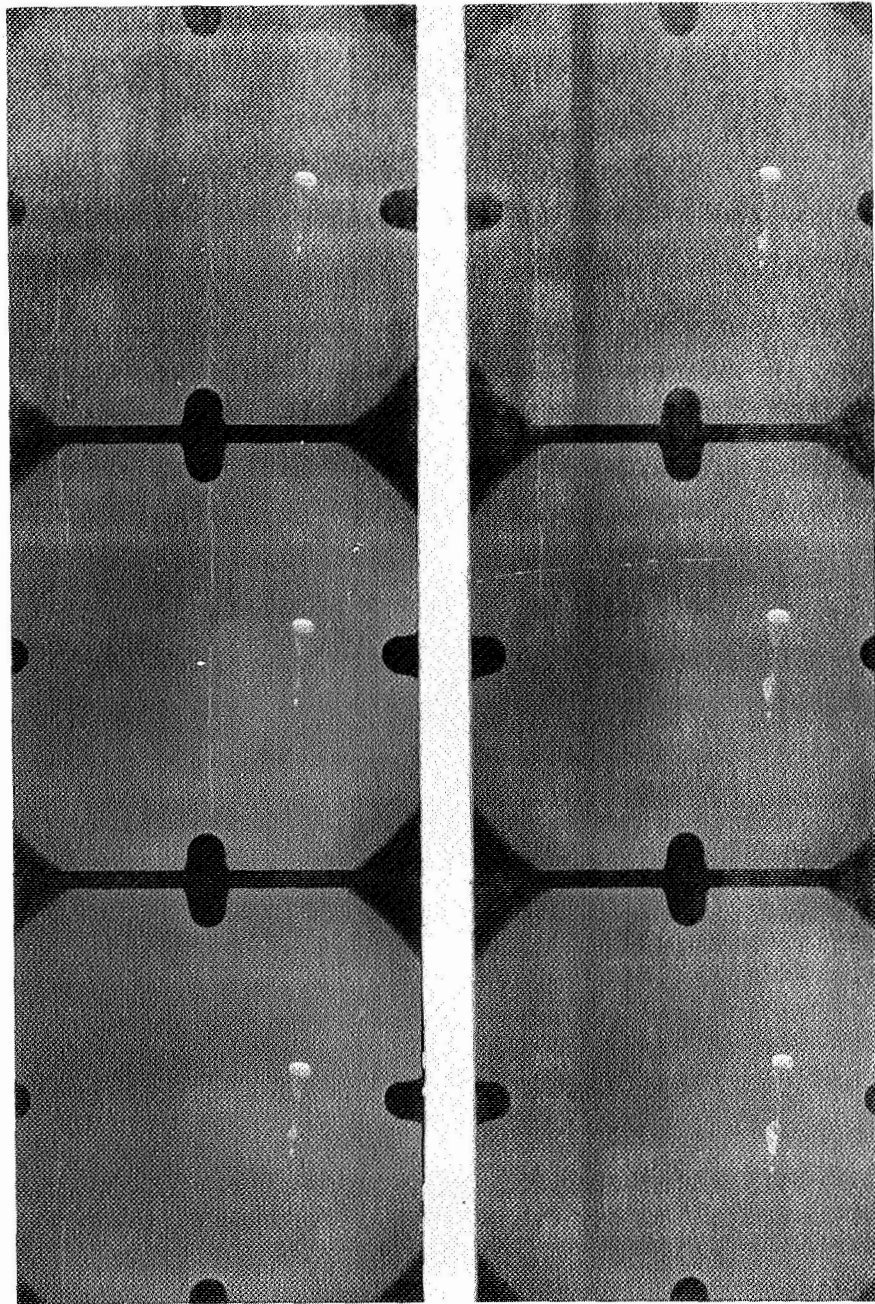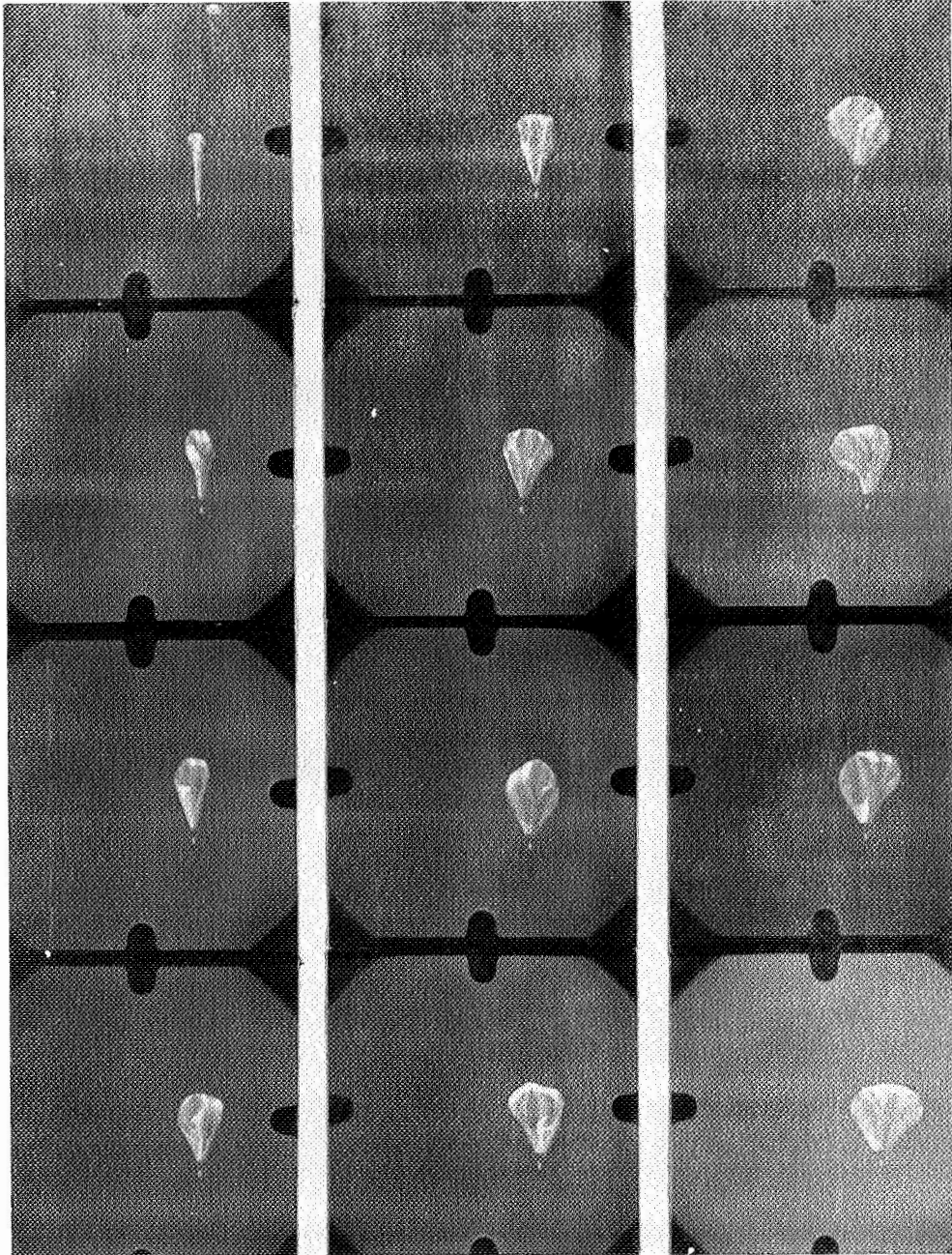
Official U. S. Navy Photograph

Figure 30.   Beginning of Deployment Sequence Showing Initial
Air Bubble - Drop Test No. 1

After inflation was 40 to 50 percent complete, envelope motions became much more serious. By this time enough air had been ingested to extend the envelope to nearly its full diameter, but the bubble inside was not large enough to keep the envelope fully expanded and prevent fabric flapping and breathing in and out. Thus, when the winds caused the throat to momentarily close, the lack of ram pressure inside the envelope allowed the fabric to move in and out. This was observed in the form of large dents running from the throat, sometimes all the way to the crown; a series of six indentations in and out of the entire envelope crown; indentations of the lower half of the envelope giving the balloon a mushroom shape; and other random motions, such as rapid ripples which ran from one end of the envelope to the other. (On the basis of frame counting in the motion pictures, the crown indentations required from 1.5 to 3.5 seconds per cycle.) These motions continued until inflation was about 90 percent complete and the air bubble inside was big enough to maintain the balloon shape against outside air forces. Descent velocities during this period ranged from 50 to 35 fps. While there were no peak axial forces recorded on the vehicle above 2 to 2.5 g's, those that were recorded showed very steep onset rates and had a short duration in spite of the damping effect of the envelope fabric and the load lines. Again, steady axial loads of 1 to 1.5 g's were noted. As the inflation neared completion, the shape of the acceleration record changed from that of a nearly steady level marked by sharp peak loads to a series of more gradual but smaller (less than 2 g's) peaks. The magnitude of the various local forces between different sections of the envelope fabric as a result of the random motions appears impossible to estimate. Figure 31 (a and b) presents ground photographs of some of the configurations taken by the balloon during inflation. The tendency of the throat to close off much of the time is quite apparent in these photographs. Complete inflation was achieved about 93.5 to 94 seconds after the event at an altitude of about 10,800 feet (4500 feet below the event).

Once inflation was complete, balloon motions during the terminal cold descent were relatively small. The envelope was somewhat out of round, causing the system to descend in a position tilted slightly to the vertical. Rotations of the

Official U. S. Navy Photograph

Figure 31. Envelope Configuration During Inflation - Drop Test No. 1

(a)
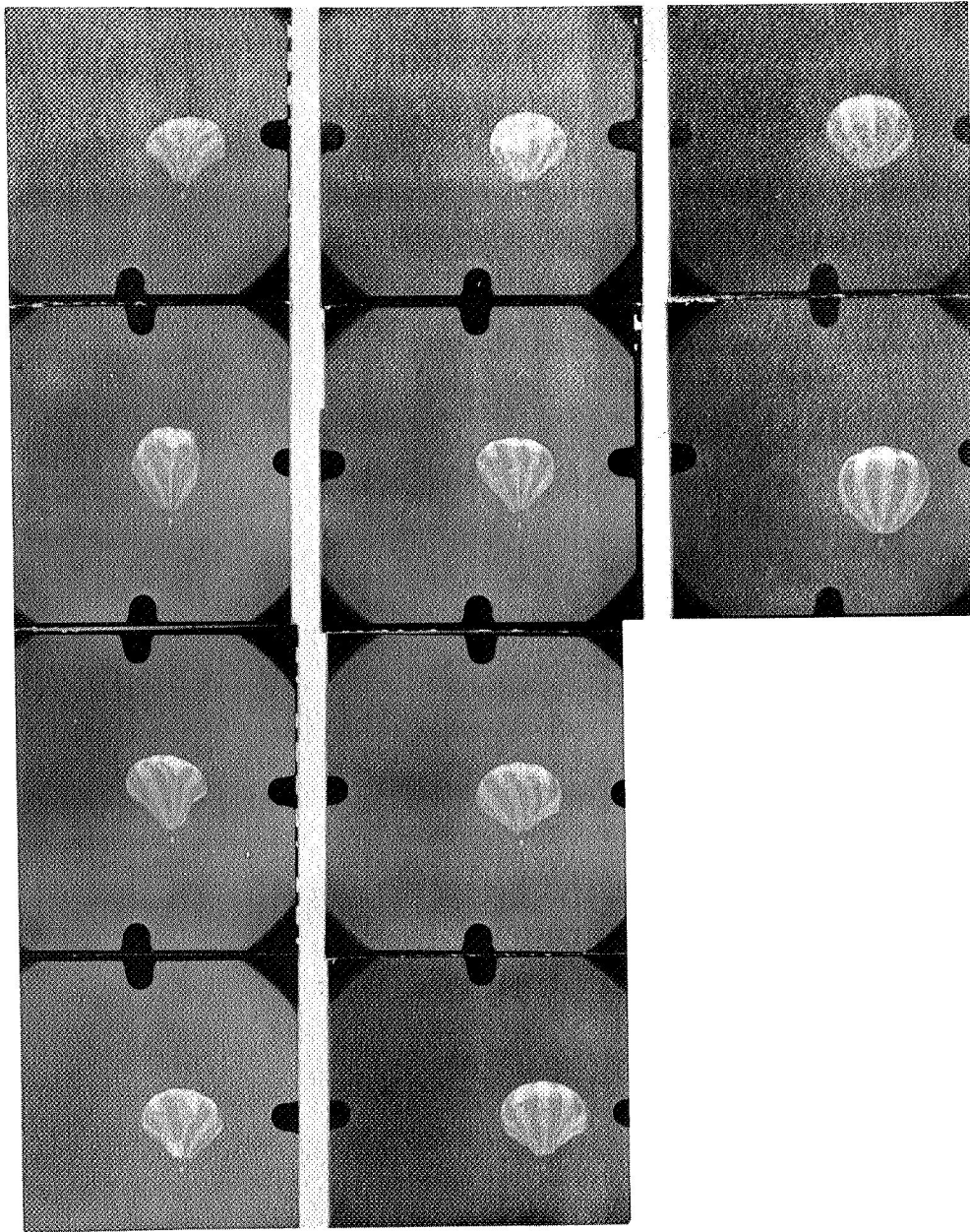
Official U.S. Navy Photograph

Figure 31. Envelope Configuration During Inflation - Drop Test No. 1
(Continued)

(b)

system were slow and were damped out within 180 degrees or less. There did not appear to be any preferred direction of rotation. No coning occurred and system oscillations were not readily apparent in the high spread motion pictures. However, review of the oscillation plots derived from the space position data revealed that small oscillations were actually present. Swings of up to seven degrees to either side of the tilted mean position of five or seven degrees off the vertical were measured. The frequency of these motions was about six cycles per minute. Reported wind velocities varied from 66 fps at the completion of inflation to 23 fps at the time of the failure. Rates of descent from 25 to 27 fps were observed during this phase.

No photographs of the terminal failure were obtained because all cameras had already expended their film. However, following the test the envelope was carefully studied, and the damage was reconstructed as diagrammed in Figure 32. Several of the reinforcing tapes in the crown showed evidence of "working" and loosening of the stitching. One of these tapes showed a frayed failure and was probably the point where total failure began. It was concluded that in the effort to reinforce the crown against possible deployment loads, areas of stress concentration, and unequal stretching resulted where the differing thicknesses of material were joined. Thus, the eventual failure was probably caused by the weakening of the structure during the many and sometimes violent motions encountered during the inflation period.

As a consequence of this failure, it was decided that the original envelope design should be revised before continuing the test program and that a second test should be made at the 100 fps event velocity. Thus, the subsequent tests all used envelopes of the simulated variable thickness design previously described.

Drop Test No. 2
_____

The second drop test was completely successful, and the program objectives were 100 percent accomplished. As had been predicted, the envelope ruptured
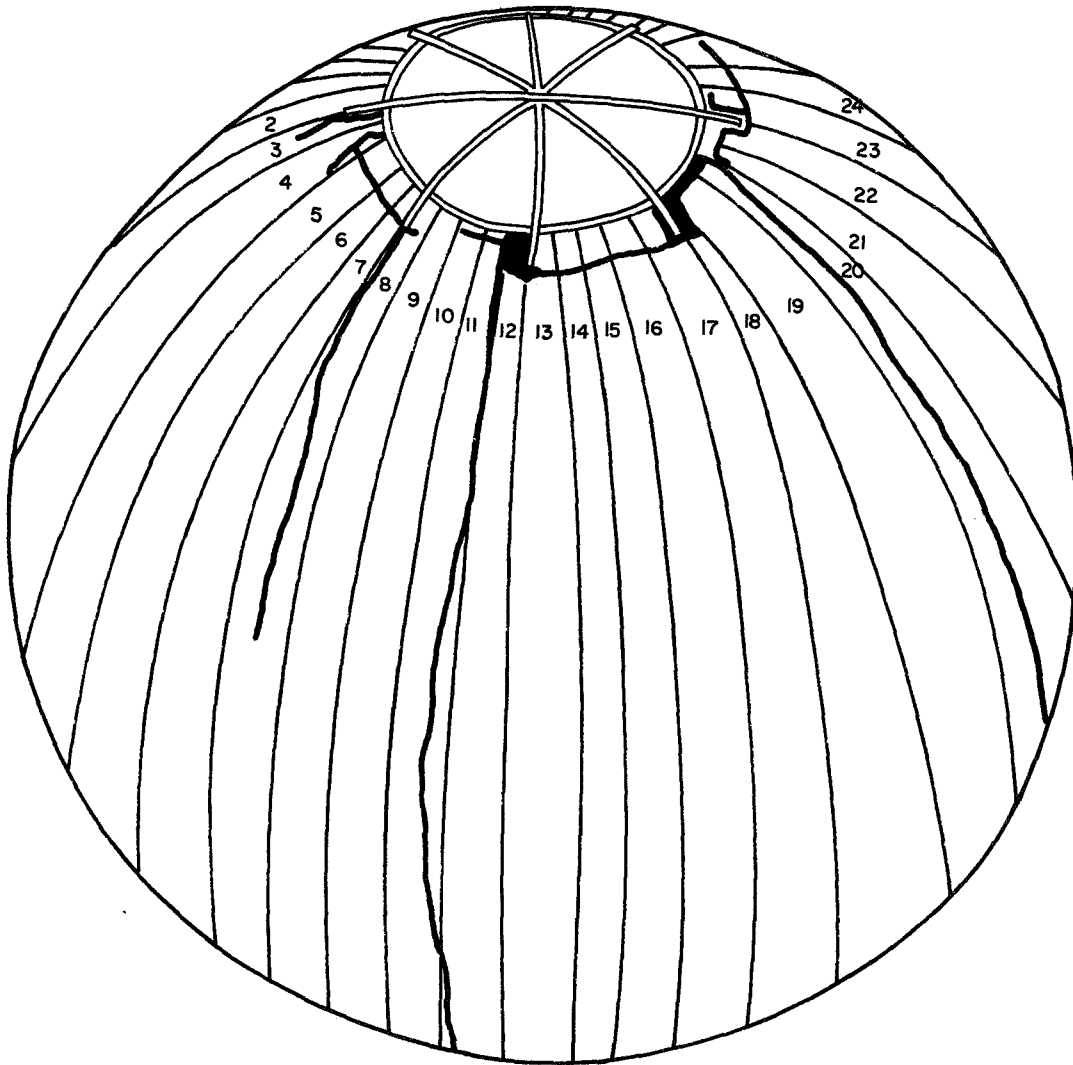
Figure 32. Envelope Damage Diagram - Drop Test No. 1

at the instant of ground impact and was severely damaged. Figure 33 shows
the "smoothed" trajectory for this flight, and it can be seen that the over-all
performance was very similar to Drop Test No. 1. However, during this
test the wind velocities at the various altitudes were only one-half to one-third
of those encountered in the previous drop.

As shown in Figure 34, deployment was about the same as in the first test,
except that the flaring of the envelope due to the initially ingested air bubble
was perhaps a little greater. The streaming from one side of the deployment
bag resulting in a question-mark shape near the end of deployment, followed
by a tendency to "whip-snap" the end of the envelope, was again present.
However, no difficulties were encountered. Frame counting in the motion
pictures revealed the following values for this sequence:

Explosive bolts fire	0	seconds
Rear closure off	0.18	
Deployment bag open	0.48	
Deployment complete	1.5	

A peak axial load on the vehicle of 2.2 g's was recorded just at the end of
deployment. No other peaks were recorded.

The inflation period was similar to Drop Test No. 1, except that the envelope
motions were much less violent, particularly during the second half of the
period. This may have been due to the revised crown design, or the lower
crosswinds aloft, or both. While again there were many fabric motions and
the same moving, sharp-edged folds in the material, the large-scale indenta-
tions in the envelope were not as severe. Two or three slight indentations
of the crown were observed, but they were not as pronounced as those in the
earlier flight in either amplitude or rate. As shown in Figure 33, the velocity
history was also about the same, with full inflation occurring about 95 seconds
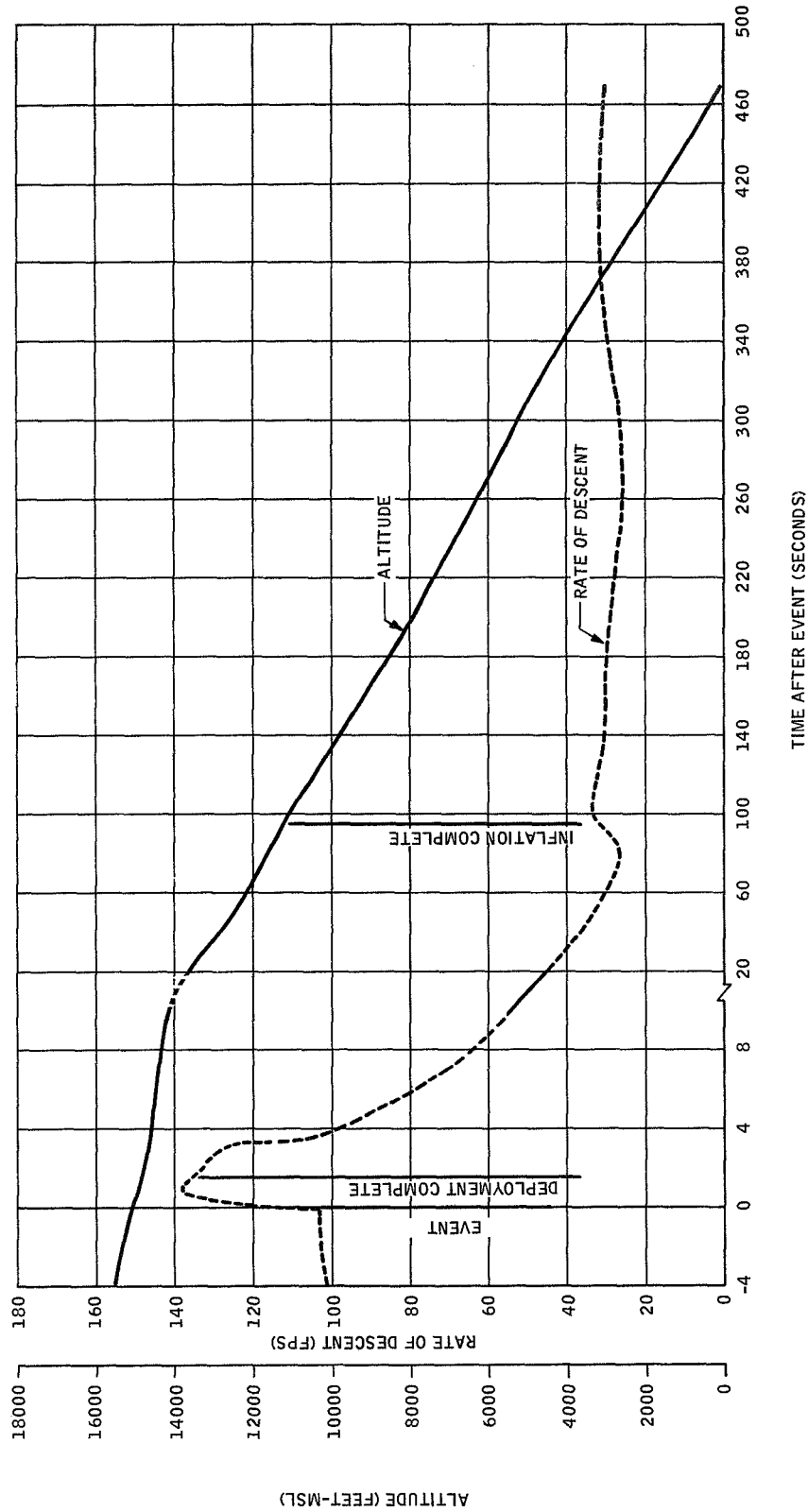after, and 3900 feet below event. In the early part of inflation, a few peak

Figure 33. Smoothed Flight Test Trajectory – Drop Test No. 2
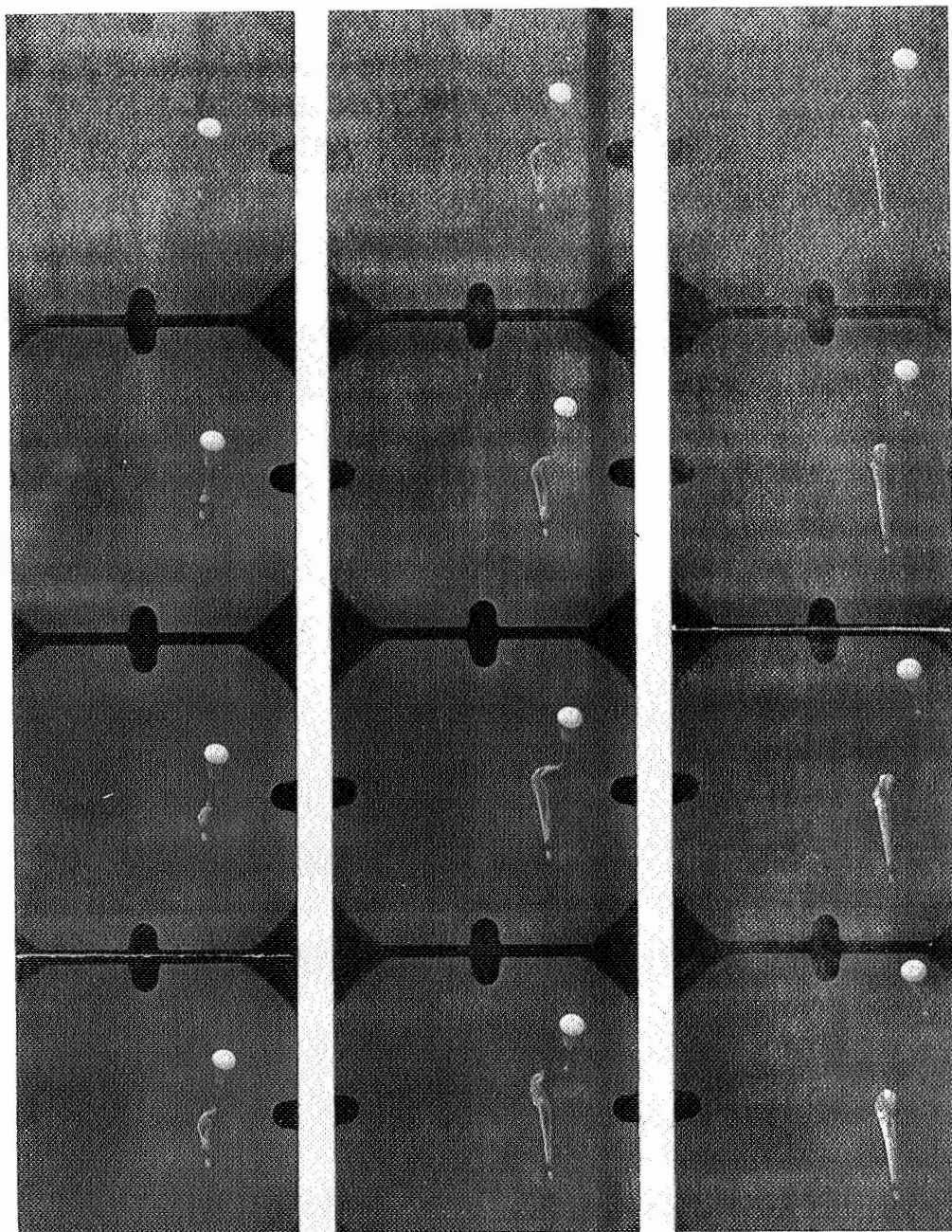
Official U.S. Navy Photograph

Figure 34. Deployment Sequence - Drop Test No. 2

axial loads of 1.4 to 1.8 g's were recorded. However, during the remainder of the flight, relatively steady loads of about 1 g were observed. Ground photographs of the inflation sequence are shown in Figures 35a and b.

Terminal cold descent, as shown in Figure 36, was similar to Drop Test No. 1, and again a low (25 to 33 fps) rate of descent was observed. This balloon was also distorted out of round and oscillations of 6 to 7 degrees around a 7- to 9-degree tilt were measured at about 8 cycles per minute. No coning occurred, and the slow system rotations were damped out within 360 degrees.

It was also found that one of the load lines was shortened by fouling with one of the clamp bands. Range safety prohibited the free jettisoning of these bands and so they were retained on the vehicle by cables after the deployment event. For the subsequent tests, springs were added to prevent a repetition of such fouling.

Post-test examination revealed no indications of fault or weakening in the revised envelope crown design. The envelope was repaired for use in a later test.

Drop Test No. 3

In this flight deployment began normally, but before it was completed the top of the envelope failed and the system plummeted to impact at about 165 fps. The test trajectory is plotted in Figure 37. It is interesting to note that this deployment was attempted at approximately the equilibrium descent velocity for the test system with the envelope in the streamed configuration. Due to the extensive damage incurred during the long fall, the envelope was a total loss, and it was impossible to reconstruct the manner of fabric failure. However, post-test examination of the vehicle, rear closure plate, and deployment bag did not reveal any abnormalities, except that the break cord had broken in the middle rather than at a knot as expected.
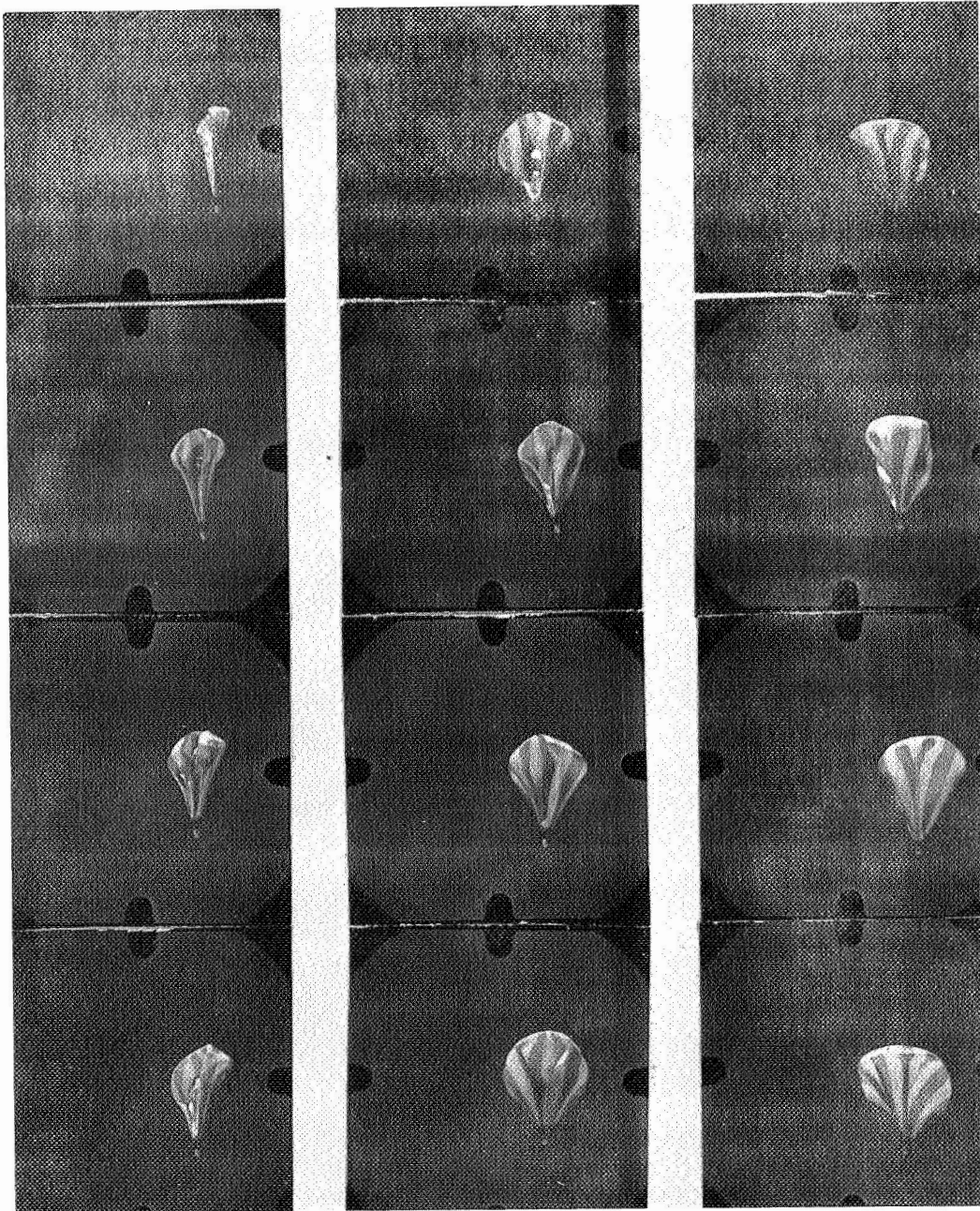
Official U.S. Navy Photograph

Figure 35. Inflation Sequence - Flight Test No. 2

(a)
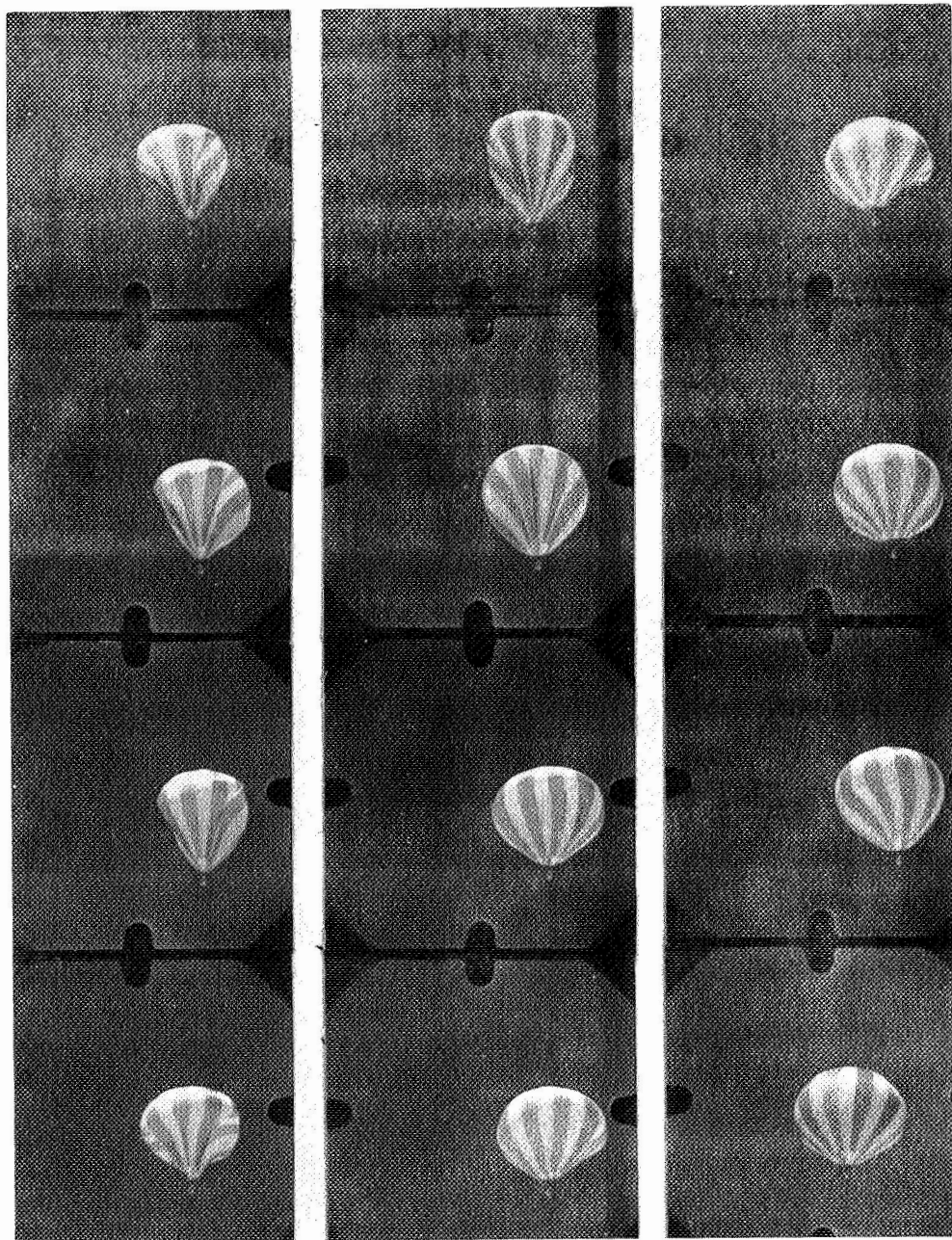
Official U. S. Navy Photograph

Figure 35. Inflation Sequence - Flight Test No. 2 (continued)

(b)
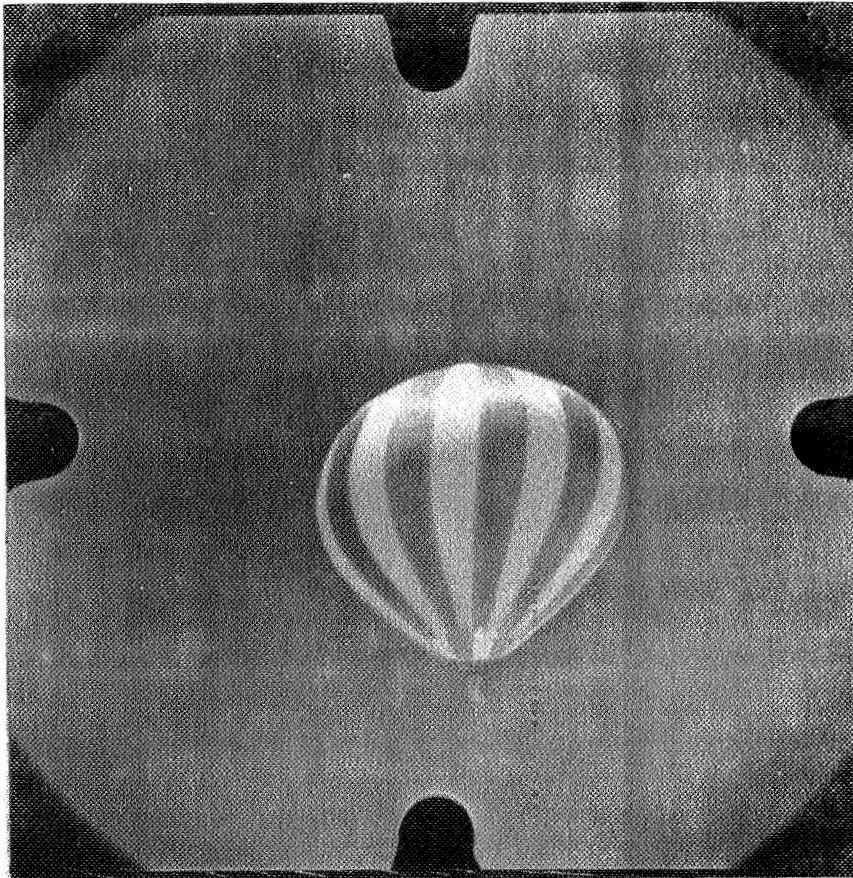
Official U.S. Navy Photograph

Figure 36. Fully Inflated 54-Foot Paravulcoon in Cold Terminal Descent
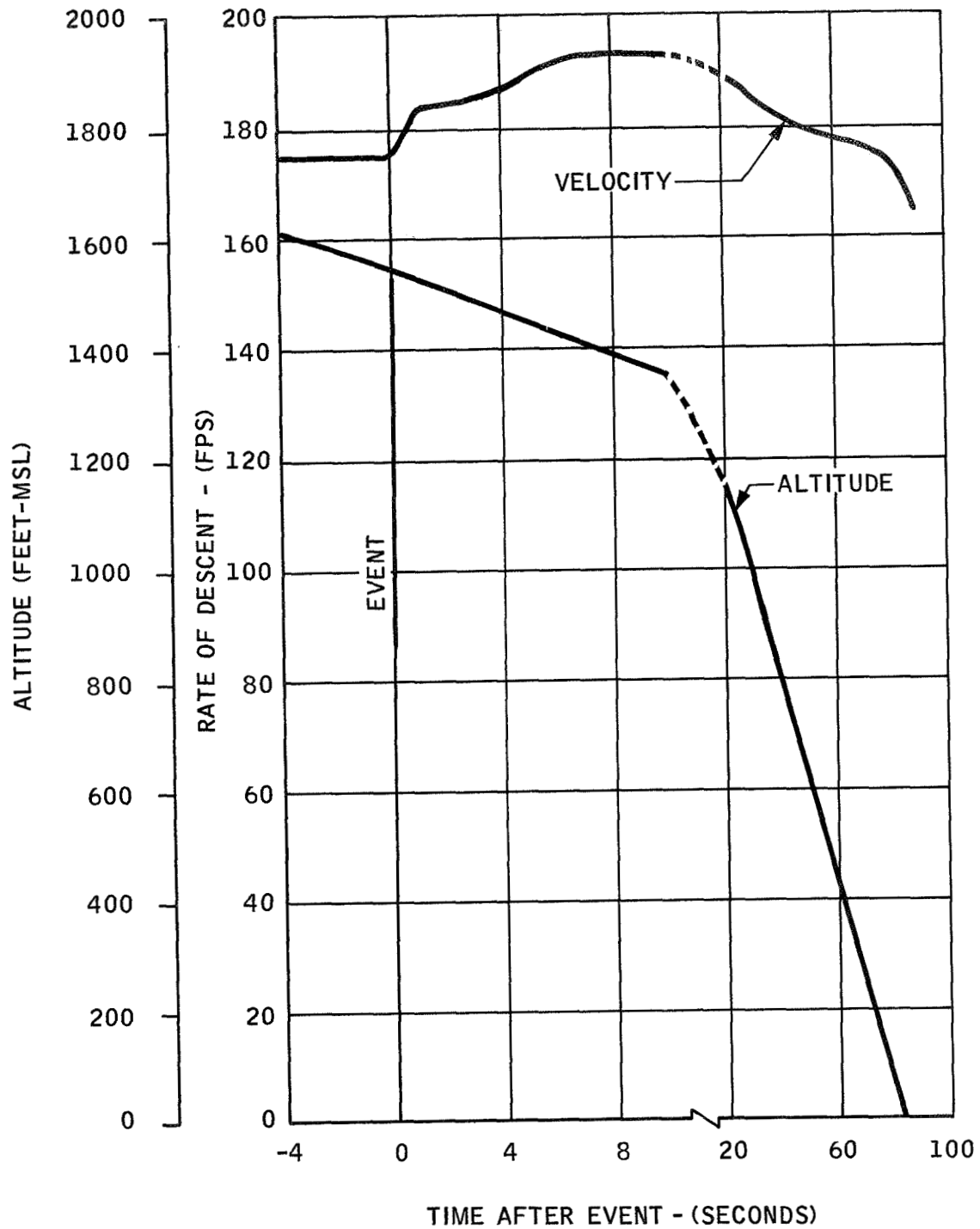
Figure 37. Smoothed Trajectory - Drop Test No. 3

Study of the test films revealed that at this higher dynamic pressure (about double the previous value) the bubble of initially ingested air was several times larger and followed closely behind the moving deployment bag. Thus, the envelope immediately flared out into a partially inflated balloon with the moving deployment bag in the center. Then, when the envelope was 75 to 80 percent deployed, the break cord broke prematurely, and the remainder of the packed envelope dropped out of the deployment bag in a wad. Apparently when this mass of folded material fell into the oncoming ram air bubble the envelope was subjected to a local overpressure which the folded material could not relieve quickly enough, and a local fabric failure occurred. The telemetry record substantiates this explanation, based on local envelope overstressing, as no axial loads on the vehicle over 1. 8 g's were noted during the first 1. 5 seconds after the event.

It was agreed that while deployment with an open envelope throat can be accomplished at 100 fps and a dynamic pressure of 10 psf, the ram air ingestion cannot be accommodated during the streaming of the envelope in a dynamic pressure of 20 psf. Thus it was decided that for the tests at higher dynamic pressures the throat would have to be temporarily reefed. Since the motion of the ingested air bubble up around the deployment bag seemed to create a region of reduced pressure in the center similar to the sucking in of the crown of large parachutes when they are deployed, there was also concern about the early breaking of the break cord. In view of this, a rig of two parallel break cords of different lengths was made for the next test, along with the throat reefing rig previously described.

Due to this deployment failure, it was necessary to rerun the same deployment event conditions with the modified rig in the next test.

Drop Test No. 4

In this test the system performed as planned, and the test was a complete success. Deployment and inflation were satisfactory, and terminal cold descent was stable. Again the envelope ruptured on ground impact. The smoothed trajectory is plotted in Figure 38.

At deployment, the envelope streamed cleanly from the deployment bag with the throat reefed. No air bubble was ingested, and the break cords appeared to hold until the envelope was fully streamed. During the deployment, an S-shaped bend in the streaming envelope followed by a whip-snap of the tip were observed. When the throat was disreefed, inflation began smoothly without any sudden bubble action. This sequence is shown in Figures 39a and b. In these pictures the throat is reefed through the last frame of Figure 39a and is just beginning to disreef in Figure 39b. Deployment required about one second, and no axial loads on the vehicle were recorded. A series of short peak loads around 2 g's were noted between one and three seconds, with a maximum value of 2.2 g's.

Inflation proceeded approximately as in Drop Test No. 2 with similar envelope motions and stable flight. As shown in Figure 38, the same rapid deceleration during the first 10 seconds to velocities of 70 fps and below was again noted. This seems to confirm, as had been heretofore believed, that system inflation is relatively independent of the deployment event velocity provided the initial envelope streaming can be sustained. During this period, peak loads of up to 3.5 g's with a 1- to 1.5-g steady load were measured. Only the steady load was measured during the remainder of the inflation which required a total of 99.5 seconds and 4690 feet for completion.

The terminal cold inflated descent was essentially the same as in Drop Test Nos. 1 and 2, but with more envelope distortion than in the other tests. Measured oscillations were approximately 7 degree swings around a 7- to 8-degree tilt angle at about 6 cycles per minute. While there was no coning, there seemed to be some insipient tendency for the system to rotate.
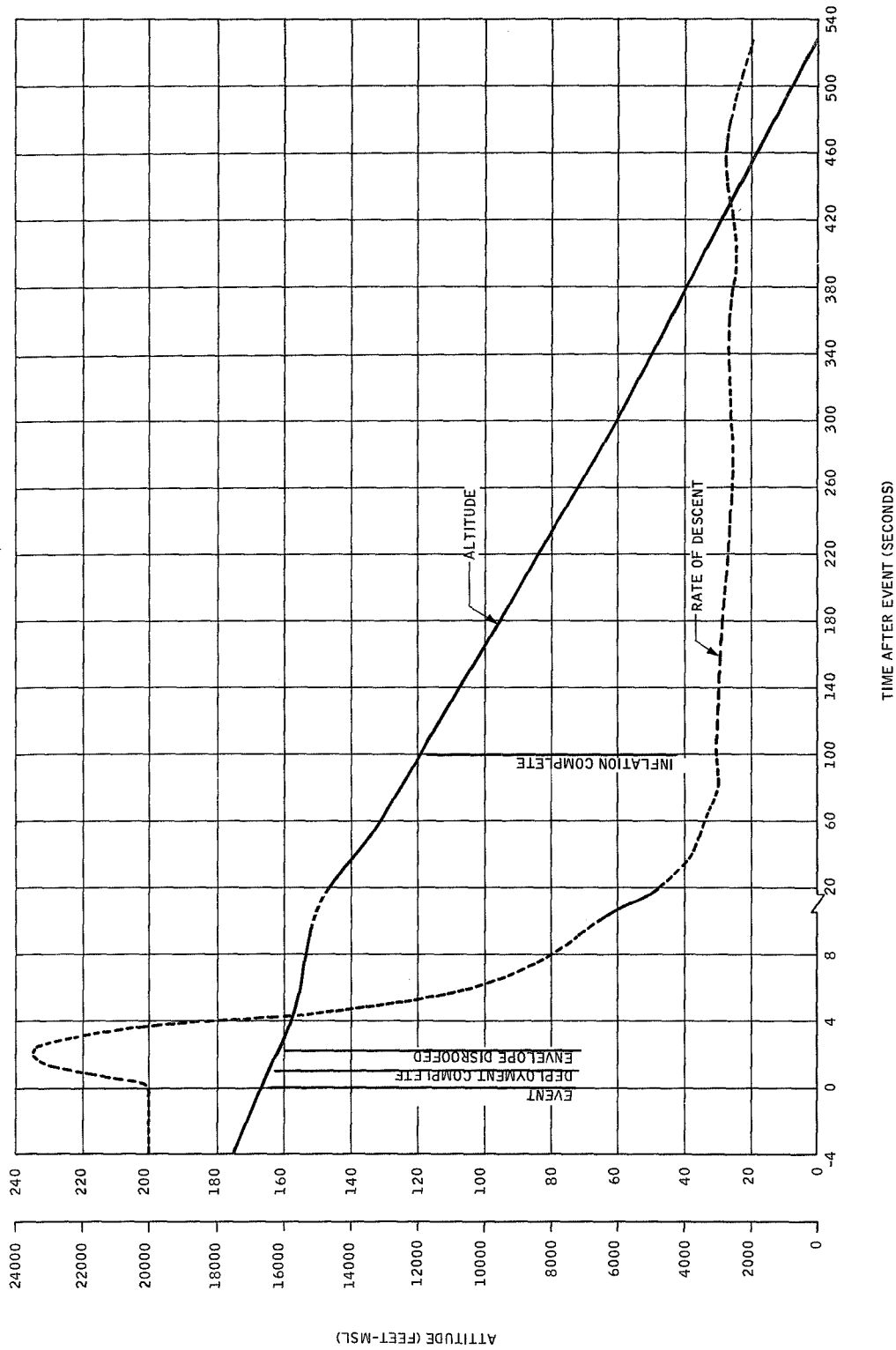
Figure 38. Smoothed Trajectory – Drop Test No. 4
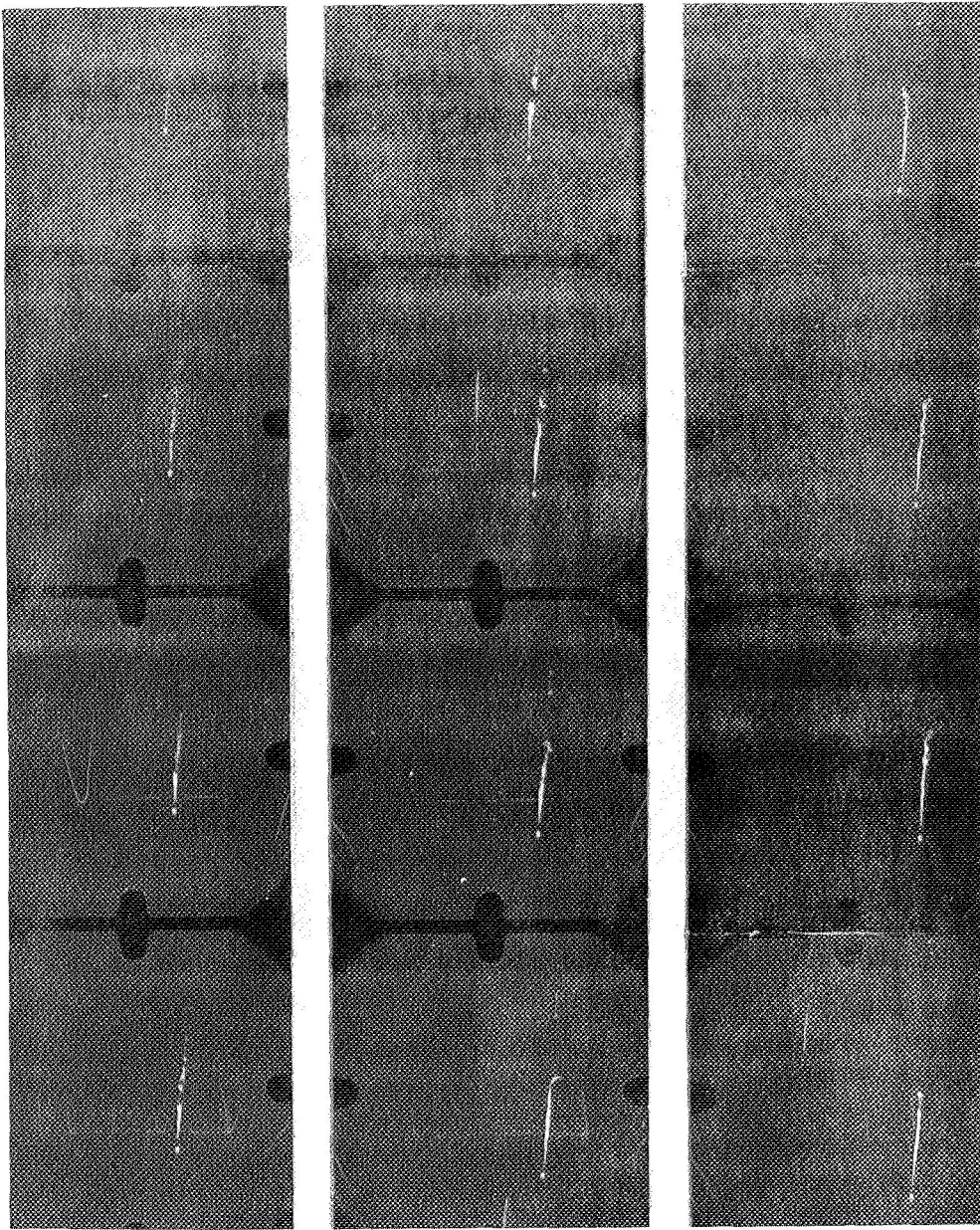
Official U. S. Navy Photograph

Figure 39. Deployment of Temporarily Reefed Envelope -
Drop Test No. 4

(a)
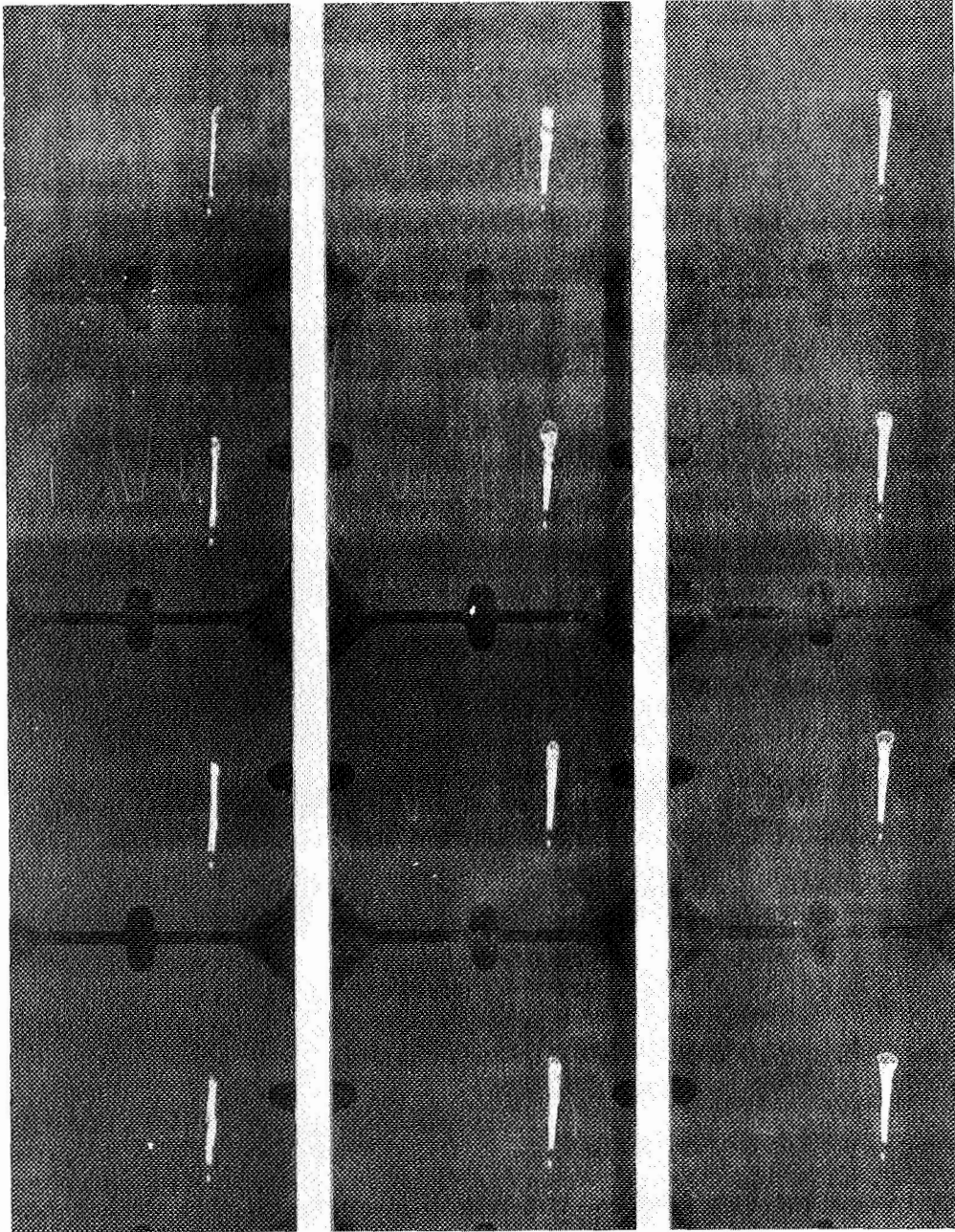
Official U. S. Navy Photograph

Figure 39. Beginning of Inflation of Temporarily Reefed Envelope
Starting from Envelope Disreef - Drop Test No. 4

(b)

The up-camera on this flight revealed two significant features of the test very clearly. The temporary reef of the throat was shown to have performed exactly as planned. Even more important was the action of the throat during the inflation. These pictures showed that the throat tended to be closed off above its opening a substantial percentage of the time until the envelope was almost fully inflated.

Ground examination of the balloon revealed the jagged hole in the apex of the envelope shown in Figure 40. This hole was approximately 16 inches in diameter and passed through all the overlapped gore layers. The apex lifting web was also missing. Examination of the deployment bag revealed that both break lines had broken at the knots next to the envelope and none of the missing pieces were attached. The missing pieces were not recovered. This hole may have been caused by (1) possible damage to the apex area when tensioning the envelope for folding and packing, (2) the initial inrush of air following the dis-reef of the throat, and (3) the whip-snapping at the end of deployment, or a combination of these. The third reason seems most likely, as in the test motion pictures there appeared to be some small pieces shed at that instant. Also, the up-camera photographs showed the hole to be present as soon as the throat had opened sufficiently for the camera to see the apex of the balloon. It is believed that this hole was too small to have any influence on the over-all inflation or aerodynamic characteristics of the system.

The flight test program was concluded at this point without attempting a deployment at 300 fps because, due to the damage incurred during the tests, there were no usable balloons left for use in another test. Funding was not available for fabricating additional balloons.

General Results and Discussion

In these four flight tests the basic program objective was demonstrated: It is feasible to aerially deploy a Paravulcoon 54 feet in diameter with a 1000-pound

Official U.S. Navy Photograph

Figure 40. Hole in Envelope Apex - Drop Test No. 4

payload at dynamic pressures up to at least 29 psf and then aerially inflate
the balloon with ram air. Furthermore, it was shown that the inflation char-
acteristics of the system are relatively independent of the deployment velocity.

Deployment was relatively simple at dynamic pressures up to at least 10 psf.
However, when deployment was attempted with a dynamic pressure of about
20 psf, the need for a positive control to prevent ingesting air into the envelope
before it has been streamed to its full length was vividly demonstrated.
A simple and reliable temporary reefing scheme will have to be developed
before operation at higher dynamic pressures is attempted. On the other hand,
with such a scheme the major limitation on deployment dynamic pressure would
appear to be the ability of the envelope to survive the whipping and flag waving
it is subjected to when in the reefed configuration. While the effect of dynamic
pressure on deployment is quite clear, insufficient tests were made in this
program to distinguish between these effects and the effects caused by deploy-
ment at high velocity. The latter would be expected to be primarily dynamic
in character.

Using this approach, the inflation mode should proceed as observed in these
tests inasmuch as system deceleration seemed to begin as soon as the envelope
was deployed to its full length. Thus, the maximum velocity which the balloon
would be subjected to as it starts to inflate would be the equilibrium descent
velocity of the system with a streamed balloon. The system drag coefficient
in this configuration was estimated from Drop Test No. 3 to be 0.0175, based
on the cross-sectional area of the inflated balloon. Based on the banner area
as used in Reference 5 (length × width of the streamer), a value of 0.188 was
estimated. This value is consistent with extrapolation of data from Reference 5
and the values obtained in the wind tunnel phase of this program.

Envelope inflation was consistent and positive and thus completely feasible.
Starting from a dynamic pressure of about 20 psf, 95 to 100 seconds and
4000 to 5000 feet of descent were required to complete inflation. Since the
system decelerated to velocities below 70 fps during the first 10 seconds of
flight (including deployment), the velocity at the beginning of inflation does not

appear to have a significant effect on the inflation time or distance. However, although the system was completely stable during this period, the motions of the envelope fabric were more severe than would be desired from the stand-point of stresses of the envelope. Thus, it appears that the inflation performance could be greatly improved by using a positive inflation control during the middle portion of this sequence (from about 30 to 85 percent inflated). Such a system would positively hold the throat open, first at a reduced diameter to preclude too sudden inflation and then at successively larger diameters, to prevent the choking off of the throat and aid in a more rapid and less violent inflation. Although they have heretofore been primarily used as supersonic inflation aids, peripheral inflation scoops might also be useful to speed inflation without over-loading the envelope.

Once a temporary reefing scheme and a positive inflation control have been perfected, there does not appear to be any apparent obstacles to the orderly development of aerial deployment and inflation of larger balloons at moderate speeds or the deployment of 50- to 60-foot balloons at higher dynamic pressures.

The over-all system performance for the three successful full scale free flight tests is summarized in Table 9.

In spite of the obvious dynamic scaling difficulties previously discussed, the wind tunnel model systems reasonably simulated the over-all deployment per-formance observed in these tests. However, while the initial sudden inges-tion of air as the envelope streamed from the deployment bag could be discerned in the wind tunnel films, it was not readily apparent. Thus, the excessive fabric stiffness and weight in the model envelopes prevented prediction of the type of deployment loads which caused the failure in Drop Test No. 3. Also, the effect of cross winds was not modeled. Similarly, the gross inflation per-formance, including the tendency of the balloon throat to be blocked much of the time, was very well modeled. On the other hand, the rapid small scale fabric motions which occurred during inflation were not present in the scale-wise heavier and stiffer model envelopes.

Table 9. Summary of Full Scale Free Flight Tests

Drop Test Number	1	2	4
Event Conditions			
Altitude (feet)	15, 300	15, 107	16, 690
Velocity (fps)	111	105	204
Dynamic Pressure (psf)	10. 0	8. 1	29. 3
Deployment Time (seconds)	~1. 3	~1. 5	~ 1. 0
Complete Envelope Inflation			
Time (seconds)	93. 5	95	99. 5
Distance (feet)	4, 500	3, 400	4, 690
Terminal Descent			
Average drag data from reduced tabulated flight data from 2, 000 to 10, 000 feet			
$C_D S$ (ft^2)	1, 160	1, 133	1, 150
C_D (based on envelope cross section)	0. 500	0. 488	0. 496
From equivalent S. L. rate of descent calculated by range			
Rate of Descent (S. L.) (fps)	25. 2	27. 8	21. 7*
C_D	0. 636	0. 523	0. 872*

*Slow rate of descent and high equivalent drag coefficient probably due to distorted shape of balloon observed during this test.

Although there was some balloon distortion and oscillation in the terminal
phase of the full scale systems, it differed from the oscillations and dimpling
observed with the light weight wind tunnel models which simulated the larger
system descent at 15,000 feet. In the 54-foot balloons, the distortion was more
of an indentation than a dimple, even though the wind tunnel model fabric was
relatively stiff. This indentation remained in a single position; it did not
form, collapse, and reform with the oscillations. There was no movement of
the envelope fabric through the indentation and with exception of Drop Test
No. 4, there was no consistent direction of rotation. Thus, on one hand it
could be inferred that the terminal performance of the large balloon was an
incipient form of the instability encountered with the model systems and as
such was predicted by the wind tunnel studies. If this was the case, the coning
encountered with the heavier models would suggest that the 1000-pound systems
would experience a similar problem if operated in the 50,000- to 60,000-foot
altitude range.

On the other hand, there were enough differences between the performance of
the wind tunnel and full scale systems to suggest that this was not the case
and that the larger systems were essentially stable. Rather, their distortion
and motions could have been the result of descending through a cross-wind or
of asymmetries in the envelope construction. (The envelope used in Drop
Test No. 4 - where there was the greatest distortion - had been patched on one
side and so could have been subject to unequal elongations of the patched and
unpatched portions under the terminal descent loads.)

While there is some inconsistency in the terminal drag data shown in Table 9,
a system drag coefficient of about 0.5, based on the horizontal cross-sectional
area of the balloon, can be conservatively concluded from these flight tests.
Although this is considerably higher than the value for a spherical shape, the
values measured in the wind tunnel with the lightweight models (15,000 feet)
were in the same range and higher. It is thus possible that there was sufficient
distortion in the larger balloons to tend to approach these values.

SECTION VII
CONCLUSIONS AND RECOMMENDATIONS

Although a reduced number of flight tests were accomplished, the principal program objective was attained. Namely, the basic feasibility of the concept of aerially deploying and inflating envelopes has been experimentally demonstrated in both wind tunnel model tests of 6-foot diameter models and free flight tests of 54-foot diameter balloons with a 1000 pound simulated payload.

The following general conclusions have been drawn from this study:

- Deployment of the envelope by streaming it out of a deployment package was found to be simple, practical, and reliable in both the model and full scale systems at velocities up to 204 fps and dynamic pressures up to 29 psf. However, for dynamic pressures above about 10 psf the Paravulcoon envelope throat must be reefed until the envelope is fully extended.

- Inflation of the Paravulcoon envelope by ingestion of air through the throat opening in its base is feasible. The time and distance required for inflation is consistant and repeatable. Since this time is relatively long, due to the tendency of the balloon throat to close off a large percentage of the time, a more practical system can be attained by providing a positive control of inflation. This will reduce the time required for inflation and thus reduce the severity and duration of the envelope motions and the accompanying stresses in the balloon fabric during the inflation period.

• A terminal instability problem was encountered with the small models, but the full scale system was found to be completely stable during the deployment and inflation phases of its activation sequence. These systems also appeared essentially stable during cold terminal descent, but some envelope distortion, small scale system oscillations, and slow damped rotations were encountered. Those were not considered serious enough to warrant a mechanical "fix".

• An average system drag coefficient of about 0.5 was found for the equilibrium cold descent of the system. Almost as large a value was observed during most of the inflation phase.

• Once the envelope had been deployed to the streamed configuration, the system descent velocity rapidly approached the equilibrium value for that configuration. Thus, the remainder of the inflation phase was found to be relatively independent of the deployment event conditions.

• No factors were encountered during this program which would be expected to hamper the reasonable extension of system capabilities with regard to balloon size and the severity of deployment event conditions or to prevent the orderly development of a practical system.

With regard to the last of these conclusions, continued study and testing are recommended in the following areas to expedite the development of a Paravulcoon System ready for practical application:

• Deployment and inflation including:

    Larger envelopes

    Higher deployment velocities and dynamic pressures

    Positive inflation control

    Temporary reefing during deployment

    Optimum envelope shape

- Initial and sustaining heat sources and their control.

- Flight test of a small system containing all the basic system components to demonstrate the overall system concept.

- Comprehensive study of the loads and stresses associated with the deployment and inflation of the Paravulcoon envelope.

SECTION VIII
REFERENCES

1. "A Document to the Marshall Space Flight Center, Paravulcoon Recovery System for the Saturn C-5 Booster," Technical Document 87762, Volume I. Honeywell Inc., in cooperation with Raven Industries, Inc., 28 March 1962.

2. Neihouse, Anshal I., and Pepoon, Philip W., "Dynamic Similitude Between a Model and a Full-Scale Body for Model Investigation at Full-Scale Mach Number," NACA TN 2062, March 1950.

3. Heinrich, H. G., and Haak, E. L., "The Drag of Cones, Plates, and Hemispheres in the Wake of a Forebody in Supersonic Flow," ASD Technical Report 61-587, December 1961.

4. Nebiker, F. R., "Feasibility Study of an Inflatable Type Stabilization and Deceleration System for High Altitude and High Speed Recovery," WADD Technical Report 60-182, December 1961.

5. Hoerner, Sighard F., Fluid-Dynamic Drag, 1958.

APPENDIX A
WIND TUNNEL STUDY DETAILS

APPENDIX A
WIND TUNNEL STUDY DETAILS

MODEL DETAILS

All load line lengths were based on the throat - forebody geometry shown
in Figure A1.. The various model details are given in Table A1.

Table A1. Model Variation Details

Material Type (oz/yd^2)	Material Weight (lb/ft^2)	Throat Percentage	Throat Diameter (inches)	Forebody Diameter (inches)	Load Line Length (inches)
1.1	0.01	25	18.0	6	6.72
1.1	0.01	25	18.0	3	8.74
0.8	0.008	20	14.4	6	4.57
0.8	0.008	25	18.0	6	6.72
0.8	0.008	30	21.6	6	8.88
0.8	0.008	20	14.4	3	6.59
0.8	0.008	25	18.0	3	8.74
0.8	0.008	30	21.6	3	10.90
0.8	0.008	40	28.8	3	15.19
1.1	0.01	25	18.0	3	12.0 ⎫
0.8	0.008	30	21.6	3	12.0 ⎬ Extra length load lines
0.8	0.008	40	28.8	3	18.75 ⎭

In addition to these variations, provision was made to bring the standard
load lines into 3-and 6-inch diameter circular rings. The 6-inch forebody
could then be suspended from either 6-or 12-inch long extension lines
below the ring. The 3-inch forebody could be suspended by 3-, 6-, or 12-inch
lines below the ring.

D_T = NOMINAL THROAT DIAMETER
D_c = DIAMETER AT BOTTOM OF CATENARY
d = FOREBODY DIAMETER
S = SPAN OF CATENARY
h = HEIGHT OF CATENARY
ℓ = THEORETICAL LOAD LINE LENGTH
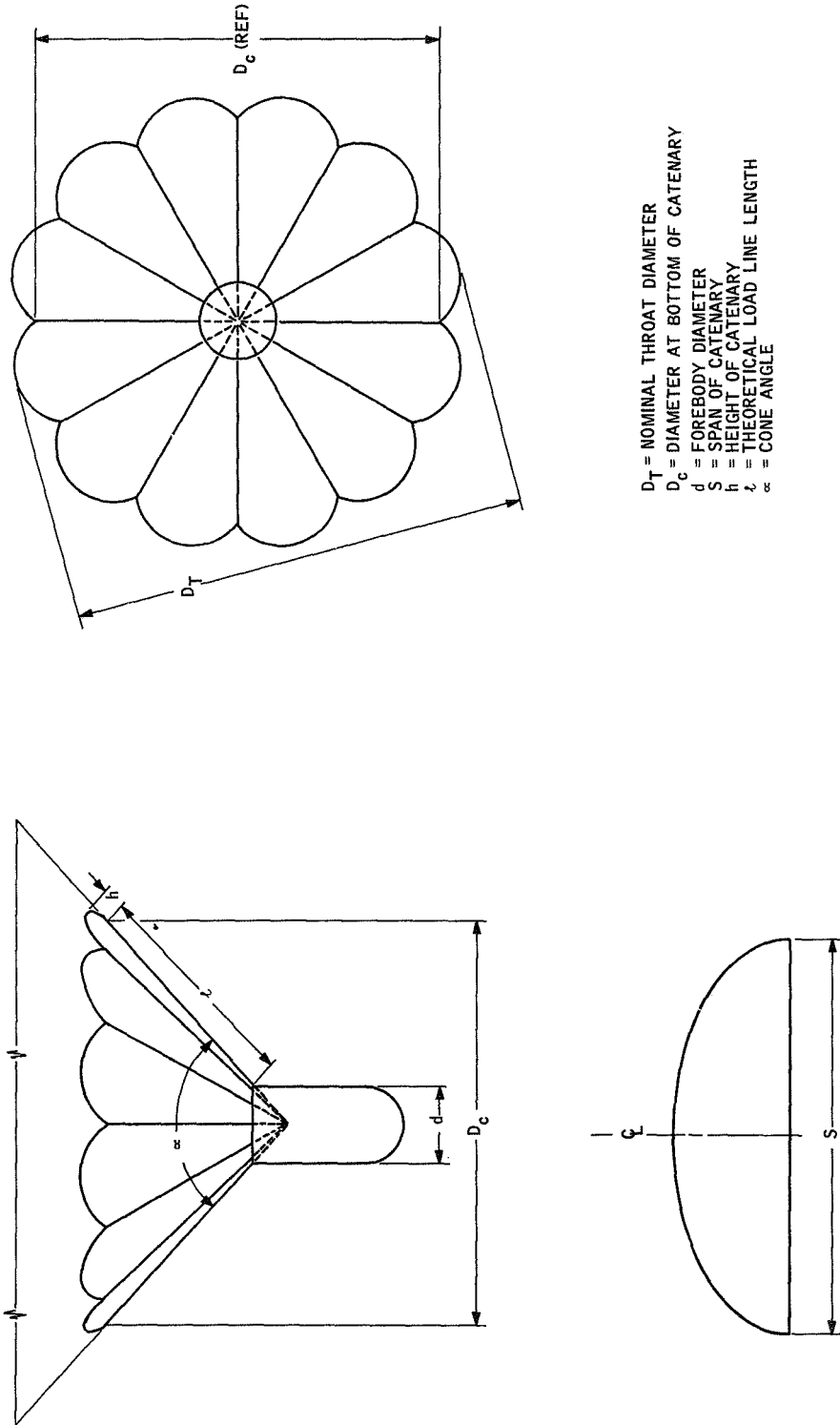α = CONE ANGLE

Figure A1.   Wind Tunnel Model Envelope Throat Geometry

TEST RESULT DETAILS

Table A2 gives a complete listing of all the tests performed in the vertical wind tunnel. Tests are listed in terms of restrained or static tests and unrestrained or dynamic tests and are grouped according to the primary purpose of the tests. In those cases where three values are shown for a single numbered test, three runs were made for a given test condition to establish the degree of repeatability of the data. Motion pictures were taken of all of the tests and are identified by the job prefix 413 followed by the specific run number. All drag coefficients are referred to the maximum horizontal cross-sectional area of the inflated envelope.

The inflation time as a function of a forebody weight is plotted in Figure A2 with various forebody sizes, throat sizes and load line configurations as parameters. From continuity considerations, an increase in mass flow through the envelope throat would be expected to decrease the inflation time. Based on this, several observations can be made from Figure A2:

- The inflation time is strongly dependent on suspended weight. An increase in suspended weight, with the corresponding increase in "float" velocity and mass flow, results in a decrease in inflation time.

- Since the mass flow through the throat is a function of throat area, inflation time would be expected to be a function of throat area. This is confirmed by Figure A2, where it is seen that an increase in throat area for a particular suspended weight results in a decrease in inflation time.

- The positively opened throat produces a marked decrease in inflation time.

Table A2. Summary of Vertical Wind Tunnel Tests

Run No.	Test Type	Forebody (in)	Weight (gm)	Envelope	Configuration	Drogue Parachute (in)	Deployment Velocity (fps)	Constant Rate of Descent (fps)	Extension Lines (in)	Average Inflation Time	Motion	C_{D_P} (Refer to inflated balloon cross-sectional area)	Dimple Size and Stability
							I. STATIC TESTS						
1	Deployment and Inflation	3			Deployment	20	30.0	---	---	20.0	---	---	---
2				125			30.0	---	---	48.0	---	---	---
6							83.2	---	---	Incomp.	---	---	---
							II. DYNAMIC TESTS						
7	Reefed Streamer Drag	4 (cylinder)	694	125	Reefed streamer	---	---	49.9	---	---	---	0.018	---
8			1000			---	---	49.1 / 59.1 / 56.7	---	---	---	0.027 / 0.019 / 0.020	---
9			1500	825		---	---	72, 60	---	---	---	0.019 / 0.027	---
54		3	1580			---	---	45.0	---	---	---	0.051	---
55			1145			---	---	41.4	---	---	---	0.044	---
56			646			---	---	32.7 / 32.1 / 29.2	---	---	---	0.040 / 0.041 / 0.050	---
11	Inflation from Streamer	3	1696	125	Inflation from Streamer	---	---	13.9	None	32.0	Rotation	0.575	Ave. Unst.
32			3744			---	---	15.4		22.5	Rotation	1.035	Large Stab.
33			1277			---	---	10.0		33.0	Rotation	0.837	Small Unst.
4			934			Effect of Extension	---	6.5	3	41.0	Ocs.	1.449	Large Stab.
12			1696			---	---	13.9	6	33.0	Rotation	0.575	Ave. Stab.
13			1696			---	---	11.7	12	33.5	Rotation	0.812	Ave. Stab.
14			1712			---	---	11.7		35.0	Rotation	0.820	Small Stab.
23		3 (cylinder)	701	820		---	---	8.0	None	73.0	---	0.717	---
17		3	1586			---	---	12.5		41.0	Rotation	0.665	Small Unst.
18			2879			---	---	13.3		29.5		1.067	Large Stab.
22		3 (cylinder)	692	825		---	---	8.0		47.0		0.708	Small Unst.
16		3	1574			---	---	11.7		30.0		0.753	Large Stab.
19			2868			---	---	14.0		24.0		0.959	Large Stab.
21		3 (cylinder)	688	830		---	---	8.0		36.0		0.704	Small Unst.

Table A2. Summary of Vertical Wind Tunnel Tests (Continued)

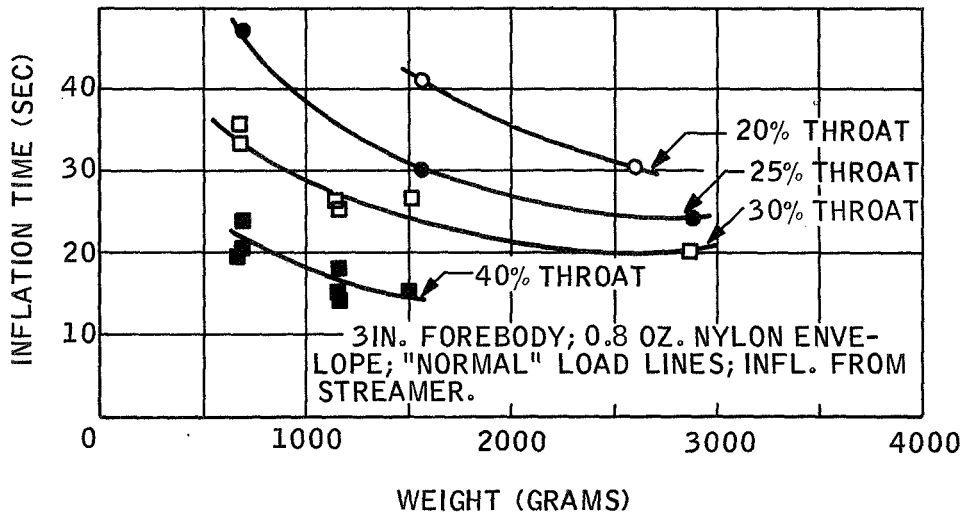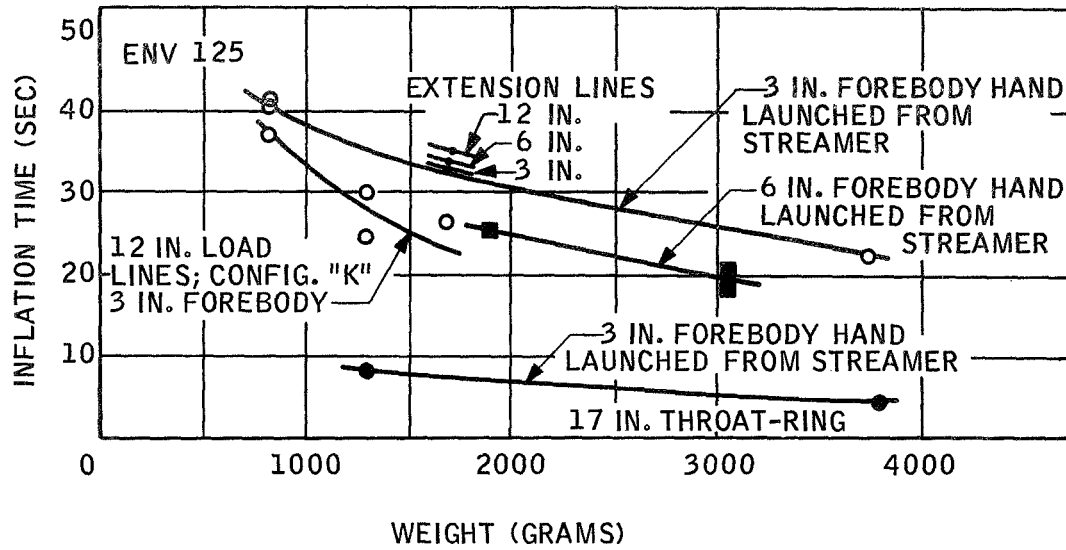| Run No.	Test Type	Forebody (in)	Weight (gm)	Envelope	Configuration	Drogue Parachute (in)	Deployment Velocity (fps)	Constant Rate of Descent (fps)	Extension Lines (in)	Average Inflation Time	Motion	C_{D_P} (Refer to inflated balloon cross-sectional area)	Dimple Size and Stability
15	Inflation from Streamer	3	1571	830	Inflation from Streamer	---	---	11.7	None	26.5	Translation	---	Small Stab.
20	→	→	2864	125		---	---	16.0	→	20.0	Rotation	0.733	Large Stab.
26		6	1885	→		---	---	12.5		26.5	Rotation	0.790	Ave. Stab.
48		→	3015	830		---	---	14.6		20.5 20.5 18.5	Rotation	0.926	Ave. Stab.
47		3	1577	→		---	---	---	12" load lines	22.5 21.0 21.0	Translation	---	Small Unst.
49			688	→		---	---	8.0	None	30.0 33.0 33.0	Translation	0.704	Small Unst.
50			1147	840		---	---	10.0	→	25.0 23.0 26.0	Translation	0.752	Small Unst.
51			1152			---	---	10.0	---	15.0 14.5 18.5	Translation	0.755	Small Unst.
52			693			---	---	8.0	---	21.5 19.0 24.0	Translation	0.710	Small Unst.
53			1585	→		---	---	11.3	---	14.5 15.0 14.0	Translation	0.813	Small Unst.
57			1155	125		---	---	9.3	---	13.5 14.5	Rotation	0.875	Ave. Stab.
24	Steady State Drag	3 (with weight)	5500	→	Launched from Pole	---	---	18.8	None	---	Oscillation	1.019	---
25			10310	125		36	---	27	---	---	Oscillation	0.926	---
27	Deployment and Inflation	6	1885	125	Deployment	30	Free Drop	---	---	---	---	---	---
28		→	→	→		---	34.0 33.4	32.7	---	---	---	---	---
29			→			---	61.9	Aborted	---	---	---	---	---
30	Inflation from Streamer with 17" ring in Throat	3	1320	125	Inflation from Streamer	---	---	10.0	None	8.2	Rotation	0.865	Small Unst.
31			3795	→	→	---	---	18.0	---	4.0	Rotation	0.767	Large Stab.
44	Observe dimple and Stability	3	1271	125	12" Load Lines	None	---	11.3	---	29.0 29.0 24.5	Rotation	0.652	Small Unst.
45	→	→	812	→	→	→	---	8.8	---	40.0 37.0 42.0	Rotation	0.687	Ave. Stab.
46			1704				---	14.6	---	26.0 25.5 26.0	Rotation	0.524	Small Unst.

Figure A2. Summary of Factors Affecting Balloon Inflation Time

●   The forebody diameters tested have a small effect on inflation time.
Since the load lines were attached to the periphery of the forebody,
the 6-inch diameter body tended to initially open more throat area
to the air stream than the 3-inch body, thus decreasing the inflation
time. For the configurations tested, there is no apparent effect of
forebody blockage.

●   It can be observed from Figure A2 that over-length load lines tend
to decrease the inflation time. The longer load lines appear to have
less tendency to hold the throat closed in the latter stages of inflation
due to a reduction in the outward force component where the load
lines join the envelope.

●   The extension lines have a negligible effect on the inflation time. Since
they do not change the throat shape, but merely vary the forebody
position with respect to the throat, there seems to be no blockage
effect here either.

●   For the two weights tested, fabric weight does not appear to have an
appreciable effect on inflation time.

APPENDIX B

FLIGHT TEST EQUIPMENT DETAILS

APPENDIX B
FLIGHT TEST EQUIPMENT DETAILS

EXTRACTION AND PARACHUTE DEPLOYMENT RIGGING

The design of the aircraft extraction and parachute deployment rigging for the 100-fps event velocity drop tests is shown in Figures B1 and B2. The design for the 200-fps tests differed only in the size of the stabilization parachute and its bridle.
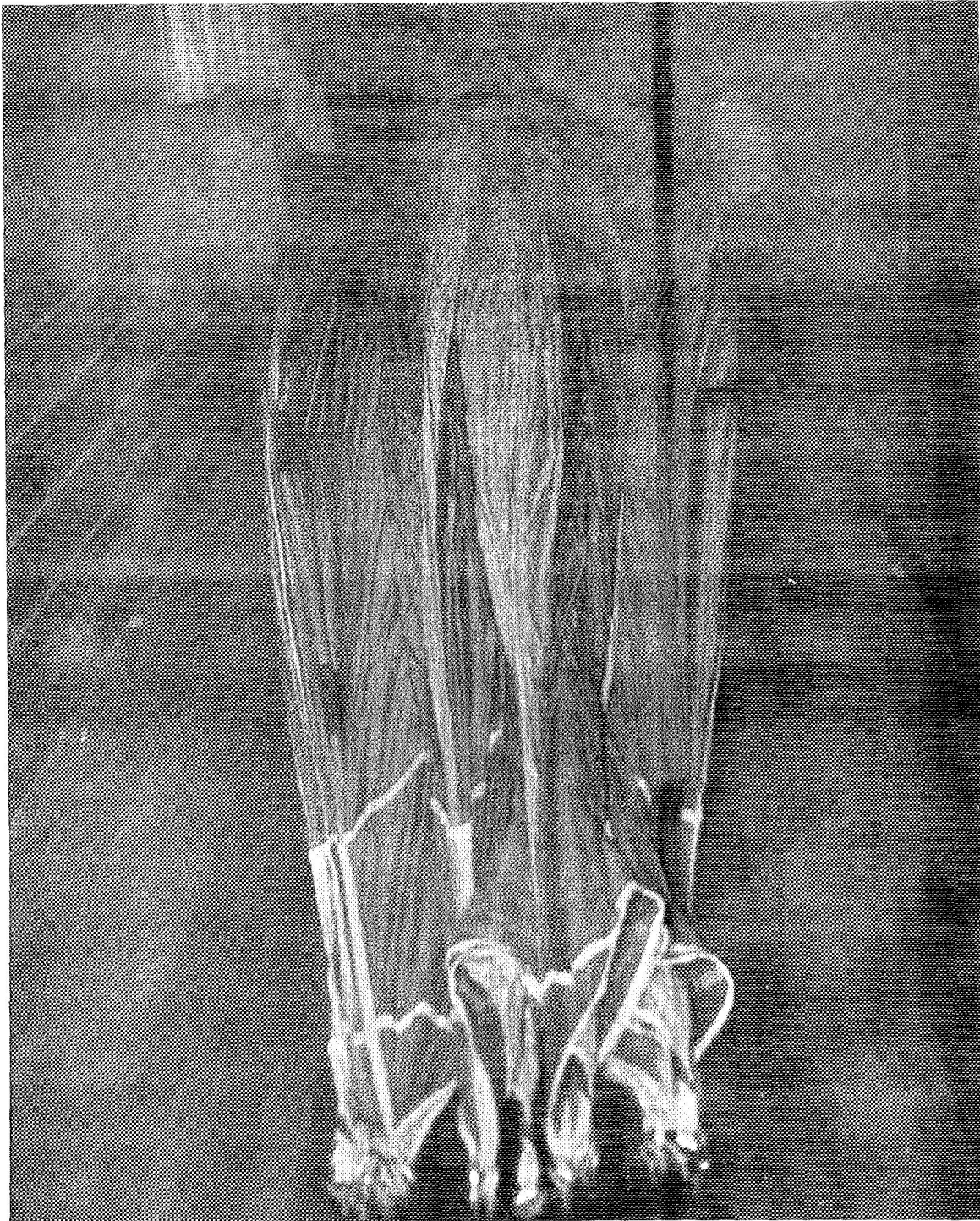
BALLOON PACKING PROCEDURE

The folding and packing of the envelope into the deployment bag is pictured in Figures B3 through B9.

DEPLOYMENT SYSTEM- LIC 9220

PAGE 1 OF 1 PAGES
SKETCH NR
9220-1

ITEM NR	DESCRIPTION
1	Static line, 24-ft. long, attached to sled, GFE
2	Deployment bag, 22-ft. ringslot, GFE
3	Breakcord, 2 turns of 80-lb. cotton tape, GFE
4	Stabilization chute, 20-ft. D_o ringslot, GFE
5	Bridle, 4-leg, 8 plies of 8700-lb. nylon webbing, 6 ft. long, GFE
6	Connector link, 30 k
7	Bridle, 6 plies of 10,000-lb. nylon webbing, 12 ft. long, GFE
8	Door, steel, CFE
9	Deployment bag, Paravulcoon, CFE
10	Balloon, Paravulcoon, 54-ft. diameter, CFE
11	Explosive bolts, door release, 20-second delay, CFE
12	Camera, GSAP, CFE
13	Telemetric Equipment, 2 channels, GFE
14	Special cylindrical vehicle, weighted to 1304 pounds, CFE
15	
16	
17	

REMARKS

DATE	APPROVED BY	PROJECT ENGINEER
13 April 1964		L. T. Byam

AFFTC FORM MAR 61 L-0-29 (FTLG)   PREVIOUS EDITIONS OF THIS FORM ARE OBSOLETE.

Figure B1. Extraction and Parachute Deployment Rigging

	DEPLOYMENT SYSTEM ████ - LIC 9220	PAGE 1 OF 1 PAGES	
		SKETCH NR	
		9220-1A	

ITEM NR	DESCRIPTION
1	Sled, wooden, weight: 200 pounds
2	Cutter line, 1 ply of 6,000-lb. 1-in. webbing, 25 ft. long w/3 Shaw knives*
3	Static line, 15 ft. long
4	Special cylindrical vehicle, rigged in accordance with sketch no. 9220-1
5	Restraint webbing, 1 ply of ████-lb. webbing, 3 required
6	Riser, 2 plies of 8700-lb. nylon webbing, 20 ft. long**
7	Sled recovery chute, 35-ft. D_0 ES with standard reefing**
8	Static line, vehicle stab. chute, 24 ft. long, tied to sled cross member
9	Vehicle stabilization chute, 20-ft. D_0 Ringslot**
10	Shear webbing, 1 ply of 1500-lb. nylon webbing
11	Bridle, 2-leg, 2 plies of 8700-lb. nylon webbing, 4-ft. long
12	Cutter line, length to suit
13	Clevis, G-12
14	Extraction line, 2 plies of 8700-lb. nylon webbing 60 ft. long
15	Extraction chute, 48-inch RGS
16	
17	

REMARKS

* Cutters to be inclosed in boots. (Item #2)

** Item #6,7 & 9: Tie parachutes and riser to vehicle with 80-lb. tape

Gross weight:	1500 lbs.
Extraction force:	650 lbs.
Extraction ratio:	.43
Extraction chute:	48" RGS
Opening force:	900 lbs.
Airspeed:	130 KEAS

DATE	APPROVED BY	PROJECT ENGINEER
13 April 1964		L. T. Byam

AFFTC FORM MAR 61 L-0-29 (FTLG) PREVIOUS EDITIONS OF THIS FORM ARE OBSOLETE.

Figure B2. Extraction and Parachute Deployment Rigging

Official U. S. Navy Photograph

Figure B3. Paravulcoon Packing Procedure (With envelope tensioned on table, gores are accordian pleated from each side with straight seams to the center.)
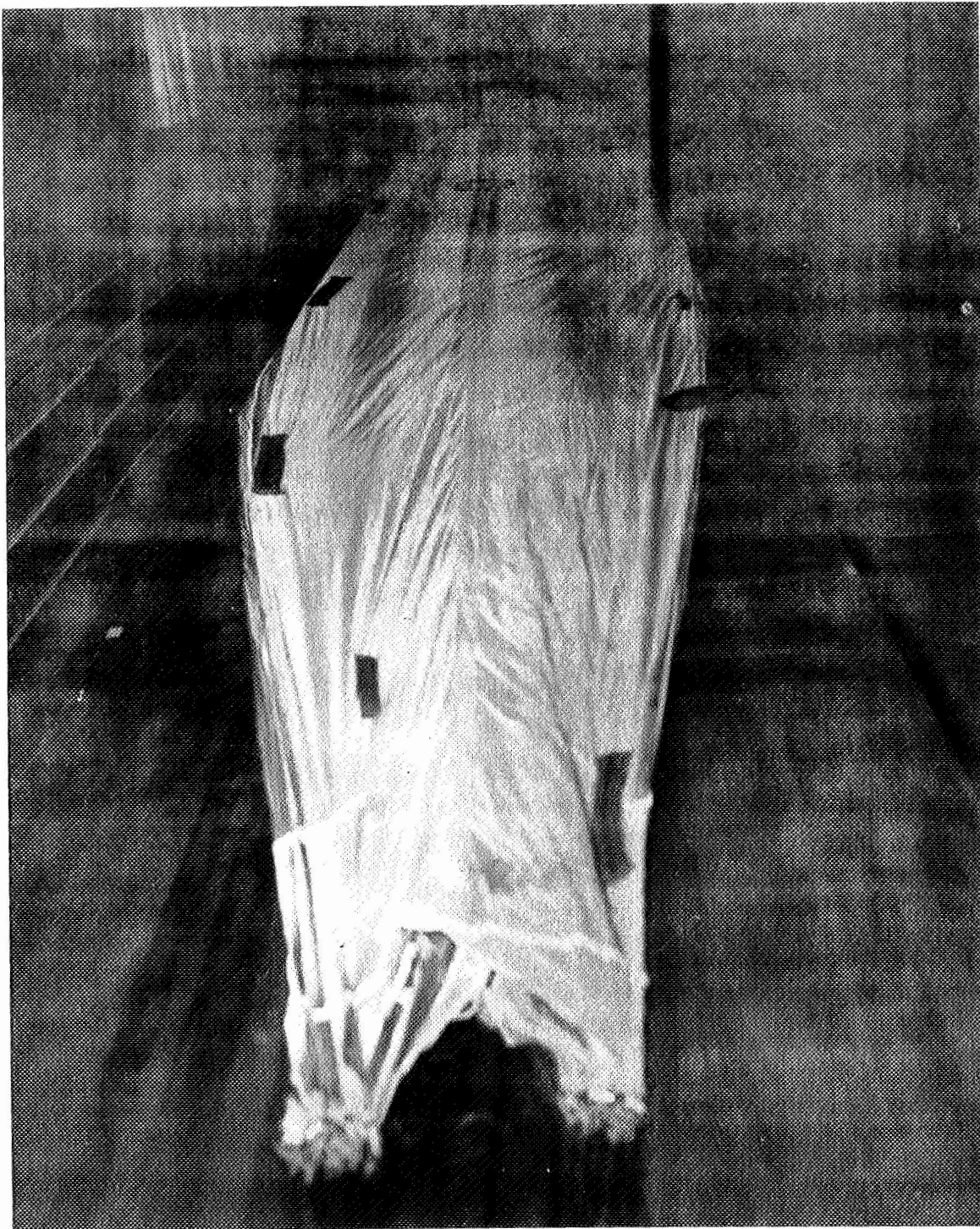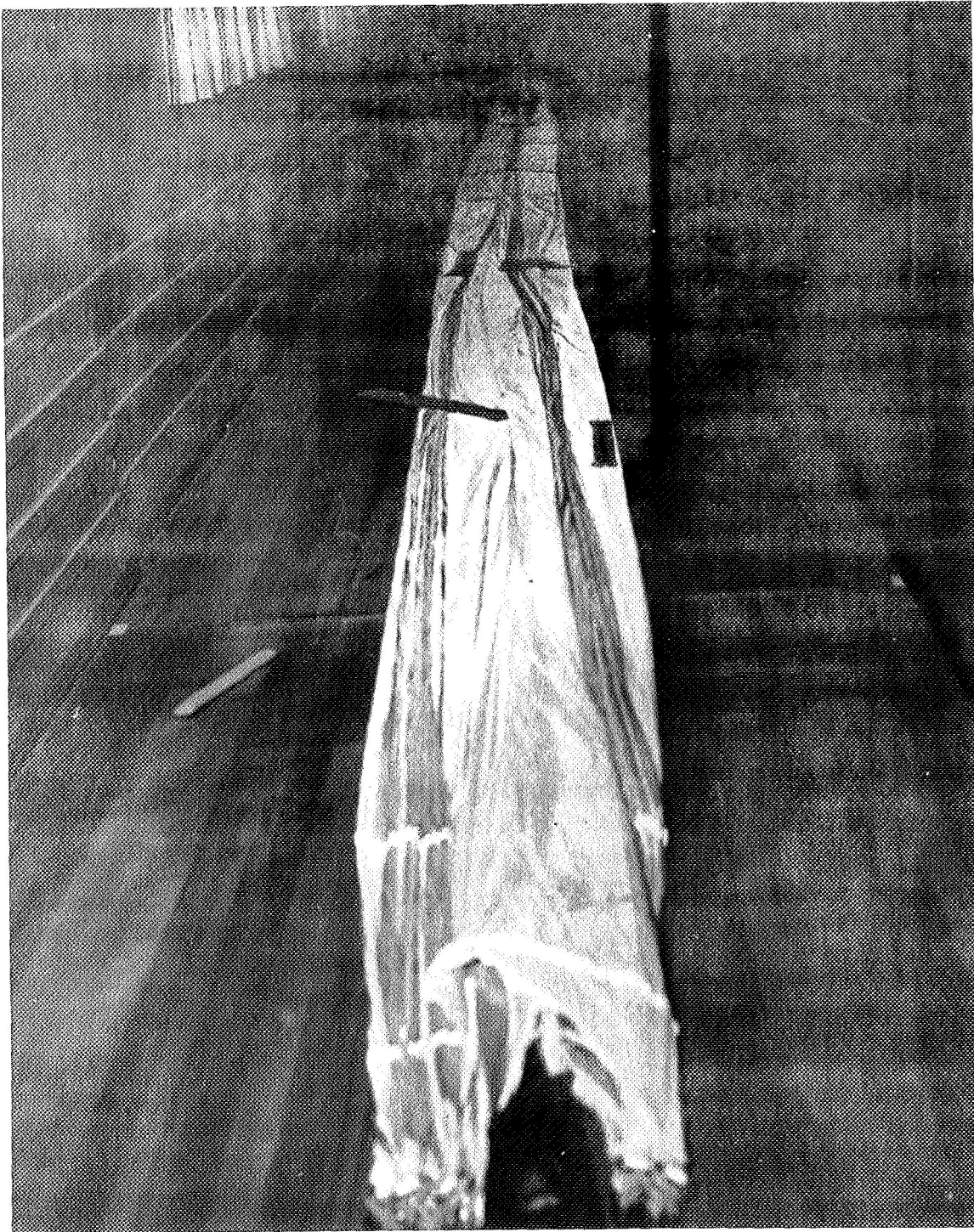
Official U. S. Navy Photograph

Figure B4. Paravulcoon Packing Procedure (envelope folded into two matching piles of 10 pleats each)

Official U.S. Navy Photograph

Figure B5. Paravulcoon Packing Procedure (matching piles of pleats folded to center and back)

Official U. S. Navy Photograph

Figure B6. Paravulcoon Packing Procedure (second folding process
completed to give a maximum width of 26 inches)

Official U.S. Navy Photograph

Figure B7. Paravulcoon Packing Procedure (with air rolled out, folded
envelope packed into deployment bag in zig-zag folds)

Official U. S. Navy Photograph

Figure B8. Paravulcoon Packing Procedure (Before closing deployment
bag, numbered load lines are indexed in special jig to ensure
proper orientation
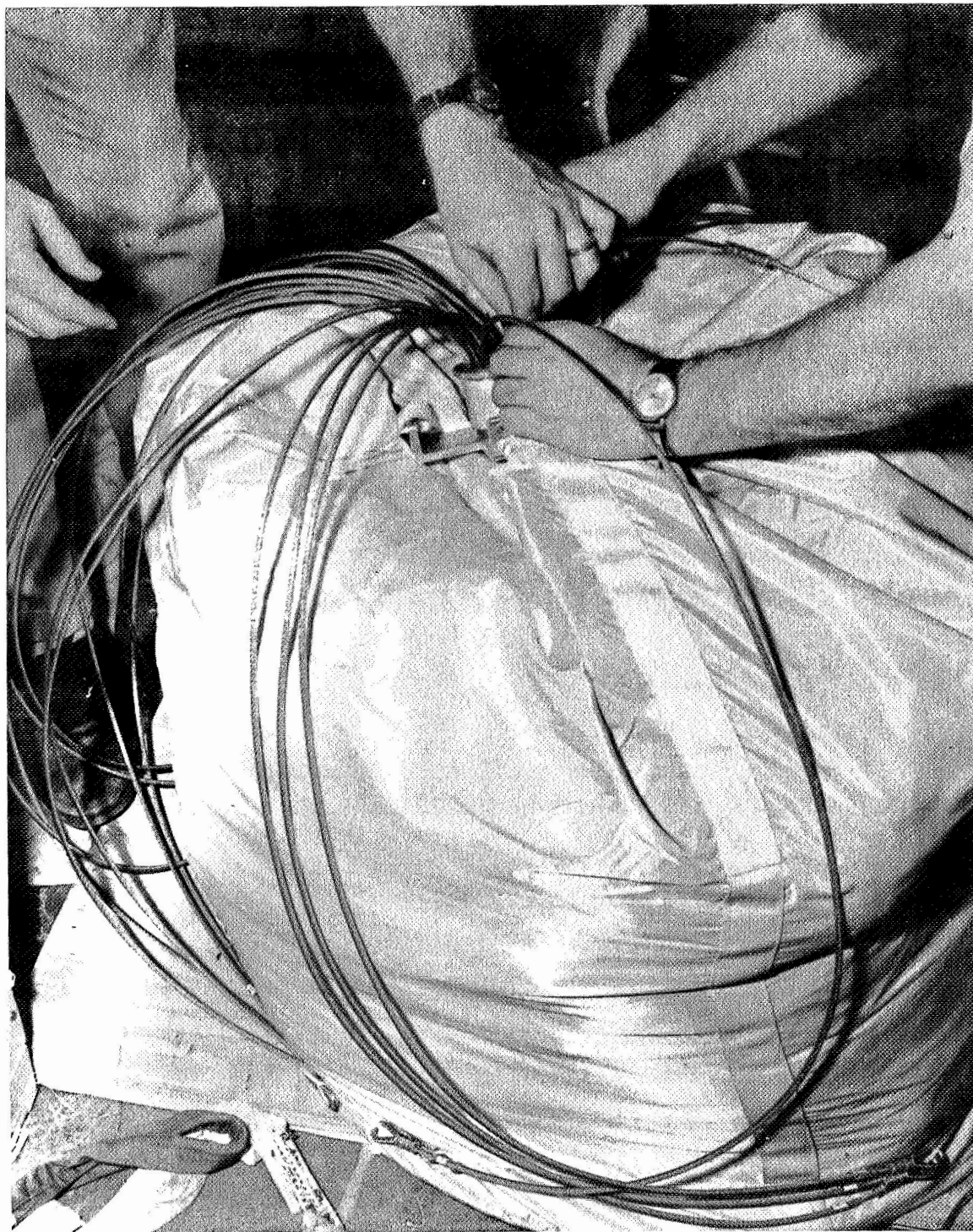
Official U.S. Navy Photograph

Figure B9. Paravulcoon Packing Procedure (breakaway spool secured and load lines inserted inside bag to give a uniform exposed length)